

# Biodistribution, Clearance, and Long-Term Fate of Clinically Relevant Nanomaterials

Joël Bourquin, Ana Milosevic, Daniel Hauser, Roman Lehner, Fabian Blank,  
Alke Petri-Fink, and Barbara Rothen-Rutishauser\*

Realization of the immense potential of nanomaterials for biomedical applications will require a thorough understanding of how they interact with cells, tissues, and organs. There is evidence that, depending on their physico-chemical properties and subsequent interactions, nanomaterials are indeed taken up by cells. However, the subsequent release and/or intracellular degradation of the materials, transfer to other cells, and/or translocation across tissue barriers are still poorly understood. The involvement of these cellular clearance mechanisms strongly influences the long-term fate of used nanomaterials, especially if one also considers repeated exposure. Several nanomaterials, such as liposomes and iron oxide, gold, or silica nanoparticles, are already approved by the American Food and Drug Administration for clinical trials; however, there is still a huge gap of knowledge concerning their fate in the body. Herein, clinically relevant nanomaterials, their possible modes of exposure, as well as the biological barriers they must overcome to be effective are reviewed. Furthermore, the biodistribution and kinetics of nanomaterials and their modes of clearance are discussed, knowledge of the long-term fates of a selection of nanomaterials is summarized, and the critical points that must be considered for future research are addressed.

## 1. Introduction

Over the past 20 years, the growth of nanomaterials research has been concomitant with an overwhelming increase in the production of nanotechnology-related products.<sup>[1,2]</sup> This increased attention in the industry is also reflected in the

amount of nanomaterials (i.e., a material with one, two, or three external dimensions on the nanoscale (<100 nm)), produced annually, which has reached values of over 1000 tons for some materials.<sup>[3,4]</sup> This new industrial revolution promises to provide an advantageous basis for numerous applications, including medicine (e.g., drug delivery, imaging, and theranostics), consumer products (e.g., food additives, cosmetics, and sporting equipment), environmental remediation, and information technology.<sup>[2]</sup>

The implementation of nanomaterials in the medical field allows a variety of biomedical applications, for instance as diagnostic or therapeutic agents and in novel vaccine formulations.<sup>[5]</sup>

The advantages of such nanomaterials are diverse and include: (i) their small size, which is in the range of biomolecules (e.g., receptors, antibodies, or nucleic acids) and enables interactions with single cells; (ii) their highly tunable surfaces for

functionalization's with biomolecules, which enables targeting of cells and/or intracellular organelles; (iii) their high surface area, which allows the attachment of more drug units than on larger particles of the same total mass, thus leading to higher loading efficacy; and (iv) their distinctive physicochemical properties when compared to their bulk materials, which can provide potential opportunities, for example in hyperthermia treatments.<sup>[6]</sup> In the last decade, a broad array of new and improved nanoscale materials has emerged, some of which draw inspiration for their design from nature. In a broad context, they are defined as materials that imitate key features of natural materials and/or biological structures at the chemical, physical, or morphological level. The list of such bioinspired materials includes systems based on lipids (e.g., liposomes), glycans (e.g., sugars), peptides, nucleic acids, and dendrimers, among others.<sup>[7]</sup> There have been major advances in the engineering of biomimetic nanomaterials that replicate features of biological systems and surfaces that mimic natural cells and viruses, such as long circulation times, few interactions with off-target molecules, and high-affinity targeting of specific cells.<sup>[8,9]</sup> These benefits add to the already interesting properties that come from the nanoscale of the material.

Despite all these interesting properties and technology advancements, very few nanomaterials have been approved by

---

J. Bourquin, A. Milosevic, D. Hauser, Dr. R. Lehner, Prof. A. Petri-Fink, Prof. B. Rothen-Rutishauser  
Adolphe Merkle Institute  
University of Fribourg  
Chemin des Verdiers 4, 1700 Fribourg, Switzerland  
E-mail: barbara.rothen@unifr.ch  
Dr. F. Blank  
Respiratory Medicine  
Department of Biomedical Research  
University of Bern  
Murtenstrasse 50, 3008 Bern  
Prof. A. Petri-Fink  
Department of Chemistry  
University of Fribourg  
Chemin du Musée 9, 1700 Fribourg, Switzerland

the Food and Drug Administration (FDA) for use in medical applications, whereas the majority have thus far failed to reach the bedside.<sup>[10]</sup> Therefore, new efforts have to focus on a detailed understanding of the interaction of nanomaterials with the cells at the fundamental level. To further increase the number of nanomaterial systems that reach clinical applications, it is important to address the possible biodistribution, clearance routes, and the long-term fate of these nanomaterials in the body. So far, little effort has been put in to studying the fate of nanomaterials over more than a few days, due to the limited detection possibilities currently available. Another reason might be the difficulty in the controlled production of the nanomaterials, for example producing materials with low polydispersity. This seems to be especially challenging when the production is upscaled to an industrial scale.<sup>[11,12]</sup>

Despite major drawbacks, a number of nanomaterials are currently being tested in preclinical and clinical phases, covering a broad spectrum from polymers, liposomes, micelles, nanocrystals, and protein-based nanomaterials to inorganic nanomaterials (for a review see ref. [13]). A recent review from 2016 identified around 51 FDA-approved nanomedicines and around 77 products in clinical trials.<sup>[14]</sup> These approved materials include gold nanoparticles (AuNPs) that, given their biologically inert properties, provide a good basis for nanosized drug delivery systems.<sup>[15,16]</sup> Additionally, a range of nanobased drug delivery systems, such as liposomal, polymeric, or bio-inspired nanoparticles (NPs), have already progressed into therapeutic applications.<sup>[17–19]</sup> Other promising classes of materials are quantum dots (QDs), semiconducting nanocrystals that contain properties suitable for imaging and diagnostic applications.<sup>[20]</sup> Even though QDs have successfully been applied as an imaging tool and provided valuable data on the behavior of nanomaterials and interactions in vivo (e.g., renal clearance), their clinical applicability remains controversial due to their potential health risks and demonstrated toxicity.<sup>[21–24]</sup> Furthermore, the already FDA-approved superparamagnetic iron oxide nanoparticles (SPIONs), i.e., NanoTherm, have drawn attention for their possible hyperthermal treatment of cancer when exposed to an alternating magnetic field, in addition to being useful as a classical drug or a gene delivery system.<sup>[25,26]</sup>

The aim of this review is to address the long-term biological fate of clinically interesting nanomaterials and present examples of materials for which reliable data have been found. We discuss the possible administration routes of nanomaterials and how their properties (e.g., size, surface charge, and functionalization) can affect their interaction at the tissue and cell membranes, their uptake and intracellular fate at the single cell level, as well as their biodistribution and clearance in vivo.

## 2. Therapeutic Nanomaterials—Possible Routes of Exposure

### 2.1. Modes of Exposure

To exert its mode of action, a drug or active agent needs to reach the organ, tissue or cell of interest. Over the course of time, different approaches have been established in order to increase targeting efficiency. In this review, we focus on the exposure



**Barbara Rothen-Rutishauser** received her Ph.D. in cell biology in 1996 from the Swiss Federal Institute of Technology in Zurich (ETHZ), Switzerland. Afterward, she worked for ten years in the research group of Prof. Gehr at the Institute of Anatomy, University of Bern, Switzerland. In 2011, she became the new chair in BioNanomaterials at the Adolphe Merkle Institute, University of Fribourg, Switzerland, a position shared equally with Prof. Alke Petri-Fink. She is an expert in the field of cell–nanoparticle interactions in the lung, with a special focus on 3D lung cell models.

routes most commonly used for nanomaterials, and their respective implications, by considering the subsequent fate of the administered nanomaterial. We not only consider the literature available describing the intentional application of biomedical nanomaterials, but also the much more extensive body of literature describing hazard/risk assessment results for the unintentional exposure of humans to nanomaterials. An overview of the commonly used routes of exposure can be found in **Figure 1**.

### 2.2. Injection

The most direct route of administration of nanomaterials is via injection. The most commonly practiced routes include intravenous, subcutaneous, and intratumoral injection. The advantage of the direct injection of nanomaterials into the bloodstream is the rapid delivery and distribution of the materials throughout the vasculature. However, one has to consider that this rapid distribution of the materials also results in their clearance by the kidneys, the liver, or via the reticuloendothelial system (RES). For the metabolism of conventional drugs, the liver is paramount. This effect, also known as the first-pass effect, can be used to engineer a nanomaterial or nanocarrier in such a way that the material or carried drug is only activated in the liver,<sup>[27]</sup> or nanomaterials can be designed so as to overcome the first-pass effect in the liver. The aforementioned limitations can be circumvented by subcutaneous or intratumoral injection, which then means that the location of the injection has to be carefully chosen for optimal effect. The fate of the nanomaterials after subcutaneous injection heavily depends on the interstitial lymphatic flow rate at the site of the injection and on the physicochemical properties of the nanomaterials. The major factor is size, as small colloids (smaller than a few nanometers) are mostly absorbed into capillaries, while nanomaterials up to a few scores of nanometers cannot be similarly absorbed and are instead drained into the lymphatic system. It has been shown that larger materials can persist longer at the injection site.<sup>[28]</sup> Finally, nanomaterials can also be

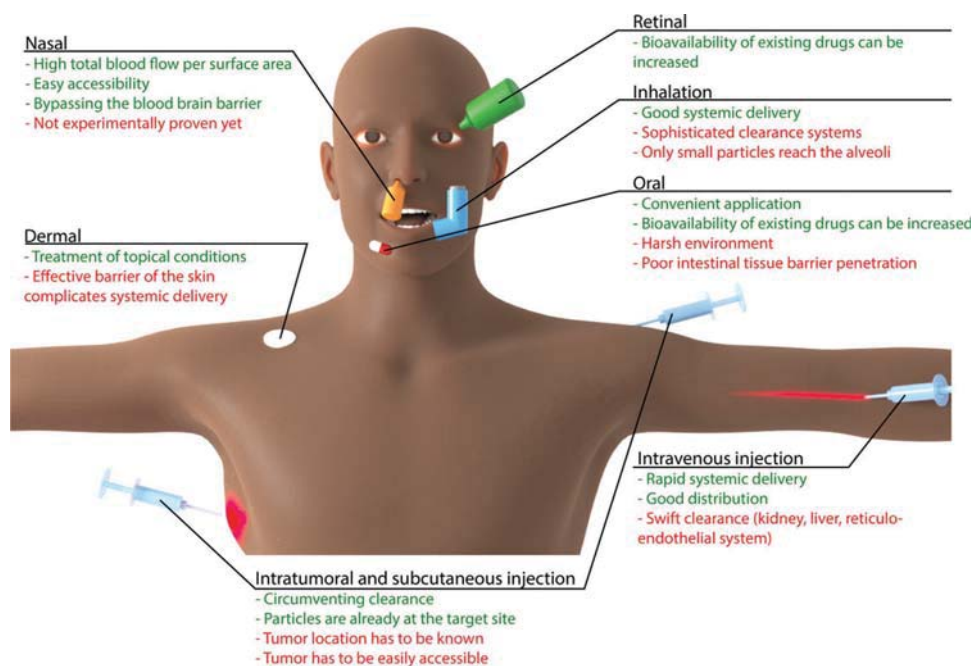


**Figure 1.** Routes of administration: summary of the routes of exposure commonly used for nanomaterial administration, including their main advantages (green) and challenges (red).

injected directly into tumor tissues, which is currently the most frequently used route in animal experimentation, as this seems to be the most promising route for successful implementation in patients. This approach overcomes the limitations arising from systemic administration, and targeting can also be optimized by delivering the nanomaterial directly to the interstitium of the cancerous tissue.<sup>[29]</sup> The parameters influencing the subsequent fate of the nanomaterials are similar to those described for the subcutaneous injection route. However, the interstitial pressure in tumors has been found to be higher than in healthy tissue, leading to a generally higher leakage of the drugs into the surrounding tissue.<sup>[30]</sup> Despite its advantages and successes, intratumoral injection is only applicable for easily accessible tumors.

### 2.3. Inhalation

Another promising and direct route for the administration of nanomaterials is via inhalation, either for the treatment of lung diseases or for systemic delivery. It was shown as early as the 1920s that inhaled insulin can lower blood sugar.<sup>[31]</sup> The lung has very interesting structure-functional properties, such as a huge internal surface area of about 150 m<sup>2</sup> (i.e., alveoli and airways)<sup>[32]</sup> and high endothelial permeability. These features facilitate systemic delivery and thus make the lung a promising organ for nanomaterial administration.<sup>[33]</sup>

Based on the particle size, it can be predicted in which compartment particles will predominantly deposit in the lung. The smaller the particles are, the deeper they penetrate into the lung parenchyma.<sup>[34,35]</sup> However, it has also been shown that nanomaterials can deposit into the olfactory epithelium and directly translocate to the brain.<sup>[36]</sup> Inhaled nanomaterials are

subject to different clearing mechanisms depending on the pulmonary compartment in which they are deposited. In the large airways, the mucociliary escalator provides rapid clearance of deposited materials. In contrast, nanomaterials that reach the gas-exchange region will be cleared less rapidly by alveolar macrophages, i.e., professional phagocytes, which may migrate out of the lung or remain in the pulmonary interstitium, or by dendritic cells, professional antigen-presenting cells, with subsequent transport to the lung-draining lymph nodes. Irrespective of the pulmonary compartment, nanomaterials can also be taken up by pulmonary epithelial cells and they may translocate across the epithelial barrier (transcytosis). In the case of an alveolar epithelium that is extremely thin, this process may lead to translocation into the blood stream.<sup>[37–39]</sup> All of these mechanisms by which the nanomaterials interact and are cleared by the respiratory tract have to be taken into account for the design of new inhaled nanomaterials/nanocarriers.<sup>[40,41]</sup>

A good example of such application has been shown by Bianchi et al.<sup>[42]</sup> They reported that the retention of gadolinium-based theranostic nanoparticles as contrast agents, administered via inhalation, shows some direct advantages, e.g., high retention in lung tumor tissue, in comparison to the classical intravenous injection route. This work was then followed up by Dufort et al. who showed that those nanoparticles do not induce inflammation and would be fit for use not only as contrast agents but also as therapeutic carriers.<sup>[43]</sup>

However, conflicting reports exist as to what proportions of nanomaterials can be systemically found after inhalation, showing major differences between animal and human models.<sup>[44]</sup> Addressing this divergence is of great importance, as the inhalation of nanoscale particulates is also of major concern with respect to their unintentional inhalation.<sup>[45]</sup>

## 2.4. Oral Administration

Oral administration of nanotherapeutics is the most preferred method of delivery, particularly due to its relatively convenient application and consequently its relatively high patient compliance.<sup>[46]</sup> Very few nanomaterial-based systems with the potential to be used as oral drugs (e.g., immunosuppressants and antiretrovirals) have been described thus far. Although this route is the most favorable one, the accompanying enzymatic degradation, the acidic environment in the stomach, and the poor penetration across the intestinal tissue barrier all result in poor oral bioavailability.<sup>[46]</sup> These challenges render the translation from benchtop to the clinic more difficult.<sup>[47]</sup> However, it has been shown that nanomaterial formulations can enhance the bioavailability of orally administered drugs.<sup>[47]</sup>

More knowledge about the interaction of nanomaterials with the gastrointestinal tract can be obtained from nanomaterials found in food or food packaging since most of these materials are metallic oxides and can be analyzed more easily. The *Project on Emerging Nanotechnologies* currently lists 118 nanotechnology-containing items in the *Food and Beverage* category, predominantly silver, nanosilicates, and titanium dioxide.<sup>[48]</sup> Silver (Ag) nanoparticles are mostly used for their antibacterial properties in packaging, and it has been shown that these particles can leach out from the packaging material over time.<sup>[49]</sup> In this context, silica (SiO<sub>2</sub>) (E551) and titanium dioxide TiO<sub>2</sub> (E171) NPs in particular should be noted since they have already been approved as dietary additives (anticaking and food whitening/brightening, respectively). The available toxicity data have recently been reviewed by McCracken et al.<sup>[50]</sup> Briefly, the available in vivo data of rats and mice are inconclusive for SiO<sub>2</sub>NPs.<sup>[50]</sup> Some studies state very little absorption of ingested NPs, whereas others state toxic effects. For TiO<sub>2</sub> NPs the data are similarly inconclusive, with some studies not finding any absorption or acute toxicity, while others do.<sup>[50]</sup>

## 2.5. Dermal Administration

The skin is the largest organ in humans and provides an effective barrier toward the environment. Recent reviews have addressed the potential interaction of nanomaterials with the skin barrier.<sup>[51,52]</sup>

A major function of the skin, particularly the stratum corneum (the outermost layer), is to provide a protective barrier against the hazardous external environment. The skin is relatively impenetrable to lipophilic molecules larger than 600 Da in molecular weight, whereas lipophilic particles smaller than this may passively penetrate.<sup>[53]</sup> In addition, it is also a potential target for drug delivery via nanocarriers.<sup>[54]</sup>

Many commercially available sunscreens contain TiO<sub>2</sub> and zinc oxide (ZnO) NPs because of their UV scattering and reflecting properties, which attenuate harmful solar radiation reaching the skin.<sup>[55]</sup> It has been shown that the presence of TiO<sub>2</sub> NPs, in combination with sunlight, can have adverse effects on DNA.<sup>[56]</sup> However, the current common consensus in the field is that the NPs present in sunscreen do not penetrate healthy or sunburnt skin.<sup>[55,57]</sup> Minor skin disruptions or psoriasis do not change this; only conditions disrupting the stratum

corneum (e.g., eczema) have been found to increase penetration of the aforementioned particles.<sup>[57]</sup>

It has also recently been demonstrated that nanoparticles originating from tattoo ink can migrate to lymph nodes and persist for extended periods of time.<sup>[58]</sup>

In general, it can be stated that healthy human skin is an efficient barrier against the most frequently applied NPs, such as the ZnO or TiO<sub>2</sub> particles in cosmetics.<sup>[59,60]</sup> Because of the barrier properties of the skin, NP formulations for systemic delivery are not very promising. On the other hand, nanomaterial formulations for the treatment of topical conditions (e.g., psoriasis) have been more heavily investigated.<sup>[61]</sup> The review of Yang et al. addresses drug delivery across the skin barrier in a complete and detailed manner.<sup>[62]</sup>

## 2.6. Other Administration Routes

Other application routes involve the retinal application of different formulations for drug delivery. Through optimization of the design of the nanomaterials used as future drug carriers, their inherently low bioavailability could be partially improved, as manifested by a number of formulations reaching clinical trials for eye applications. Some examples of this are hydrogel formulations for the topical treatment of ocular hypertension and cyclodextrin-based eye drops for open-angle glaucoma.<sup>[63]</sup> Another possibility is the coating of implants with Ag NPs, which have antibacterial properties.<sup>[64]</sup> It has been shown that implants treated with Ag NPs are biocompatible and show promising results toward the attenuation of infectious diseases.<sup>[65,66]</sup>

Furthermore, a number of ongoing projects are concerned with the application of nanomaterials as delivery systems to overcome mucosal barriers, such as those of the nose or mouth. There are a variety of benefits of nasal application for a patient, for instance the high total blood flow per unit of surface area, easy accessibility, and the direct transport of drugs to the brain via the olfactory nerves.<sup>[67]</sup> Currently, efforts are concentrated on bypassing the very selectively permeable blood–brain barrier (BBB) and thereby delivering drugs directly into the brain.<sup>[68]</sup> However, the efficacy of this route is yet to be experimentally proven.<sup>[68,69]</sup> In comparison, most of the research into the buccal administration route is performed in order to increase retention time and to increase mucoadhesion so as to prevent the drug from being washed away by saliva.<sup>[70,71]</sup> However, this field has not yet been comprehensively explored.

The review of Kermanizadeh et al. gives a good overview of different exposure routes and the possible adverse effects of nanoparticles following such administrations.<sup>[72]</sup>

## 2.7. Protein Corona

As elaborated above, nanomaterials may be administered to the human body via different methods such as by inhalation, injection, ingestion, and application to the skin. Independent of the administration route, the particles inevitably encounter a complex physiological fluid environment populated with a wide range of biomacromolecules, e.g., proteins, vitamins, lipids,

and salts/ions.<sup>[73]</sup> Upon contact with physiological fluids, the formation of a surface-bound protein layer, particle dissolution, or aggregation might occur, which are expected to have a crucial impact on cellular, tissue, and organ interaction.<sup>[74]</sup> For the subsequent fate it is important to understand the consequences of the interactions of nanomaterials with physiological fluids including mucus (gastrointestinal (GI) or respiratory tract), aqueous lining layer covered by surfactant (lung parenchyma), the blood or the lymphatic fluid, as well as available analytical methods to investigate the possible interactions.<sup>[75]</sup>

The description of the protein corona formation depending on the physicochemical properties of the nanomaterials is beyond the scope of this review and has been thoroughly presented elsewhere.<sup>[76–82]</sup> We have, however, included relevant literature for the later discussed materials.

### 3. Biological Barriers

#### 3.1. Tissue Barriers

A variety of biological barriers exist, and nanomaterials or drug nanocarriers must either be designed to be effective at the diseased barrier itself or to overcome the barrier to provide an effective concentration of the therapeutic drug at the diseased site. Depending on the mode of exposure and the route of administration, external and internal biological barriers can be differentiated.

The skin and the mucosa form primary structural barriers that separate the hosts from the external environment. External barriers include the epithelia of the skin, the nasal tract and the respiratory system, the retina, and the gastrointestinal tract. The stratum corneum comprises the physical barrier of the skin, whereas the other barriers are covered with a mucosal layer that has to be overcome by a nanomaterial via the aforementioned exposure routes in order to reach the blood circulation and/or the targeted tissue.

Internal or secondary biological barriers include the endothelium of the blood vessels, the BBB, the blood–testis barrier (BTB), the placental barrier, the interstitial space and extracellular matrix (ECM), and reticuloendothelial system.

Normally, blood endothelial tissue is tight and does not allow nanomaterials to translocate. However, cancerous tissue, as well as inflammatory reactions causing activation and secretion of proinflammatory cytokines (tumor necrosis factor (TNF), interleukin (IL)-1, IL-6, vascular endothelial growth factor (VEGF)), shows induction of endothelial fenestration, i.e., a loss of cellular integrity inducing a gap between the endothelial cells.<sup>[83,84]</sup> This feature can enable the nanomaterials to extravasate from the blood system into the cancerous and/or inflamed tissue. Another possibility is the clearance of the nanomaterials via the lymph system. After extravasation of nanomaterials from the blood system, they face the dense interstitial space and ECM, a network of collagen, proteins, and elastic fibers that provide the structural integrity to the tissue.<sup>[85,86]</sup> Diseases such as cancer and liver fibrosis reveal an altered ECM and an increased number of fibroblasts, which affect the penetration of nanomaterials through the tissue.<sup>[87]</sup>

The BBB, which is one of the tightest barriers in the human body, protects the central nervous system from toxins and restricts the diffusion of large, hydrophilic molecules into the cerebrospinal fluid. The efficient BBB is formed by endothelial cells, the capillary basement membrane, astrocyte end-feet encircling the vessels, and pericytes forming an additional continuous layer that separates the blood vessels from brain tissue.<sup>[88]</sup> The endothelial cells from the BBB differ from endothelial cells found in the rest of the body since they show no fenestrations, form very tight monolayers ( $>1000 \Omega \text{ cm}^2$ ), and exhibit reduced pinocytotic vesicular transport.<sup>[89]</sup> It has been shown that only small lipophilic molecules and molecules with molecular weights less than 400 Da can diffuse through the BBB.<sup>[90]</sup> Specific brain pathologies, e.g., stroke, and Alzheimer's and Parkinson's diseases, can cause an impairment of the BBB, making it more permeable to different molecules that can induce inflammatory responses or neuronal damage.<sup>[91]</sup> Despite this increased permeability, challenges for the efficient delivery of nanomaterials into the brain still remain.

The BTB protecting the male germ line is also one of the tightest blood–tissue barriers in the mammalian body. The BTB regulates the entry of nutrients (e.g., sugars and amino acids) and vital molecules (e.g., hormones and electrolytes) into the compartment that is important for sperm cell development.<sup>[92]</sup> Male germ cells are protected from harmful substances by Sertoli cells forming the BTB.<sup>[93]</sup> Sertoli cells are connected by basal ectoplasmic specializations, gap junctions, and desmosome-like junctions.<sup>[94]</sup> Lan et al. have proposed that nanomaterials can display adverse effects on spermatogenesis by activating the release of (pro-)inflammatory cytokines, leading to a weakening of the BTB that allows the nanomaterials to cross the barrier.<sup>[95]</sup>

In females, the placenta protects the developing fetus during pregnancy and also changes its properties, such as thickness and permeability, during pregnancy. During the early days of pregnancy, an epithelial cell called a syncytiotrophoblast is formed, which represents the primary barrier between fetal and maternal tissue. Both the syncytiotrophoblast and the fetal capillary endothelium express a variety of transporters that take part in drug transport.<sup>[96,97]</sup> During the first trimester the barrier is thicker and less permeable than during the last three months, whereupon it gets thinner, more permeable, and therefore increases the chances of nanomaterials crossing the membrane. Exposure to nanomaterials in the third trimester can potentially cause severe damage to the placenta and a high possibility of miscarriage and embryo malformation.<sup>[98]</sup> However, newly engineered nanomaterial-based drug delivery systems could enable new therapeutic approaches during pregnancy to treat a diseased embryo/fetus in situ.

Another possibility is the clearance of the nanomaterials via the lymph system. After extravasation of nanomaterials from the blood system, they face the dense interstitial space and ECM, a network of collagen, proteins, and elastic fibers that provide the structural integrity to the tissue.<sup>[68,69]</sup> Diseases such as cancer and liver fibrosis reveal an altered ECM and an increased number of fibroblasts, which affect the penetration of nanomaterials through the tissue.<sup>[70]</sup> Furthermore, nanoparticles can be cleared by the RES. The RES is part of the immune system and contains monocytes and macrophages located in the various tissues, which retain and rapidly remove nanomaterials from the blood circulation through opsonization.<sup>[82]</sup>

The translocation of particles from one side of a tissue barrier to the other is a phenomenon observed in many different tissues and organs. How this transport works in detail, i.e., if the transport occurs by trans- or paracellular routes, and what determines the fate of the internalized particles, is not yet fully understood.<sup>[99,100]</sup> The size dependency for the translocation of gold (Au) NPs across the lung epithelium was also confirmed by Kreyling et al. in 2014.<sup>[101]</sup> The authors reported that, in rats, the size, the material, specific surface area, and surface charge are all essential factors, with smaller particles translocating more easily. Several *in vitro* studies have investigated the internalization and translocation of polystyrene NPs in intestine cell monocultures and more complex human intestinal cell models. Walczak et al. showed in 2015 that the translocation of NPs across the intestinal barrier is dependent on their size, charge, and surface chemistry.<sup>[102]</sup> However, the surface chemistry seems more important, as the two types of negatively charged NPs investigated showed a greater than 30-fold difference in translocation.<sup>[103]</sup>

### 3.2. Cellular Barriers

Once nanomaterials have overcome the tissue barriers and reached their target cells, or if they interact with cells at the tissue barrier itself, several other barriers remain, including the outer cell membrane and the intracellular membranes surrounding the different compartments. The cell membrane consists of a phospholipid bilayer containing various lipids, carbohydrates, and membrane proteins, which regulate the entry of small and large molecules into the cell and are held together mainly by noncovalent interactions.<sup>[104]</sup> In cell membranes, the lipid molecules are arranged as an  $\approx 4\text{--}5$  nm thick, continuous double layer that is not rigid but rather dynamic, serving as a relatively impermeable barrier to the passage of most water-soluble molecules.<sup>[105]</sup> The fluidity of the phospholipid bilayer results in changes in the arrangement of the different components into a nonhomogenous distribution pattern, described as the fluid mosaic model by Singer and Nicolson in 1972.<sup>[106]</sup> Different cellular uptake routes exist for macromolecules or materials entering a cell, such as passive diffusion through the membrane, transport-mediated uptake via transmembrane proteins serving as pumps or channels, or catalyzing membrane-associated reactions and vesicular uptake mechanisms, including endocytotic processes such as pinocytosis and phagocytosis.<sup>[107–109]</sup>

Specific targeting of a diseased tissue or cell represents a major challenge for effective nanomaterial formulations. Targeting strategies involve either passive targeting, by the enhanced permeability and retention (EPR) effect through the increased permeability in the cancer vasculature, or active targeting, via receptor–ligand-mediated interactions for cell binding, or direct intraarterial injection into the diseased area.<sup>[110]</sup> A more detailed overview about the EPR effect for macromolecular therapeutics can be found in the review by Maeda et al.<sup>[111]</sup> Subsequent to internalization by cells, nanomaterials are eventually transported through endocytic vesicles to the lysosomes. The lysosomal compartment is a low-pH environment, which may lead to potential degradation of

ingested nanomaterials; however, it also provides new opportunities such as the possibility of theranostic approaches or controlled or triggered drug release.<sup>[112]</sup> Carbon nanotubes (CNTs) show great potential as pH-sensitive nanocarriers in cancer therapy, as this nanomaterial shows enhanced release of conjugated drugs in low-pH environments. Consequently, with the help of CNTs an anthracycline drug like doxorubicin selectively becomes effective in the extracellular environment of tumors that show low pH or inside the lysosomal compartment of cancer cells following targeted uptake.<sup>[113,114]</sup> Various strategies are employed to address this issue, such as the implementation of fusogenic peptides or pH-sensitive nanomaterials.<sup>[115]</sup> Endosomal escape is one of the key challenges for the clinical application of therapeutic drug delivery to target cells with subsequent access to other compartments, e.g., mitochondria or cell nuclei. However, with the development of medical science, the organelle-specific delivery of bioactive molecules has become more important for achieving maximum therapeutic effect with minimum side effects and has emerged as a new research field for the development of future drug delivery systems.<sup>[116]</sup> Mitochondria are one of the main classes of organelles that mediate apoptosis. Their dysfunction can cause neurodegenerative and neuromuscular diseases, diabetes, obesity, and cancer.<sup>[117–119]</sup> Mitochondria are composed of two membranes, featuring a high membrane potential across the inner membrane and a protein import machinery at the outer membrane, both features being used as possible targeting strategies.<sup>[120]</sup> The nucleus presents a further important intracellular barrier, but nevertheless constitutes a popular target for drug delivery systems as it regulates gene expression and other cellular processes.<sup>[121,122]</sup> A range of drugs act on the DNA level, preventing its replication and decreasing or inhibiting gene transcription. The major barrier for nanomaterials targeting the nucleus is represented by the nuclear membrane pores, which prevent entry of NPs larger than 9 nm.<sup>[123]</sup>

## 4. Cellular Uptake and Fate of Nanomaterials

### 4.1. Nanomaterial Uptake

The uptake of nanomaterials by mammalian cells occurs mainly via endocytotic pathways. Two types of endocytosis are distinguished: pinocytosis (“cellular drinking”) involves the ingestion of fluid and molecules via small vesicles ( $<0.15$   $\mu\text{m}$  in diameter), whereas phagocytosis involves the ingestion of large particles, such as microorganisms and cell debris, at formations of large vesicles called phagosomes (generally  $>0.25$   $\mu\text{m}$  in diameter) (for reviews see refs. [124,125]). The term pinocytosis includes macropinocytosis, clathrin- and caveolin-mediated endocytosis, and clathrin- and caveolin-independent endocytosis.<sup>[124]</sup>

Phagocytosis is carried out by professional phagocytes (i.e., monocytes/macrophages, neutrophils, and dendritic cells), which form intracellular phagosomes. Macromolecule or particle internalization is initiated by the interaction with specific receptors on the surface of the phagocyte. This leads to the polymerization of actin filaments at the site of ingestion, i.e., membrane ruffling, and after internalization the

phagosome matures by a series of fusion and fission events with components of the endocytic pathway, culminating in the formation of the mature phagolysosome.<sup>[126]</sup> Macropinocytosis triggers actin formation and the macropinosomes form large intracellular vesicles. However, instead of invaginating a ligand-coated particle, they collapse onto and fuse with the plasma membrane to generate large endocytic vesicles called macropinosomes, which sample large volumes of extracellular milieu.

Caveolin-mediated endocytosis is mostly used for the transport of serum proteins. Caveolae are static, flask-shaped invaginations of the plasma membrane that are slow in uptake and are observed in several cell types, including capillary endothelium, type I alveolar epithelial cells, smooth muscle cells, and fibroblasts.<sup>[124]</sup> This mechanism is generally connected to cholesterol-rich microdomains, called rafts, with a diameter of 40–50 nm.<sup>[127,128]</sup> Clathrin-mediated endocytosis is very well studied and is, like most pinocytic pathways, a form of receptor-mediated endocytosis, which is in general very fast. It occurs in all mammalian cells and carries out the continuous uptake of essential nutrients, such as the cholesterol-laden low-density lipoprotein particles that bind to the low-density lipoprotein receptor and iron-laden transferrin that binds to transferrin receptors.<sup>[129,130]</sup>

The endocytosis of (nano)materials is not just one mechanism, and depends on the physical interaction of the material with the cell wall, the material itself, and also the cell type. Different nanomaterial properties, such as size, shape, material, and surface coating, have an impact on which uptake mechanism will be activated.<sup>[108,131,132]</sup> In addition, the cell type plays a significant role since each cell type might have different uptake mechanisms and can react differently to nanomaterials.<sup>[133,134]</sup>

All of the previously presented endocytic pathways have at least one aspect in common: that the internalized particle is ultimately located in an intracellular vesicle. However, studies have reported that the intracellular localization of nanomaterials of different materials is not membrane-bound, thus indicating alternative pathways for particles to enter cells.<sup>[135–138]</sup> Among other possible mechanisms, passive diffusion through membrane pores and passive uptake by van der Waals or steric interactions (subsumed as adhesive interactions) are suggested by the authors of these studies.<sup>[139]</sup> However, it is not yet known which chemical and physical properties of the cellular membrane and particles are responsible for the translocation of nanomaterials into cells, the nucleus and organelles, either *in vitro* or *in vivo*. It is, however, important to mention that the localization of nanomaterials in the cytosol is only rarely observed and the majority of nanomaterials are found inside vesicular structures.

## 4.2. Endosomal Maturation

After the cellular uptake, nanomaterials end up in endocytic vesicles that fuse together to form early endosomes (EE). There, a complex machinery sorts the vesicles according to the type of the internalized materials and membrane-associated proteins to mature either into k, translocation or degradation vesicles. EE allow for  $\approx 10$  min to fuse with other endocytic vesicles, and during this time the membrane and internal fluids are

constantly recycled, while the cargo (such as nanomaterials or other particles, e.g., viruses) is retained inside.<sup>[140–143]</sup> The material that stays inside the vesicle is then destined to end up in the lysosome. This occurs by the maturation of the EE into late endosomes (LE), which starts by association of cytosolic proteins, the so-called retromer, with the outer surface of the EE membrane.<sup>[144]</sup> These proteins, with Rab5 being the major factor, are also important markers for clear identification of endosomal vesicles and can also be used to show nanomaterial internalization in endosomes by colocalization studies.<sup>[145,146]</sup> During this maturation, the EEs are constantly exchanging vesicles with the trans-Golgi network (TGN), which sends bidirectional exchange crucial proteins for the lysosomal digestion system, such as hydrolases or membrane-attached transport proteins, into the degradation pathway.<sup>[147]</sup>

The formation of the so-called intraluminal vesicles begins already in EE.<sup>[148]</sup> This vesicle formation is driven by the endosomal sorting complex required for transport (ESCRT). A machinery consisting of four main proteins (ESCRT 0–III) and other associated proteins sorts membrane-bound proteins according to their ubiquitination state.<sup>[148,149]</sup> It has been shown that only a minor fraction of the uptaken cargo can be excreted again into the extracellular space via slow/fast recycling endosomes and by this bypassing the possible lysosomal degradation.<sup>[150]</sup>

During the whole endosomal maturation process, the transport of vesicles between the endosome and the TGN is very important as it promotes the maturation by removal of endosomal components while delivering lysosomal parts into the vesicle. Additionally, the vesicles initially formed at the cell membrane travel to the perinuclear area along the microtubule (MT) network (MN) propelled mainly by a dynein-driven translocation. This translocation can be observed by live cell imaging, by tracking particles that colocalize with endosomes along the microtubular network.<sup>[151–153]</sup>

While the exact process of LE formation is not yet clearly understood, it is clear that LEs have very little in common with EEs. The dominant marker Rab5 is exchanged by Rab7 and the internal pH is decreased to around 5–6, which is achieved by proton pumps that influx  $H^+$  ions into the vesicle against the concentration gradient by hydrolyzing adenosine triphosphate (ATP).<sup>[154]</sup> During this maturation the LEs fuse with each other to form larger structures and finally combine with preexisting lysosomes to form the so-called endolysosomes. After this final fusion, the majority of the endosomal components are degraded and the lysosomal parts are preserved.<sup>[155]</sup> This preservation is achieved by protecting the lysosomal-facing membrane part from degradation by excessive glycosylation.<sup>[156,157]</sup> This results in lysosomes being able to then be specifically marked using antibodies against lysosomal-associated membrane proteins.<sup>[158]</sup> The fusion of endosomes with lysosomes is essential as the transport of freshly produced lysosomal components to lysosomes is only achieved during this fusion and for a few subsequent minutes, as transports between the TGN and mature lysosomes have never been observed.<sup>[157,159]</sup> The whole process of endosomal maturation is summarized in **Figure 2**.

The reviews of Huotari and Helenius and Hu et al., respectively, contain more detailed descriptions of endosomal maturation and the endosomal–lysosomal system.<sup>[159,160]</sup>

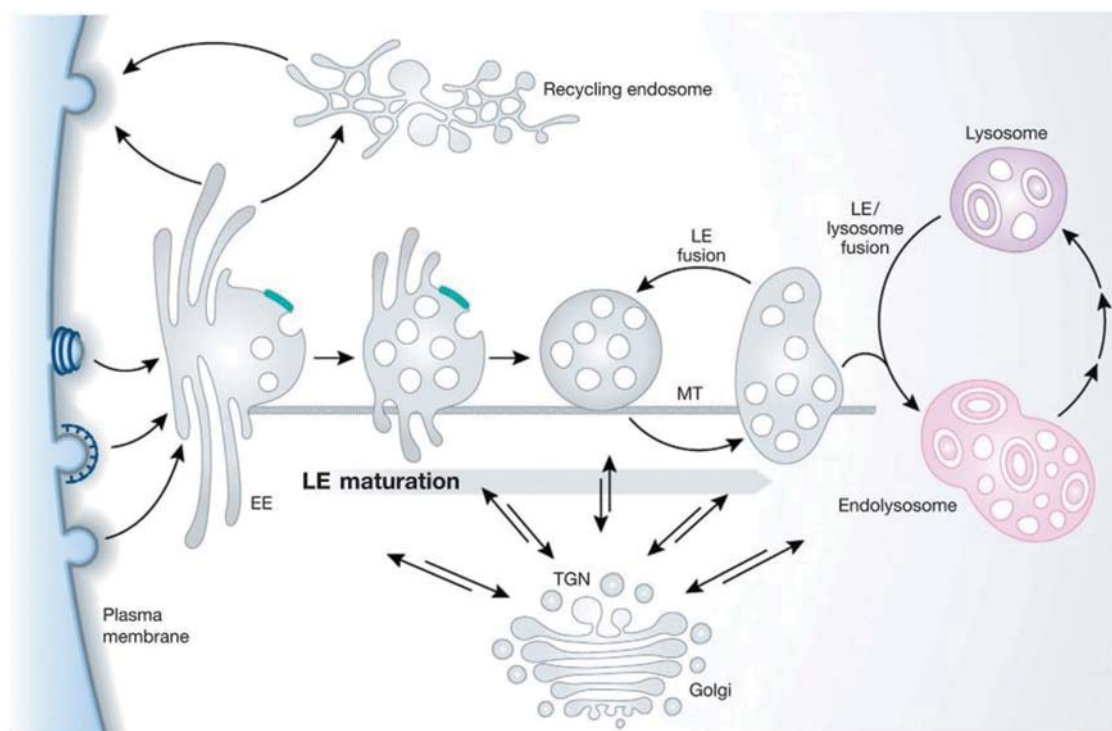


**Figure 2.** Endosomal maturation: After endocytosis, the endosomes travel along the microtubule (MT) network to the inner part of the cell. The constant exchange of cargo and membrane components with the trans-Golgi network provides the essential proteins for the endosomal maturation. In the end, the late endosome fuses with a lysosome to form an endolysosome, which delivers essential lysosomal components to the lysosome. Reproduced with permission.<sup>[159]</sup> Copyright 2011, John Wiley & Sons.

#### 4.3. Degradation of Nanomaterials in Lysosomes

The degradation of nanomaterials inside the cells can mainly be attributed to the harsh environment found in the lysosomes.<sup>[161–164]</sup> Inside the lysosomal compartment, nanomaterials are exposed to an acidic pH (between 4.5 and 5), high ionic strength, and up to 50 different degrading enzymes. These acid hydrolases can degrade biomolecules such as DNA, RNA, proteins, lipids, and polysaccharides.<sup>[154,165,166]</sup>

Proteases, for example, cathepsin L, an unspecific protease that cleaves up to a third of the entire human proteome, have been identified to degrade the protein corona that can be attached to the nanomaterial surface as well as peptides conjugated onto the surface of AuNPs.<sup>[167,168]</sup> Wang et al. showed that human brain astrocytoma cells were protected from the toxic effects of cationic NPs by this protein corona. Only when the corona was degraded in the lysosomes did the NPs induce a loss of lysosomal integrity, followed by a release of lysosomal components into the cytoplasm leading to a cathepsin-induced apoptosis. Ma et al.<sup>[169]</sup> showed that the degradation speed of the protein corona is dependent on the corona composition. The authors compared the effects of AuNPs coated with either human serum albumin, human  $\gamma$ globulin, or human serum fibrinogen on cell viability. They reported that the same particles with different corona provoke different biological responses, suggesting that both the speed and the cytotoxic effect can vary when different protein corona are present.

It has also been reported that enzymes in the lysosomes can dissolve the polymer coatings often used to stabilize the nanomaterials and/or to add a specific functional surface. This phenomenon has been shown by Kreyling et al. in 2015, who used radiolabeled AuNPs coated with a radiolabeled indium polymer shell.<sup>[170]</sup> They showed in vitro that the particles ended up in endosomes and lysosomes after endocytosis. There, a separation between the inorganic gold core and the organic polymer coating was observed. In an in vivo study they showed that the particles accumulated in the liver, where they were endocytosed and processed in the lysosomes of liver cells. Subsequently, parts of the digested polymer shell were exocytosed, then filtered by the renal system, and finally excreted via the urine.

In addition to the digestion of protein coronas or surface modifications of nanomaterials in lysosomes, the dissolution of metal oxide NPs has also been shown.<sup>[171,172]</sup> In 2015 Jiang et al. published a report showing a time-dependent dissolution of AgNPs, subsequent to their endocytosis into epithelial cells.<sup>[173]</sup> The authors compared the Ag particle/Ag ion ratio in media at pH 4.5, simulating the environment inside lysosomes, and the media at pH 7, to the ratio of AgNPs and Ag ions found in the cell cytoplasm. They reported that the major fraction of the particle dissolution was probably caused by enzymes. This conjecture was based on the fact that only 7.5% of the total Ag was dissolved into ions when incubated in acidified media, in contrast to the dissolution of up to 80% of the total Ag after endocytosis by epithelial cells. Similar effects were also observed for other metal-containing NPs such as Zn, Fe, and Au NPs.<sup>[174]</sup>

In contrast, a number of other nanomaterials, such as mesoporous silica NPs, have been found to be degraded in a phosphate buffered saline (PBS) solution in the absence of degrading enzymes.<sup>[175,176]</sup> The composition of the degradation media (pH, flow, protein content, etc.) plays a crucial role in the degradation kinetics of any nanomaterial.<sup>[177]</sup> Additionally, the properties of the nanomaterials themselves, such as porosity and surface oxidation, have a great impact on their degradation speed. An in-depth discussion of silicon-based particles is included in the review of Croissant et al.<sup>[177]</sup> The clearance of silicon nanomaterials is addressed in Section 7.5 of this review.

#### 4.4. Exocytosis

While endocytosis of nanomaterials has been intensively investigated in recent years, there are only a limited number of reports showing exocytosis of nanomaterials. Two pathways of exocytosis have been described, one constitutive and one that is regulated.<sup>[157,178]</sup> Constitutive exocytosis is observed in all cell types. Proteins are secreted by being packaged into transport vesicles in the Golgi apparatus and then transported to—and incorporated into—the plasma membrane. The regulated pathway is found in cells that are specialized for secreting their products, such as hormones, neurotransmitters, or digestive enzymes. This process is performed rapidly and on demand, which is often triggered by an influx of  $\text{Ca}^{2+}$  ions. To study exocytosis, it is possible to incubate cells at 4 °C or to expose them to different chemical inhibitors such as sodium azide or drugs that inhibit lysosomal exocytosis.<sup>[174,179,180]</sup> There may also be an eventual loss of the total nanomaterial load per cell as a result of mitotic division, nanomaterial exocytosis, and/or transcytosis (for reviews see refs. [132,181,182]).

It has been shown that endocytosis and exocytosis are coupled, and can stimulate or compensate for each other.<sup>[179]</sup> Furthermore, endocytotic processes occur much faster than exocytotic routes, where the excretion rate even decreases with increasing particle size, as shown for 14, 50, and 74 nm AuNPs in HeLa cells.<sup>[183]</sup> It is also known that many parameters, such as the cell type,<sup>[184]</sup> nanomaterial properties (i.e., size, surface, and shape), and their applied concentration and exposure time, can affect exocytosis significantly (for a review see ref. [185]). Since the nanomaterial surface can change during uptake and lysosomal processing, the exocytosed NPs may also exhibit a different surface and therefore recognize different targets or receptors on the cellular surface.<sup>[185,186]</sup>

### 5. Biodistribution and Biokinetics

The activity of any nanomaterial at the tissue or cellular level is dependent on the rate and extent of the material absorption, distribution, metabolism, and elimination (ADME) (Figure 3). In nanoscience, these processes are referred to as biokinetics, i.e., uptake, biodistribution, and elimination.<sup>[187,377]</sup>

The physicochemical properties of nanomaterials can differ quite a lot from their bulk materials as they inherit a vastly different volume-to-surface ratio.<sup>[188]</sup> These differences not only affect the biodistribution but also the biodegradation

rates observed in vivo. For soluble nanomaterials, the degradation products, mostly ions, share the same fate as their corresponding chemical solutes.<sup>[189–191]</sup> This leads to a systemic distribution, but also includes local retention in tissues or cells. In brief, the biodistribution of nanomaterials is controlled by many factors, such as size, surface properties, and dissolution rate of the nanomaterial, as well as tissue- or organ-dependent

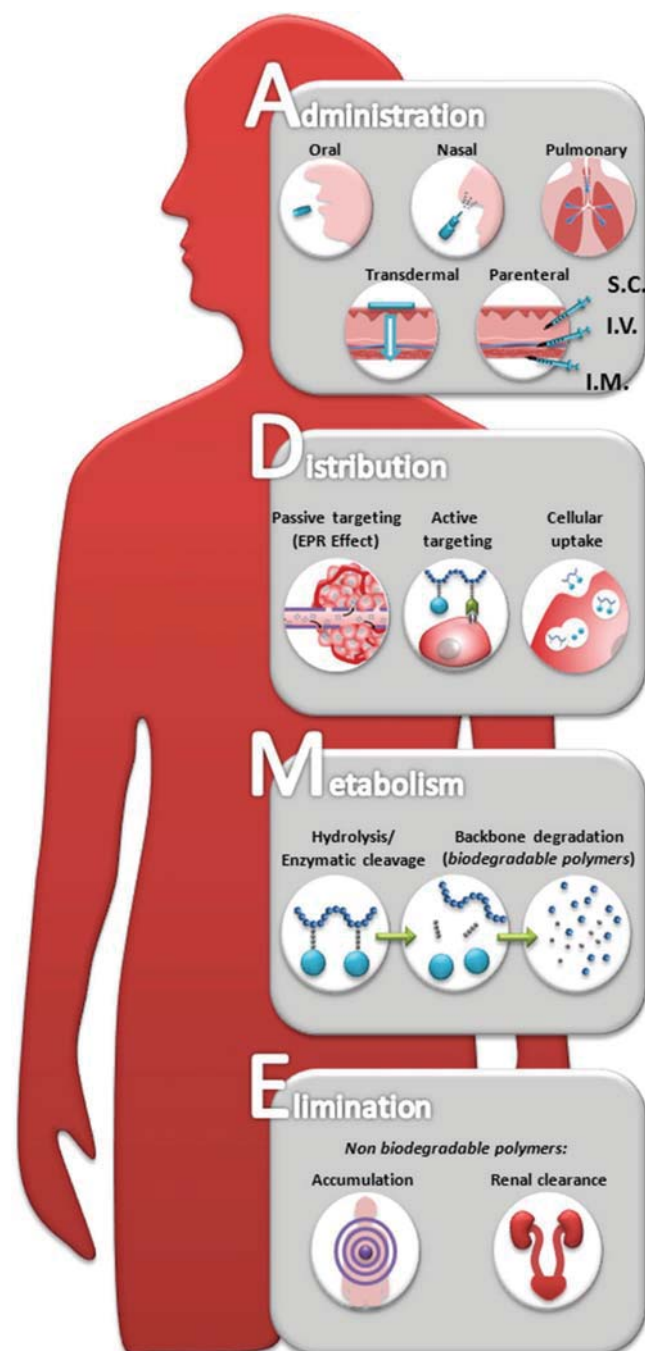


**Figure 3.** The biokinetics of nanomaterials: ADME stands for administration, distribution, metabolism, and elimination, and describes the common path all drugs follow when administered. A detailed understanding of the ADME is important to bring new medicines in the market. Reproduced with permission.<sup>[377]</sup> Copyright 2012, Elsevier.

factors such as permeability or barrier tightness.<sup>[192–194]</sup> In general, after inhalation, oral exposure, or intravenous injection, nanomaterials can be found in the liver, spleen, kidneys, bone marrow, the central nervous system (CNS), and local and systemic lymph nodes.<sup>[162,194–196]</sup> Therefore, studies focusing on the biokinetics of nanomaterials should include these organs in their screening, in addition to their specific targeted organs.<sup>[186]</sup> To perform an accurate dosimetric risk extrapolation, it is necessary to accurately correlate the effects to the retained drug dosage.<sup>[197,198]</sup> The guidelines for designing and testing new materials or drug delivery systems should include retention kinetics in the targeted organs or tissues as well as the adverse or beneficial effects observed there.

The effect of the different protein coronas that form in primary or secondary organs, which has been reported by various *in vitro* studies, is yet to be confirmed by appropriate *in vivo* studies.<sup>[169]</sup> The lack of such studies makes it difficult to evaluate the effects of the different corona on particle distribution or cell interactions as *in vitro* data often fail to accurately foresee *in vivo* results.<sup>[199,200]</sup>

The systemic biokinetics of a nanomaterial depends not only on the physicochemical properties of the nanomaterials but also on their biodurability/biodissolution and the point of entry. Biodurability has been defined as the tendency to resist dissolution and biotransformation within biological and environmental media, which in turn may lead to bioaccumulation of nanomaterials.<sup>[189,201]</sup> Thus, this definition of biodurability essentially measures the dissolution rate of nanomaterials in all types of media and physiologically relevant solutions such as lysosomal fluid.

The route of exposure is also an important factor. The biokinetics and biodistribution of nanomaterials following intravenous exposure is different from the biokinetics/biodistribution of nanomaterials administered to the respiratory tract as described earlier.<sup>[101,202,203]</sup> In addition, a very recent series of three publications by Kreyling et al. showed that the biokinetics of intravenously injected nanomaterials does not represent a surrogate biokinetic approach for pulmonary or oral routes of exposure.<sup>[204–206]</sup> The authors employed 70 nm radiolabeled TiO<sub>2</sub> NPs containing <sup>48</sup>V in rats to study the biokinetics and biodistribution in various tissues over the period of 1 h to 28 d. After intravenous injection, the highest titanium accumulation was found in the liver, followed by the spleen, carcass, skeleton, and blood after 1 h, after which the blood content decreased rapidly, while the distribution in the other organs and tissues remained constant until day 28. After oral administration, the predominant fraction was cleared via fecal excretion, whereas 0.6% of the administered dose translocated across the GI tract and was finally found in liver, lung, kidney, brain, spleen, uterus, and skeleton. The exposure via intratracheal instillation resulted in a 4% translocation rate of the initial administered dose after 1 h and was retained mainly in the carcass, and this percentage decreased to 0.3% after 28 d. The organ fractions in the liver and kidneys remained constant. The clearance from the lungs via the larynx increased from 5% to 20% for all translocated/absorbed particles.

Physiologically based pharmacokinetic (PBPK) models have been developed that can accurately predict such relationships, and most of these models describe the fate of intravenously

injected nondegradable nanomaterials.<sup>[207,208]</sup> It has been shown that the most important factors are the physicochemical properties of the nanomaterials (e.g., size and shape), blood/tissue coefficients of permeability, as well as the phagocytotic uptake by macrophages.<sup>[209]</sup> For the lung, a novel two-step approach to assess the biokinetics of inhaled nanomaterials has recently been presented. For this purpose, the translocation kinetics of aerosolized gold nanoparticles across the epithelial tissue barrier was assessed *in vitro*, and then in a second step the distribution to secondary organs was predicted with a PBPK model.<sup>[210]</sup>

## 6. Mode of Clearance

Nanomaterials entering the vascular system can interact with cells from the blood circulation but will most probably be further distributed to peripheral organs. The distribution to peripheral organs, and especially their clearance, is highly dependent on their physicochemical properties, particularly their size and surface structure/modifications. Understanding the biodistribution and possible subsequent clearance from the body is of paramount importance for their further application. However, nanomaterials that are not efficiently cleared from the body have a higher probability of interacting with cells, tissues, and organs and accumulating in the body due to their prolonged circulation time. Clearance of nanomaterials from the body can happen via different pathways. Renal clearance is the most effective excretion, but due to the related size restrictions (6–8 nm) many nanomaterials cannot be efficiently cleared via this route and undergo biliary excretion where nanomaterials are processed by the liver and become excreted via the GI. Mucociliary clearance in the upper airways can be closely correlated with GI clearance, as nanomaterials trapped in the mucus are typically transported to the pharynx and then swallowed. While clearance via the kidneys and liver can occur over a timescale from 30 min to a few days, nanomaterials that have been internalized by mononuclear macrophages can persist for a long time, trapped within the RES. The following section provides a brief overview of the potential clearance pathways (from the fastest, i.e., renal to the potentially slowest, i.e., RES) and considerations relevant to nanomaterial excretion. An overview of the clearance organs is found in **Figure 4**.

### 6.1. Renal Clearance

The kidneys are involved in a number of crucial physiological functions, such as the regulation of blood (ionic concentration, pH, volume, pressure, and osmolarity), production of hormones, and the excretion of foreign substances and waste.<sup>[211,378]</sup> Following administration and their entrance to the vascular circulation, nanomaterials can be efficiently excreted through the kidneys along with the urine. This form of clearance strongly depends on the size of the materials. Renal clearance is favorable as it requires minimal interaction and metabolism within the body, which reduces possible toxic effects.<sup>[212]</sup> Although beneficial from a toxicological aspect, renal clearance significantly limits the circulation time of nanomaterials, which can have an impact on their efficacy. The excretion of substances and



**Figure 4.** Biodistribution of nanomaterials: following administration, nanomaterials can either interact with the primary tissue barriers and translocate into the blood circulation, or be directly injected into the blood from where they can be distributed to peripheral organs. Upon distribution, depending on their properties, nanomaterials can undergo renal (through kidneys, purple), hepatic (through liver, red), mucociliary (through lungs, blue), and gastric clearance (through GI, yellow), or reside within reticuloendothelial system (green).

production of urine is performed by three basic processes of the nephrons and collecting ducts—glomerular filtration, tubular reabsorption, and tubular secretion. Nephrons are the functional units of kidneys, built up by renal corpuscle and tubules, where blood plasma is filtered and the filtered fluid passes through. The renal corpuscle consists of the glomerulus, i.e., capillary network, and the glomerular capsule, i.e., the double-walled epithelial cup that surrounds the glomerular capillaries. Glomerular capillaries have a high surface area and are completely encircled with podocytes. Their particular anatomy allows formation of a “leaky” barrier that is up to 50 times more permeable than in other tissues and can act as a filtration membrane.<sup>[211,213,214]</sup> Substances filtered from the blood pass through the glomerular endothelial cell membrane, basal lamina, and the filtration slit formed by podocytes. At the level of the glomerular endothelial cell, the membrane is porous, with size limitations of  $\approx 70\text{--}100\text{ nm}$ , which prevents filtration of blood cells. At the level of the basal lamina, proteoglycans prevent filtration of larger proteins, while podocyte expansions, i.e., pedicels, form filtration slits and slit membranes with a cutoff of  $6\text{--}7\text{ nm}$ .<sup>[211]</sup> A schematic of the renal filtering system is depicted in **Figure 5**. Due to the slit membrane limitations, filtration of nanomaterials and renal clearance is strongly dependent on the particle’s hydrodynamic size. It has been shown that nanomaterials larger than  $8\text{ nm}$  cannot be cleared and renal clearance is limited to nanomaterials smaller than  $6\text{ nm}$ .<sup>[213–215]</sup> Filtration of intermediate-sized nanomaterials, i.e., between  $6$  and  $8\text{ nm}$ , is dependent on the nanomaterial surface and the surface charge.<sup>[22]</sup> For QDs, it has been shown that the diameter should be less than  $5.5\text{ nm}$  for efficient renal clearance.<sup>[22]</sup> The nanomaterials tend to interact with proteins in the blood, forming a protein corona, which leads to an increased hydrodynamic diameter that can have an impact on the clearance. Furthermore, the fate of the nanomaterials can also depend on the interactions of charged materials within the nephron during filtration.<sup>[213]</sup> Studies have shown that anionic NPs are filtered less successfully than neutral NPs, and even less than cationic ones.<sup>[22,213,214,216,217]</sup>

As previously mentioned, aside from renal filtration and secretion, one of the basic renal functions is renal reabsorption. During this process, most of the filtered ions, and small molecules such as glucose and amino acids, are reabsorbed by epithelial cells of the proximal tubules via specialized pathways, while most of the peptides and proteins are reabsorbed via pinocytosis.<sup>[211]</sup> Resorption of nanomaterials on the level of proximal tubules is still poorly understood or incompletely investigated, and the available data are inconclusive. It should also be noted that several studies exist showing that silica NPs with sizes significantly larger than  $8\text{ nm}$  can be cleared via the urine.<sup>[218–220]</sup> The mechanism is far from fully understood, but a plausible hypothesis suggests that excretion of NPs can occur at the level of the proximal tubules.<sup>[221]</sup>

## 6.2. Hepatic Clearance

After the skin, the liver is the largest human organ and performs a range of functions. It is involved in macromolecule metabolism, storage, production, and conversion of molecules into waste products that can be excreted via the kidneys and

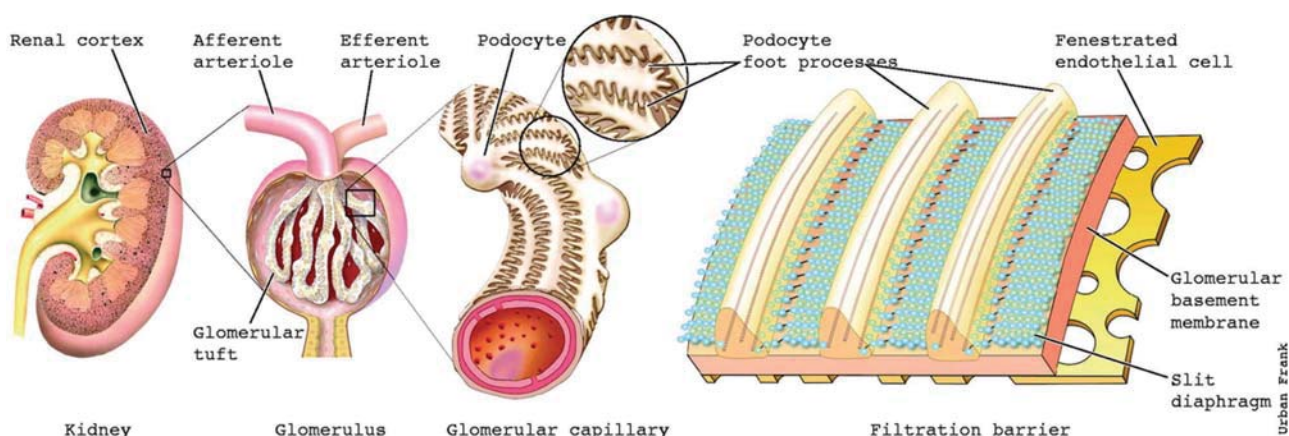


**Figure 5.** Renal filter system: renal filtration and clearance are performed by the glomerular filtration. The glomerulus is the capillary network, and the glomerular capsule is the double-walled epithelial cup that surrounds the glomerular capillaries. Glomerular capillaries are completely encircled with podocytes, which form a filtration membrane. Substances that are filtered pass through the glomerular endothelial cell membrane, basal lamina, and the filtration slit formed by podocytes. Reproduced with permission.<sup>[378]</sup> Copyright 2005, The American Physiological Society.

the intestinal tract.<sup>[211,379]</sup> Hepatic clearance represents the predominant route for the excretion of nanomaterials that cannot be cleared via the kidneys. The liver consists of two lobes separated by the middle hepatic vein. Blood is delivered to the liver via the hepatic artery and the portal vein. The portal vein further delivers blood from the spleen, pancreas, and intestines, while blood is drained via the left, middle, and right veins. This organ consists of specialized epithelial cells, i.e., hepatocytes, phagocytic Kupffer cells, resident immune cells, as well as additional specialized endothelial and epithelial cells (see **Figure 6**). The hepatocytes are the key cells of relevance to the clearance of nanomaterials. These cells excrete nanomaterials into the small intestine via the bile, after endocytosis and enzymatic

breakdown.<sup>[222]</sup> As for the clearance via the kidneys, hepatic clearance is likewise highly influenced by the physicochemical properties of the nanomaterial, i.e., its size, shape, and surface charge.<sup>[215,223]</sup> Upon entrance to the liver via the blood circulation, nanomaterials can also be internalized by the Kupffer cells, which are specialized macrophages in the liver. Kupffer cells can internalize nanomaterials up to several hundreds of nanometers in size by phagocytosis or other endocytotic uptake mechanisms.<sup>[219,224]</sup> Nanomaterials smaller than 200 nm can either pass through or undergo transcytosis in order to interact with abovementioned hepatocytes.<sup>[225,226]</sup> The impact of the surface charge upon cellular uptake has also been postulated. Kupffer cells are efficient in

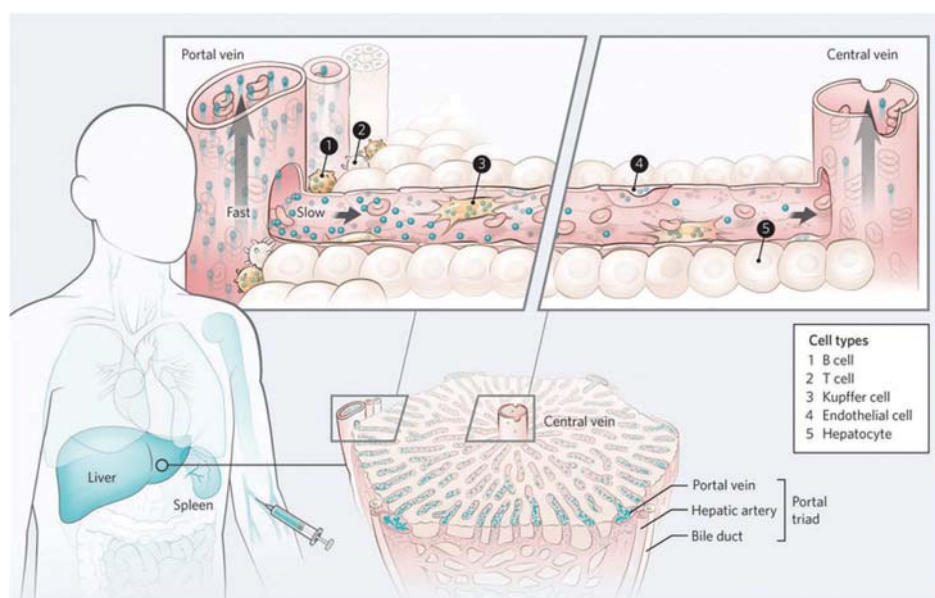


**Figure 6.** Hepatic filter system: the liver consists of two lobes, separated by the central hepatic vein, while the blood is delivered to the liver via the hepatic artery and the portal vein. The liver consists of specialized epithelial cells, i.e., hepatocytes, phagocytotic Kupffer cells, resident immune cells (B cells and T cells), as well as additional specialized endothelial and epithelial cells. Reproduced with permission.<sup>[379]</sup> Copyright 2016, Nature Publishing Group.

the internalization of anionic NPs, while hepatocytes have a preference for cationic NPs.<sup>[226–229]</sup> In general, Kupffer cells are more efficient in nanomaterial removal than hepatocytes; however, it should be noted that only nanomaterials processed via hepatocytes can be cleared through the bile and gastrointestinal tract, while NPs captured by Kupffer cells remain in the RES.<sup>[230]</sup>

### 6.3. Mucociliary Clearance

As mentioned above, one of the potential exposure scenarios for nanomaterials is inhalation. The further fate of the nanomaterials and clearance depends on the lung compartment in which they have been deposited. The deposition of nanomaterials is size dependent. Larger materials (1–10  $\mu\text{m}$ ) are preferentially deposited in the conducting airways (i.e., trachea and bronchi) with ciliated epithelial cells, whereas smaller materials (i.e., nanomaterials (<100 nm)) are localized in more peripheral lung regions (i.e., alveoli).<sup>[35]</sup> The first line of defense from inhaled materials and the fastest route of clearance is mucociliary transport, whereas penetration into the bronchial conducting pathways and lung periphery epithelium is a slower process.<sup>[231]</sup>

Mucus is secreted by airway epithelial goblet cells and sub-mucosal glands. The mucus is formed by a two-layer mucus blanket over the ciliated epithelium, i.e., a low-viscosity sol layer, covered by a high-viscosity gel layer. Insoluble materials are trapped in the gel layer and are moved toward the pharynx (and ultimately to the GI) by the upward movement of mucus generated by metachronous beating of the cilia. The mucus blanket consists of a surfactant as an outermost layer, mucus, and the proximal periciliary layer. This periciliary layer has a less dense structure and, as proposed in 2012 by Button et al., a very distinct brush structure that enables penetration into the mucin layer and hence efficient beating of the cilia.<sup>[232]</sup> The conducting airways are lined by epithelial cells covered with numerous cilia at their apical side, which are  $\approx 6 \mu\text{m}$  long with a diameter of 250 nm.<sup>[233]</sup> Cilia have microtubulae structures and their movement is generated by ATPases.<sup>[234]</sup> The metachronous ciliar beating moves the mucus to the pharynx together with particulate matter trapped inside it.<sup>[235]</sup> Mucus activity is dependent on the number of ciliated cells and their beating frequency, which can be 10–20  $\text{mm min}^{-1}$  in trachea.<sup>[236]</sup> Mucociliary clearance via the pharynx is the most common clearance route for nanomaterials deposited on the upper airway surface and was first described by Kilburn in 1968.<sup>[235]</sup> Mucin with trapped materials will be directed to the pharynx via ciliar beating and can also be stimulated additionally via coughing, if ciliar beating is insufficient.<sup>[237–239]</sup> The efficiency of the translocation of nanomaterials through pulmonary mucus is not yet fully understood, but it has been shown that nanomaterial mobility in the mucus is dependent on the adhesive or inert properties of the material, as well as on its size.<sup>[240,241]</sup>

The clearance kinetics in the lung periphery is much slower due to the absence of mucociliary action. The nanomaterials either can be eliminated by: (i) phagocytosis and subsequent transport by macrophages, (ii) by alveolar epithelium

translocation into the blood circulation, or (iii) sequestration by dendritic cells and transportation to the draining lymph nodes.<sup>[40]</sup>

### 6.4. Gastrointestinal Clearance

When nanomaterials are either ingested or inhaled, and then cleared via mucociliary clearance, they pass from the mouth into the laryngopharynx. The laryngopharynx continues into the esophagus, which delivers swallowed nanomaterials to the stomach. The stomach connects the esophagus with the duodenum, which is the first part of the small intestine.<sup>[211]</sup> One of the main functions of the stomach is to digest, mix, and store the food until the duodenum is ready for the next digestion steps. Due to its role in digestion, the surface of the stomach is quite complex as it has to provide acids and enzymes for digestion, but at the same time has to protect itself from digestion. For that reason, the surface of the stomach is organized into gastric pits made of surface mucous cells and mucous neck cells secreting mucus, parietal cells secreting hydrochloric acid and intrinsic factor, chief cells secreting pepsinogen and lipase, and finally hormone-producing G cells secreting gastrin.<sup>[211]</sup> In summary, the stomach secretes gastric juice (mainly aqueous HCl), which can induce protein denaturation. This is performed by pepsin, which starts the digestion of proteins, and gastric lipase, which assists in the digestion of triglycerides. The stability and integrity of nanomaterials in the stomach is strongly dependent on their chemical structure. Nanomaterials consisting of proteins, lipids, and acid-sensitive material will already be degraded at this step of the clearance process.

The small intestine has a specially adapted structure for the digestion and absorption of nutrients. Even though the intestine is highly efficient in absorption and digestion due to its length ( $\approx 3 \text{ m}$ ), its performance is additionally increased and optimized by the formation of folds, villi, and microvilli structures that significantly increase the surface area. As previously mentioned, nanomaterials that have been internalized by hepatocytes are typically excreted via bile to the intestines, and can either be translocated across the intestinal barrier or excreted from the body via feces.<sup>[230]</sup>

### 6.5. The Reticuloendothelial System

The term RES is used to describe the group of phagocytic cells, i.e., monocytes, macrophages, dendritic cells, and neutrophils, which form a network or a reticulum in different organs, whereas “endothelial” refers to their proximity to the vascular endothelium.<sup>[242]</sup> One of the main functions of this system is the sequestration and clearance of materials found in the blood and lymph nodes.<sup>[211]</sup> The RES predominantly spreads across the liver and spleen, although cells of the RES can be found in all major organs. The liver is considered to be the major part of the RES and its residing macrophages, i.e., Kupffer cells, are crucial for RES function.<sup>[211]</sup> It is interesting to note that Kupffer cells were isolated by Rous in 1933 by injecting magnetic particles intravenously and following the phagocytosis by Kupffer cells.<sup>[242,243]</sup> Cells belonging to the RES are also found in the lungs, where airway and alveolar macrophages perform

phagocytosis of inhaled foreign materials.<sup>[40,211]</sup> The existence of microglia cells in the brain is also an indicator of how vital the cells of the RES are for the function of all organs. These cells have been shown to be able to both phagocytose and migrate,<sup>[242,244]</sup> although they do not often come in contact with particles due to the tight BBB. In general, tissue-resident macrophages originate from precursors that arise during embryonic development and are maintained through self-renewal, independent of adult hematopoiesis. However, during inflammatory response, blood monocytes may enter the tissue and differentiate into monocyte-derived macrophages.<sup>[245]</sup> In general, nanomaterials can be removed by the macrophages, which function as sentinels at all epithelial tissue barriers in the human body. Nanomaterials with a protein corona on their surface, and more specifically those tagged for opsonization, are prone to this type of clearance.<sup>[246]</sup> Once they are in phagocytes, nanomaterials will be processed and degraded in the lysosomes when possible. Chemically inert nanomaterials will remain in intracellular compartments until sequestered at the level of the spleen and liver, making their clearance significantly slower.<sup>[215,223,247,248]</sup> Even the death of the cells does not necessarily mean that the nanomaterials will be cleared because the cell debris (including the nanomaterials) can be collected and taken up by other phagocytes, resulting in chronic persistence. In general, dead cells are promptly recognized and cleared after efficient signaling, which includes signals by which phagocytes are attracted and stimulated to engulf dead cells. Dead cells engulfed by phagocytes are then digested.<sup>[249,250]</sup>

The RES is usually closely correlated with the long-term fate of nanomaterials in an organism, as nanomaterials captured by these cells persist for a long time in RES organs, especially if nanomaterials do not undergo degradation in the lysosomes and/or exocytosis.

The surface charge and hydrophobicity of nanomaterials also represent a key feature for overcoming rapid clearance and prolonging circulation lifetime, which is often desired for drug delivery systems. The overall interactions of nanomaterials with biomolecules are highly dependent on the size and the surface of nanomaterials, as previously demonstrated in several studies by Dawson and co-workers.<sup>[76,77,82]</sup> Nanomaterials with positively charged surfaces show high binding affinity to negatively charged molecules found in the blood, such as serum proteins and sugar moieties from cell membranes. In contrast, neutral and negatively charged particles show reduced binding to serum proteins, leading to prolonged circulation time.<sup>[251]</sup> It has been shown that surface modifications using the synthetic polymer polyethylene glycol (PEG) and “self” peptide CD47 induce a reduction of the clearance by the RES, resulting in an increase in blood circulation time and better pharmacokinetic properties.<sup>[252,253]</sup>

## 7. Long-Term Fate of Clinically Relevant (Bioinspired) Nanomaterials

For the design and optimization of biomedical nanomaterials it is not only important to address their efficacy *in vivo*, but also to investigate their fate and possible clearance. In particular, the long-term fate of nanomaterials that are biopersistent and can stay longer in the human body, *i.e.*, from weeks to years, has to

be considered. *In vitro* experiments might be applied to obtain an initial mechanistic insight into uptake, possible degradation and/or release at the cellular or tissue level. However, to understand the long-term biokinetics, *in vivo* experiments are needed.

### 7.1. Liposomes

Liposomes are probably the most commonly used nanomaterials for drug delivery. These are bioinspired vesicles consisting of a phospholipid membrane structure mimicking the cell membrane, and are one of the most frequently applied drug delivery systems due to their biodegradability, low immunogenicity, and toxicity. These vesicles allow the loading of various soluble drugs into the hydrophilic, aqueous center, the lipophilic membrane, or the interface between.<sup>[254]</sup> Being able to incorporate drugs into the liposomes provides the advantage of protecting the active compound from degradation and increases the half-life in the body. A large amount of research has been conducted on this topic since the first description of liposomes in the 1980s.

The first generation of liposomes had short *in vivo* half-lives, being cleared very quickly. In 1985, Scherphof et al. showed that the RES rapidly cleared the intravenously injected liposomes out of the body.<sup>[255]</sup> This finding helped to develop drug formulations to target diseases affecting the RES, such as microbial or parasitic infections.<sup>[256–258]</sup> While the RES does not recognize the liposomes themselves, a number of groups showed that the attachment of certain serum proteins, the so-called opsonins, is the major factor that leads to the rapid clearance of the liposomes.<sup>[259–263]</sup> In contrast to opsonins, dysopsonins have also been identified that help to prevent the phagocytosis and thus increase the liposomal half-life. Furthermore, the complement system is another line of defense the body possesses against liposomes. Most important here is the assembly of the membrane attack complex, which forms lytic pores that lead to the release of the liposomal content.<sup>[264]</sup>

In order to avoid the fast clearance of the liposomes by the RES, other approaches have also been attempted. The first idea was to modulate the size and surface charge. It was found that larger liposomes, such as multilamellar liposomes (MLV) with sizes of around 500–5000 nm, are cleared faster than the smaller single lamellar liposomes (SLV).<sup>[265,266]</sup> In addition to the size, the charge of the liposomes also influences their fate in the body. Negatively charged liposomes are cleared more rapidly from the blood than their neutral counterparts, while positively charged liposomes appear to be toxic and are cleared from the body even faster.<sup>[267–269]</sup> Another method proposed to overcome the fast clearance is to expose the body to empty liposomes prior to the application of the drug-containing derivatives. This would lead to the saturation of the RES and thus longer circulation times for the drug-containing liposomes.<sup>[192,270]</sup>

Second-generation liposomes were then developed by the modification of surface properties, by adding coatings of glycolipids, sialic acid, or PEG around the membrane.<sup>[271,272]</sup> These surface modifications substantially increased the half-life of liposomes and enabled the use of these drug delivery systems for new applications since long-circulating liposomes could profit from the EPR and accumulate in tumors or sites of

inflammation.<sup>[273]</sup> In particular, PEG has already received much attention for its beneficial effects combined with drugs or nano-carrier systems, such as increasing stability and solubility, or decreasing toxicity and antigenicity.<sup>[274,275]</sup> As PEG is a synthetic polymer, the molecular weight and its structure can be modified to fit individual needs. The increased circulation time due to the reduced uptake in the RES is attributed to the reduced interaction of PEG with serum proteins, which is presumably due to steric hindrance.<sup>[276,277]</sup> In 1991, Allen et al. showed that the length or molecular weight of the PEG, and the density of the PEG packing onto the liposomal surface, influence this stealth effect. In general, longer PEG chains and denser packing lead to longer blood circulation times.<sup>[271]</sup> Together with the EPR effect, PEGylated liposomes have now become a commonly used and accepted system for drug delivery, but there are still limitations one has to consider. For instance, the drug release needs to be controlled at the target site, as only the free, released drug is able to diffuse into the cells and there perform its action.<sup>[278,279]</sup> This also results in difficulties in quantification—the ratio of released drug to encapsulated drug determines the efficiency of the system, but the determination of this ratio is challenging.<sup>[280]</sup>

To overcome some of these problems, liposomes have been developed where the PEG coatings are detachable in acidic pH, an environment that has been found in close proximity to tumors, where they are subsequently taken up by the cancer cells.<sup>[281]</sup> Another approach was to conjugate targeting molecules on top of the PEG, instead of simply relying on passive targeting via the EPR effect. These targeting moieties could be specific antibodies, receptor ligands, or other biomolecules.<sup>[282–284]</sup>

Interestingly, Laverman et al. and Ishida and co-workers reported in 2001 and 2008, respectively, that PEGylated liposomes have altered pharmacokinetic behavior after an initial dose if the second dose is administered within a few days of the first dose. They report that the clearance of this second dose happens at a much faster rate than initially expected. This effect is called accelerated blood clearance and has been reported extensively in connection with PEG.<sup>[285–289]</sup> To overcome this issue, PEG has been under heavy investigations and also PEG alternatives were studied. A detailed review about this topic can be found in the review of Knop et al.<sup>[290]</sup>

While this review is focused on the long-term fate of the nanomaterials, there are few reported studies that investigate the biodistribution of the administered liposomes after more than one week. This is somewhat understandable for a number of reasons. First, the detection of liposomes in the body can be quite challenging, as they are vesicles where the composition barely differs from other membranes in the human body (if they are not labeled). When radiolabeled, for example with <sup>111</sup>In, which is commonly used for this purpose, then the question remains if the indium is still in or attached to the liposomes, or if the liposomes are degraded and the indium persists in the body.<sup>[279,291–293]</sup> Another problem is the fast clearance of the liposomes out of the body, as mentioned above. While this is advantageous for some applications, it makes long-term studies of their biodistribution difficult to perform.

The biodistribution at early time points (up to 3 d postadministration) has been extensively studied. For radiolabeled (<sup>186</sup>Re) Doxil (liposomal-encapsulated doxorubicin), Soundararajan et al.

found that 4 h after the intravenous administration to rats, the liposomes were found mainly in the spleen.<sup>[294]</sup> The distribution was found to have changed after 48 h, where they began to be localized in the kidneys. However, the amount of liposomes in the spleen remained constant until 96 h postexposure. The liver seemed not to be a target. This is in contrast to the findings of Chang et al.,<sup>[295]</sup> who reported the biodistribution of PEGylated <sup>188</sup>Re-BMEDA-liposomes in mice to show accumulation in the liver over 72 h. Up to 4 h after the injection, the main load was still found in the blood. The distribution then shifts and most of the liposomes were found in the feces. The liver and the lungs immediately showed some accumulation, but the lung burden was cleared within 24 h, while the liver showed increased values over the whole 72 h period. The spleen began to accumulate the liposomes after 4 h, where it reached similar levels to the liver, while the kidneys showed immediate accumulation, which decreased over the first 24 h. Chow et al. reported the comparison of <sup>111</sup>In-labeled liposomes with either 0.9 or 6 mol% PEG.<sup>[291]</sup> This study again demonstrated the influence of the PEG density on the biodistribution. The authors reported a much higher retention in the blood and accumulation in tumors when the mice were exposed to highly PEGylated liposomes. On the other hand, the accumulation in the spleen, liver, and kidneys was found to be significantly lower.

## 7.2. Micelles

Micelles are monolayers of aliphatic molecules, which means that classically they possess a hydrophobic core, in contrast to liposomes, which have hydrophilic cores. They offer the possibility of incorporating hydrophobic drugs that would not otherwise be soluble under physiological conditions. Commonly used micelles are formed using either synthetic polymers (e.g., polypropylene) or bioinspired polymers like polysaccharides (e.g., cellulose, heparin, and dextran).<sup>[296,297]</sup>

Similar to the liposomes, micelles are quite difficult to detect in the body and require special labeling in order to do so. This has either been done by incorporating fluorescent dyes, metal particles, or radioactive labels.<sup>[298–300]</sup> However, the detection methods for the labels are indirect and after being administered the micelles can potentially separate from their cargo, making the observed biodistribution questionable. These issues have led to a lack of long-term biodistribution data for micelles, as most studies only focus on the first few hours or days.

There are two main factors that influence the fate of micelles *in vivo*, namely their size and degree of PEGylation. In 2015, Wang et al. investigated these influences on the accumulation of micelles in tumors in mice.<sup>[300]</sup> Their findings, which are summarized in **Figure 7**, show that the half-life of micelles increases with size and PEGylation degree, which they define as the mass fraction of the PEG moiety relative to the total block copolymer. However, the half-life, which is at most 15 h, still remains short. The biodistribution analysis in this study only included data from the liver, spleen, and kidneys after 24 h postinjection, suggesting that the clearance is mainly performed by the liver and the spleen, while the kidneys are not significantly burdened.

Ebrahim Attia et al. presented biodistribution data of fluorescently labeled, PEGylated diblock copolymeric micelles up

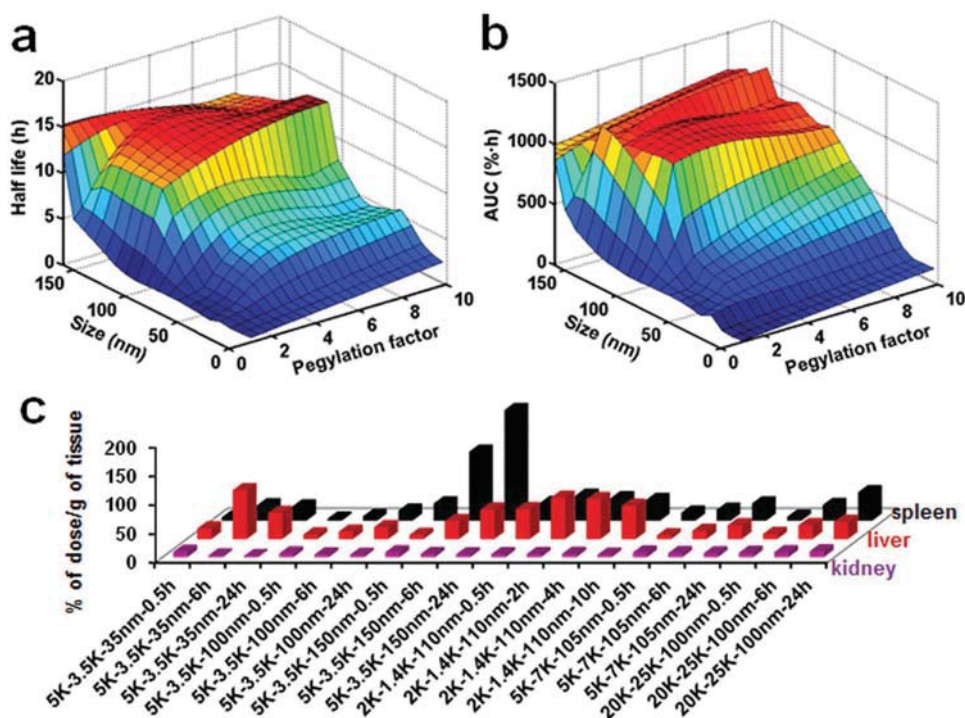


**Figure 7.** Half-life and biodistribution of differently sized and PEGylated micelles: the a) half-life, b) area under curve (AUC), and c) biodistribution of micelles as a function of size and amounts of PEG. Larger micelles with high amounts of PEG stay longer in the circulation and are predominantly cleared by the spleen and the liver, whereas the kidneys are not heavily burdened. All of the experiments were carried out in mice. Reproduced with permission.<sup>[300]</sup> Copyright 2015, American Chemical Society.

to 96 h postinjection in mice.<sup>[301]</sup> Their data suggest, in agreement with Wang et al., that the main load of the micelles is cleared mostly by the liver, and to a lesser extent the spleen. In addition, an accumulation of the PEGylated particles in the tumor tissue was also observed. The kidneys showed only weak fluorescent signals and the heart and the lungs were both below the detection limit for the epifluorescence.

### 7.3. Gold Nanoparticles

Although not strictly bioinspired, gold nanoparticles or nanoclusters are used extensively for medical applications, such as imaging, cancer irradiation therapy, or as drug delivery systems. Their inert properties also make them a reliable tool for biomedical studies.<sup>[302,380,381]</sup> However, the available data on acute toxic effects of these materials are frequently contradictory, with *in vitro* studies variously reporting both cytotoxic effects and no impact.<sup>[303]</sup> The main conclusion that can be drawn from present *in vitro* data is that the measured toxicity strongly depends on the surface modification; however, the biological system, concentration, and application method also have to be considered.<sup>[304]</sup> Concerning *in vivo* toxicity, in 2009 a study was conducted comparing different sizes of noncoated AuNPs. It was found that at a dose of 8 mg kg<sup>-1</sup> per week, particles with diameters of 3, 5, 50, and 100 nm did not have a toxic effect, while 8, 12, 17, and 37 nm sized NPs had severe effects on the mice's health.<sup>[305]</sup> However, concerning the long-term fate of these particles, data are scarce. The studies covered in this

review are summarized in **Table 1**. In a recent study carried out by Wang et al., the influence of the charge of  $\approx 3.5$  nm nanoparticles on retention in kidneys and accumulation in tumor tissue in mice was investigated over a period of 90 d. In all of the tested tissues except the kidneys, there was still a detectable amount of gold present regardless of the charge of the particles.<sup>[306]</sup> Those findings stand in contrast to a study published by Naz et al., who investigated AuNPs with sizes of 2, 5, and 10 nm over 90 d and found a more complete elimination of all sizes in all tested organs.<sup>[307]</sup> The findings of these conflicting studies are summarized in **Figure 8**. With increasing size, the data become more concise: Fraga et al. used 16 nm AuNPs to study their long-term fate in rats.<sup>[308]</sup> The particles were coated with citrate or the pentapeptide CALNN (cysteine–alanine–leucine–asparagine–asparagine), forming a water-excluding layer on the NPs. The authors reported an elimination of gold from almost all tested organs (thymus, heart, lung, kidneys, brain, muscle tissue, small intestine, femur, testis, and blood), a 50% reduction in the liver and spleen, and persistence in the tail. Furthermore, another study investigated the fate of 20 nm AuNPs in rats over a period of two months. The highest relative levels of NPs were found in the liver, spleen, and kidneys. Other tested tissues, such as the blood, small intestine, tongue, adrenal gland, and testis, showed persistent AuNPs concentration, but to a lower relative degree, while the remaining samples (lung, heart, aorta, thymus, esophagus, stomach, cecum, colon, pancreas, bone tissue, muscle tissue, skin, olfactory bulb, frontal cortex, hippocampus, striatum, thalamus/hypothalamus, brainstem, cerebellum, bladder, feces, and urine)

**Table 1.** Long-term biodistribution data on gold-based nanomaterials.

Material	Size [nm]	Animal	Investigated tissue <sup>a)</sup>	Longest timepoint	Reference
Ethanediamine-coated Au NPs	3.2	Mouse	<b>K, TT, Te, Li, L, H, S</b>	90 d	[306]
Ethanedioic-acid-coated Au NPs	3.7				
Au NPs	2 ± 0.5 5 ± 1 10 ± 2	Mouse	<b>Li, S, L, H, K, Br</b>	90 d	[380]
CALNN-coated Au NPs	16	Rat	Th, H, L, K, Br, M, SI, Fa, Te, <b>Bl, Li, S, T</b>	28 d	[308]
Citrate-coated Au NPs					
Au NPs	20	Rat	<b>Li, S, K, Bl, SI, To, AG, Te, L, H, A, Th, E, St, C, Co, P, Bo, M, Sk, OB, FC, Hi, Sa, Th, BT, Cb, Bd, Fa, U</b>	2 months	[309]
Au nanorods	55 × 13	Rat	<b>Fa, M, L, H, Br, K, S, Li</b>	28 d	[227]
Au NPs	40	Mouse	<b>Li</b>	180 d	[223]
CYT-6091 (PEGylated Au NPs containing TNF- $\alpha$ )	27	Mouse	<b>S, Li, K, L</b>	120 d	[311]
PEG stabilized silica coated Au NPs	110	Mouse	<b>Bl, Li, L, S, M, K, BT, Br</b>	28 d	[381]

<sup>a)</sup>E: esophagus; A: aorta; TT: tumor tissue; H: heart; L: lung; K: kidney; Br: brain; M: muscle; SI: small intestine; Te: testis; Bl: blood; Li: liver; S: spleen; T: tail; To: tongue; AG: adrenal gland; St: stomach; C: cecum; Co: colon; P: pancreas; Bo: bone; Sk: skin; OB: olfactory bulb; FC: frontal cortex; Hi: hippocampus; Sa: striatum; Th: thalamus; BT: brainstem; Cb: cerebellum; Bd: bladder; Fa: feces; U: urine; F: femur; and the bold letters indicate that the organ tested positive for nanoparticles.

showed negligible concentration.<sup>[309]</sup> Finally, gold nanorods  $\approx 55$  nm in length and 13 nm in width were tested over a period of 28 d in rats. In feces, bone tissue, muscle tissue, lung, heart, and brain, the gold concentration showed a decreasing trend (but was still detectable), while the concentrations inside the kidney, spleen, and liver either increased or were stable.<sup>[227]</sup> For 40 nm AuNPs, a more extensive study was conducted on mice, revealing similar results: substantial amounts of gold were found in the liver even after 180 d postinjection, supporting the claim that biological systems lack a suitable system for clearing the injected particles.<sup>[223]</sup> Similarly, Goel et al. tested CYT-6091, a prototypal nanomedicine consisting of a PEGylated colloidal gold core 27 nm in size, with TNF- $\alpha$  attached to the surface to target cells present in the tumor interstitium in mice, over 120 d.<sup>[310]</sup> This study supported the persistence of the NPs in the spleen, liver, and kidneys.<sup>[311]</sup> Finally, 110 nm Au-cored NPs with 10 nm silica shells were tracked in mice for up to 28 d. The measurable concentrations of gold in the spleen and liver at the endpoint were also in line with the above studies. In conclusion, the available data point toward a long persistence of AuNPs, especially above a certain threshold of size. Inversely, literature addressing AuNPs below that threshold suggests a rather complete (>70%) and fast clearance via the urine of the animal as it was observed exemplarily for the imaging agent Au@DTDTPA 72 h postexposure by Alric et al.<sup>[307,312]</sup> Therefore, the further investigation of possible chronic implications, especially of AuNPs of greater size, is of utmost importance in order to safely promote the translation of AuNPs to clinical use.

#### 7.4. SPIONs/Iron Oxide

Superparamagnetic iron oxide nanoparticles are currently being extensively investigated for a variety of applications. Because of their particular magnetic properties, they have already been approved as contrast agents in magnetic resonance imaging techniques, and they are also used for hyperthermia-based cancer treatment due to their ability to generate heat when exposed to an alternating magnetic field, as in the case of FDA-approved NanoTherm.<sup>[313–315]</sup> Since SPIONs have already made their way into the clinic, their biological effects have already been extensively investigated, indicating no major signs of acute toxicity.<sup>[316,317]</sup> However, less effort has been put into understanding their long-term fate, but it has been shown that iron oxide can be recycled the same way as the iron oxide present as ferritin in hemoglobin.<sup>[318]</sup> Ferritin consists of an iron oxide core of  $\approx 8$  nm and a surrounding protein shell that increases the hydrodynamic diameter up to 13 nm.<sup>[319]</sup> When red blood cells (RBCs) are aged or damaged they are taken up by macrophages, and the protein shell around the ferritin complex is rather quickly digested by enzymes present in lysosomes. Subsequently, the iron oxide core also dissolves readily in the acidic lysosome and can be reused in the bone marrow to make new RBCs.<sup>[318,319]</sup> It is thought that iron oxide nanoparticles, which end up in lysosomes, are dissolved and recycled similarly to ferritin.<sup>[319]</sup> For instance, Gazeau and co-workers followed iron oxide nanocubes in vivo for a maximum of 14 d by aberration-corrected high-resolution transmission electron microscopy.<sup>[320]</sup> The authors found a stochastic corrosion process to be governing degradation

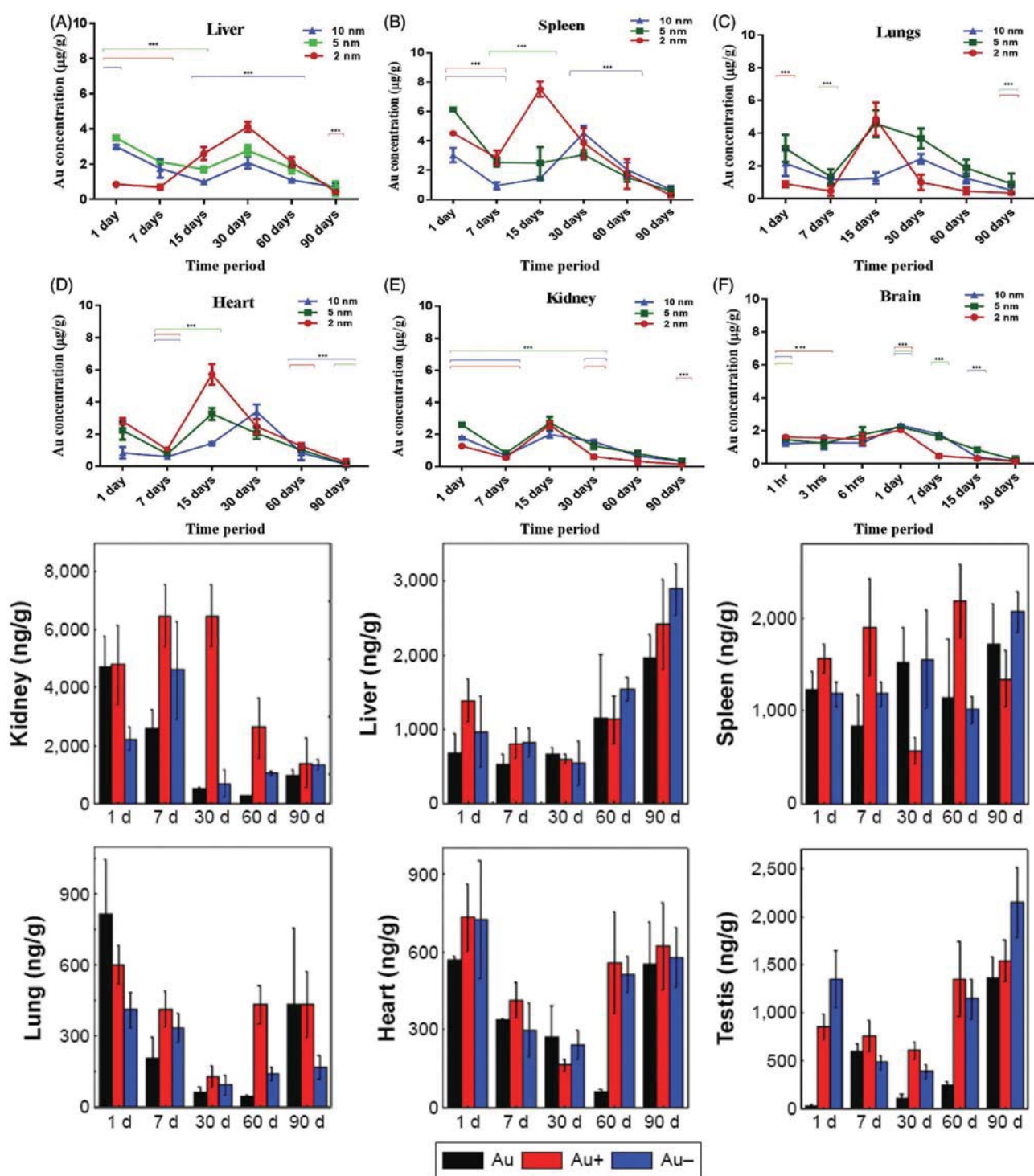


**Figure 8.** Gold nanoparticle biodistribution up to 90 d: graph plots showing results obtained by Naz et al. indicating a substantial clearance of 2, 5, and 10 nm Au NPs after 90 d measured by ICP-AES. The bar plots, on the other hand, depict the results obtained by Wang et al. with ICP-MS. Here, the authors did not observe a clearance independent from the charge of the roughly 3.5 nm Au NPs. Upper panel block (A-F): Adapted with permission.<sup>[380]</sup> Copyright 2016, Taylor & Francis. Lower panel block (bar charts): Adapted with permission.<sup>[306]</sup> Copyright 2016, DOVE Medical Press.

in vivo as well as in vitro, as well as an enrichment in iron-filled proteins close to lysosomes at day 14 postexposure, providing further evidence for the importance of the ferritin pathway for iron oxide NP long-term fate.<sup>[320]</sup> Taking this into account, the

long-term biopersistence of SPIONs in cells or tissue is rather unlikely. Nevertheless, a couple of long-term studies were conducted (as summarized in Table 2): Briley-Saebø et al. investigated rat livers after injection of the commercially

**Table 2.** Long-term biodistribution data on iron-based nanomaterials.

Material	Size [nm]	Animal	Investigated tissue <sup>a)</sup>	Longest timepoint	Reference
Clariscan (monocrystalline SPION)	5.6 ± 1.2	Rat	Li	133 d	[321]
P904 (glucose-derivative-coated maghemite SPIONS)	8	Mouse	Li, <b>S</b>	90 d	[323]
Ferucarbotran (carboxy-dextran-coated multicore magnetite SPION) LS-008 (PEG-coated single-core magnetite SPIONS)	3–5 (26.3 ± 1.5)	Rat	Li, <b>S</b> , <b>Bl</b> , <b>K</b> , <b>L</b> , <b>H</b>	70 d	[324]

<sup>a)</sup>H: heart; L: lung; K: kidney; Bl: blood; Li: liver; S: spleen; and bold letters indicate that the organ tested positive for nanoparticles.

available contrast agent Clariscan over a time frame of 133 d postinjection.<sup>[321]</sup> Even though the plasma half-life of the compound was determined to 50 min at the highest administered concentration in pigs,<sup>[322]</sup> in the rat liver the study found longer half-lives by relaxometry, a technique to analyze magnetic particles.<sup>[321]</sup> In the same study, the concentration of Clariscan dropped below the detection limit of inductively coupled plasma atomic emission spectroscopy (ICP-AES) after 45 d, but could still be measured by relaxometry.<sup>[321]</sup> This indicates a lack of sensitivity of ICP-based measurements when compared to relaxometry. Furthermore, the study found a strong correlation between clearance time and administered dosage. This is in line with the work of Levy et al., which showed residual characteristic magnetization measured by ferromagnetic resonance and a superconducting quantum interference device after 90 d in mouse liver and spleen, indicating the presence of ferromagnetic nanoparticles.<sup>[323]</sup> Recently, Keselman et al. used magnetic particle imaging (MPI) to study SPIONs over a period of 70 d.<sup>[324]</sup> The authors found that the SPIONs were cleared out of the blood within hours and the liver and spleen showed SPION activity even after 70 d, as shown in **Figure 9**, indicating that SPIONs persist for a long time in the body.<sup>[324]</sup>

### 7.5. Silica

Amorphous SiO<sub>2</sub> NPs, in particular mesoporous NPs, are interesting materials for biomedical applications due to their porosity and high surface area, and hence high drug loading capacity. On the other hand, SiO<sub>2</sub> NPs fall into the category of bioinspired materials, as silicon can be naturally found in the body, in particular in bone, cartilage, and supportive connective tissue. As such it can be used as a supplement or an adjuvant in drug preparation, and it has been approved by the FDA since it is generally regarded as safe. Amorphous silica has been used in drug delivery since 1983.<sup>[325]</sup> Thus far, the only type of silica that has gained approval for human clinical trials by the FDA is the Cornell dots (C-dots), while polysiloxane-based AGuIX (activation and guiding of irradiation by X-rays) nanoparticles have entered clinical trials. AGuIX is a magnetic resonance contrast agent based on gadolinium with a hydrodynamic diameter of ≈3 nm and is used for radiosensitization and multimodal imaging. It has been showed in the mouse model that AGuIX

NP formulations allow efficient renal clearance and a minimized NP localization outside of the kidneys (only 0.2% were detected). After four weeks, most of the NPs are excreted via the kidneys (0.5% of initial dose remains), and the NPs do not undergo degradation.<sup>[326]</sup> Although lanthanide-based NPs show great promise for their safe application in nanomedicine they will not be covered in this review as this subject has been

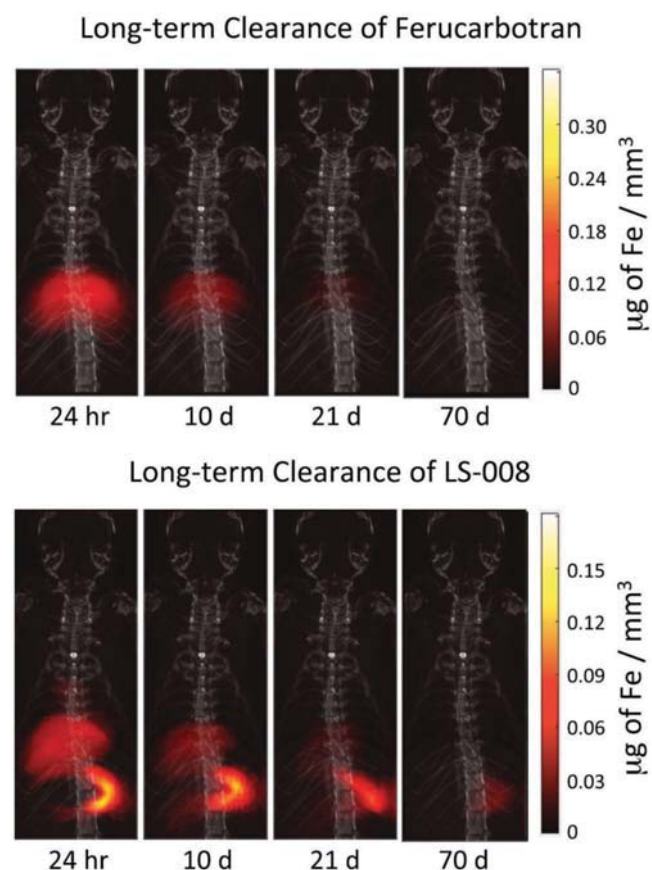


**Figure 9.** Long-term clearance of SPIONs (Ferucarbotran and LS-008) tracked with MPI in rats: even after 70 d, a residual signal could be observed in the spleen and liver, indicating slow clearance for both. Furthermore, LS-008 shows predominant clearance by the spleen, and Ferucarbotran by the liver. Reproduced with permission.<sup>[324]</sup> Copyright 2017, IOP Publishing.

**Table 3.** Long-term biodistribution data on silicon-based nanomaterials.

Material	Size [nm]	Animal	Investigated <sup>a)</sup> tissue	Longest timepoint	Reference
PEG mesoporous SiO <sub>2</sub> NPs; mesoporous SiO <sub>2</sub> NPs	80–390	Mouse and Rat	<b>S, Li, L, K, H</b>	1 month	[331]
<sup>14</sup> C-SiO <sub>2</sub> NPs	33	Mouse	<b>S, Li, L, K, CLN, BM,</b> Br, M, Ad	8 weeks	[221]
<sup>125</sup> I-SiO <sub>2</sub> NPs	20	Mouse	<b>Li, S, L, K, St, Bl, Br, In</b>	30 d	[333]
Rhodamine B SiO <sub>2</sub> NPs	80	Mouse	<b>K, Li, S, Fa,</b> Br, L	4 weeks	[332]
	50				
	100				
Mesoporous hollow SiO <sub>2</sub> NPs	110	Mouse	<b>S, Li, L, K,</b> Br, Te	45 d	[338]
SiO <sub>2</sub> NPs	110	Mouse	<b>Li, S, L, K, In, Fa,</b> M	7 d	[337]
Rod-like SiO <sub>2</sub> NPs-FITC and PEG	185 AR = 1.5 720 AR = 5	Mouse	<b>Li, S, L, Br, K, Bl</b>	18 d	[195]
Cationic mesoporous SiO <sub>2</sub> NPs	80	Mouse	<b>H, L, Li, S, K, St, In, P,</b> Fa, Bd, Te	3 d	[334]
C-dots	10	Human	<b>Pl, U, S, Thy, Pa, K, Li, L,</b> M, Sp, <b>Bd, Br, GI, H</b>	3 d	[329]
AGulX	3 nm	Mouse	Li, Bl, S, <b>K</b>	4 weeks	[326]
<sup>125</sup> I-SiO <sub>2</sub>	115 AR = 1	Mouse	L, Li, S, <b>K</b>	3 d	[336]
	120 AR = 1				
	139 AR = 7.6				
ORMOSIL nanoparticle	20	Mouse	<b>In, Li, K, Sk</b>	15 d	[382]
SiO <sub>2</sub> NPs	20	Rat	<b>Br, K, Li, L, S, Te,</b> Ov	14 d	[339]
	100				
SiO <sub>2</sub> NPs	150	Rat	<b>K, L, H,</b> Li	4 d	[340]
SiO <sub>2</sub> NPs	20	Rat	<b>Pl</b>	28 d	[383]
	100				
SiO <sub>2</sub> NPs (3 different shapes)	85 AR = 1	Mouse	<b>Li, L, S, K, In</b>	7 d	[384]
	175 AR = 5				

<sup>a)</sup>H: heart; L: lung; K: kidney; Br: brain; M: muscle; Te: testis; Bl: blood; Li: liver; S: spleen; P: placenta; Fa: feces; St: stomach; Sk: skin; Bd: bladder; BM: bone marrow; Ad: adipose tissue; CLN: cervical lymph nodes; Ov: ovary; Pl: plasma; In: intestine; U: urine; Thy: thyroid; Pa: parotid; Sp: spine; GI: gastrointestinal tract; AR: aspect ratio; and bold letters indicate that the organ tested positive for nanoparticles.

previously reviewed.<sup>[212,327,328]</sup> The particles consist of fluorescent molecules encapsulated in a silica core that is overcoated with a silica shell, further functionalized with polyethyleneglycol. By attaching peptides that recognize receptors on cancer cells, this hybrid system is primarily used as a cancer diagnostic tool. The main challenges for efficient cancer targeting are the renal clearance and unspecific biodistribution. Due to the small size of C-dots (10 nm) and their specific functionalization (integrin targeting), the nanoparticles are efficiently cleared via the kidneys, and RES uptake has been minimized. C-dots (formulation-<sup>124</sup>I cRGDY-PEG-C dots) have been monitored for their tissue distribution and clearance in humans using quantitative PET imaging, which showed a half-life of 13–21 h mostly due to the fast clearance by the kidneys (90%). The remaining

10% has been postulated to be cleared via hepatobiliary system, taking into account that all hepatic activity is ultimately excreted via the hepatobiliary route.<sup>[329]</sup> A previous mouse study from the same group showed that most of the C-dots (<10 nm) without a PEG coating ended up in the liver, whereas <sup>124</sup>I-cRGDY-PEG-C-dots were cleared by the urinary system.<sup>[330]</sup> Interestingly, C-dots did not show accumulation in the liver, spleen, lung, or bone marrow. These C-dots are currently the only silicon-based nanomaterials approved to be used in humans; however, the long-term fate of the NPs and their biodistribution has so far only been studied in animal models, predominantly in mice and rats (as summarized in **Table 3**). He et al. investigated the effects of PEGylation and size on the in vivo biodistribution of mesoporous silica nanoparticles (see **Figure 10**). In this study,

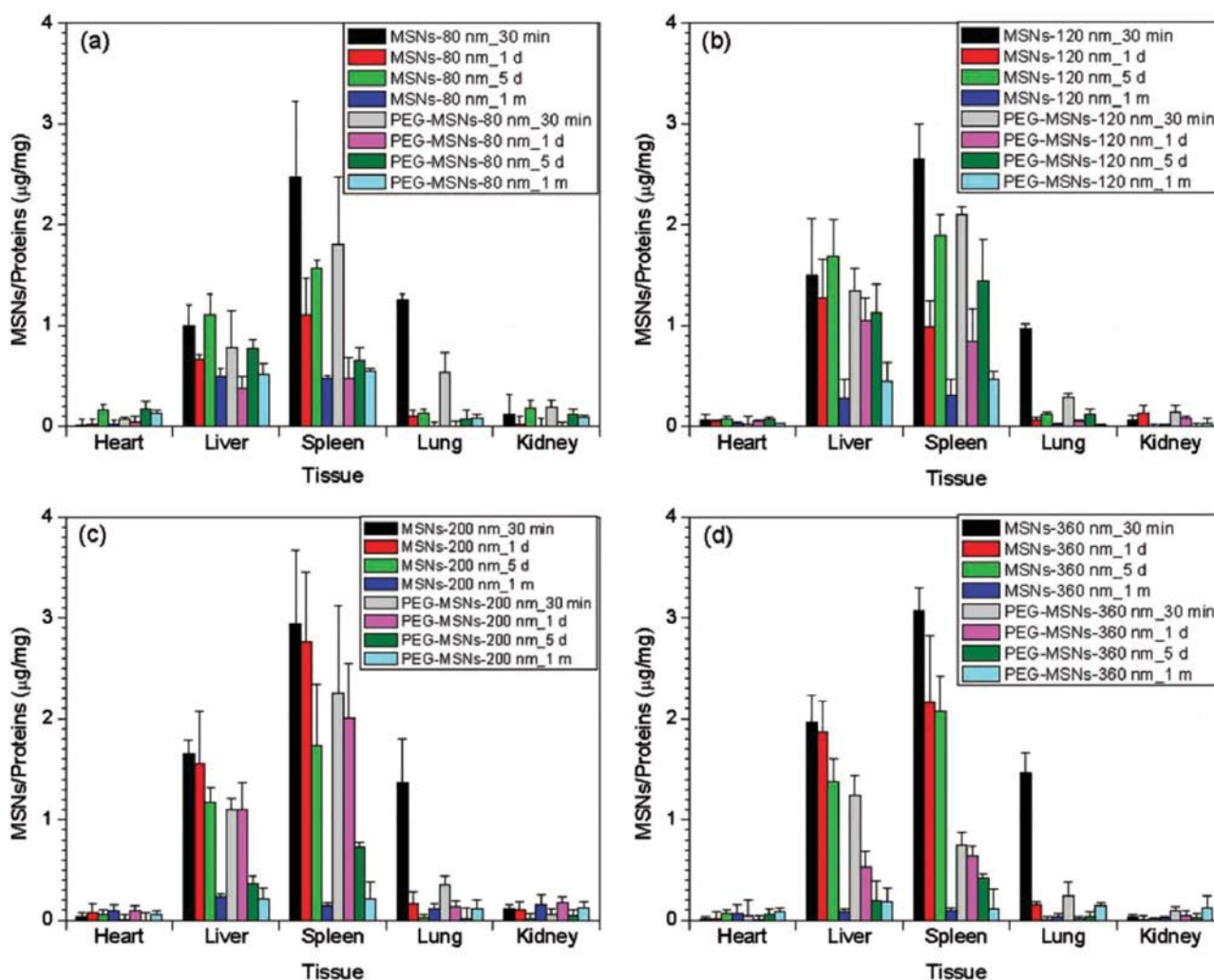


**Figure 10.** Biodistribution of mesoporous silica nanoparticles (MSNs) of different sizes: biodistribution percentages of MSNs and PEG–MSNs of particle sizes a) 80, b) 120, c) 200, and d) 360 nm in the heart, liver, spleen, lung, and kidney of ICR mice after tail intravenous injection at different time periods (30 min, 1 d, 5 d, and 1 month), respectively. Adapted with permission.<sup>[331]</sup> Copyright 2010, John Wiley & Sons.

NPs of sizes 80–390 nm were injected into the tail vein of mice and rats. The biodistribution of the NPs was tracked over one month by taking advantage of their fluorescein isothiocyanate (FITC) functionalization. The particles were detected mostly in the spleen, liver, and in lower concentrations in the lungs, kidneys, and heart. The authors observed that the smallest analyzed nanoparticles (80 nm) showed the longest circulation time, especially for the PEGylated particles. While PEGylation hindered the sequestration of NPs and increased circulation time, increasing the size of the NPs had an opposite effect. Larger NPs showed faster degradation, possibly due to the fact that they were more efficiently captured within the RES. In general, during the first month postadministration of larger particles (>80 nm), the amount of silica present in the liver decreased and silica degradation products were detected in the urine. Their biodistribution data are summarized in Figure 10.<sup>[331]</sup> Although this study provides extensive information on how size and PEGylation can play a role in the long-term fate of NPs, it should be noted that fluorescence-based measurements mainly provide semiquantitative information. Malfatti et al. used

accelerator mass spectrometry with high sensitivity to track the fate of 33 nm <sup>14</sup>CSiO<sub>2</sub> NPs up to 56 d postinjection.<sup>[221]</sup> In all mouse tissues, the maximum concentration occurred 2 h postinjection via an implanted jugular vein catheter. The NPs showed fast clearance from the plasma and subsequent accumulation in tissues, mostly in the spleen and liver, with higher concentrations found in the liver. Lower amounts of NPs were also detected in kidneys and lungs, and some in the bone marrow and cervical lymph nodes. NPs were not detected in muscle or adipose tissue, or in the brain. After 56 d, a significant decrease of NP concentration in the kidneys and lungs was observed (20%), with even larger decreases in the spleen (57%) and liver (72%). Although the amount of NPs gradually decreased, a significant proportion remained in the body even after eight weeks. Renal clearance occurred as early as 2 h postinjection, as opposed to hepatobiliary clearance, which was observed after 21 h. Malfatti et al. postulated that NPs are secreted in urine via tubular secretion.<sup>[221]</sup> The size impact on the biodistribution of SiO<sub>2</sub> NPs was further addressed by Xie et al., who tracked the fate and toxicity of 20 and 80 nm SiO<sub>2</sub> NPs

modified by  $^{125}\text{I}$  over one month, while Cho et al. investigated 50, 100, and 200 nm rhodamine  $\text{SiO}_2$  NPs over the same time period.<sup>[332,333]</sup> Xie et al. showed that size had no significant effect on the biodistribution of the NPs and that all particles were mostly found in liver, spleen, and lungs (and at low concentrations in the blood, heart, kidneys, intestine, stomach, and brain). Although the distribution patterns did not differ, the amount of 200 nm NPs in tissues was higher. After 30 d, the amount of 20 nm NPs found in the liver and spleen had significantly decreased compared to that found for 80 nm particles.<sup>[333]</sup> Cho et al. observed all of the investigated NPs in the liver and spleen after four weeks, and their distribution correlated with the distribution of RES within the liver and spleen. The concentration of the smallest NPs (50 nm) peaked in the urine after 12 h, while it took 24 h for the larger NPs (100 and 200 nm). It is worth noting that both particle types are significantly larger than the membrane pores in kidneys, thus clearance by glomerular filtration cannot be expected. The same pattern was observed for hepatobiliary excretion, where 50 nm NPs were detected in feces after 24 h and 100 nm NPs after 72 h. The 200 nm NPs were less efficiently excreted via both above-mentioned routes and remained mainly within the RES of the spleen and liver.<sup>[332]</sup> As the physicochemical properties of the NPs typically determine their fate in the body, the effect of shape on the clearance of mesoporous silica NPs has been investigated by Huang et al.<sup>[195]</sup> The authors used FITC- and PEG-functionalized nanorods: short NRs (185 nm, aspect ratio 1.5) and long NRs (720 nm, aspect ratio 5). All NRs were detected in spleen and liver, and their localization correlated with localization of the RES. It has been observed that the fluorescent signal decreased after 7 d, especially in the case of long NRs, which has been postulated to be due to the degradation of silica. Although NRs were not detected in lymph nodes and the brain, some were detected in kidneys. Inductively coupled plasma optical emission spectroscopy (ICP OES) analysis showed that short NRs were located predominantly in the liver while longer NRs were located in the spleen. PEGylation decreased the amount of NRs found in the liver but increased that found in the lungs, while slowing down the clearance. The short NRs were also more efficiently cleared via the urine and feces than long NRs. It is worth noting that, based on biochemical assays, NRs were observed to induce dysfunction in biliary excretion and glomerular filtration.<sup>[195]</sup>

The impact of the surface charge on the long-term fate and biodistribution of  $\text{SiO}_2$  NPs has not yet been fully studied. Short-term studies provide approximations of the potential impact of surface charge on the long-term fate of NPs.<sup>[334–336]</sup> By varying the NP porosity, size, and geometry, Yu et al. showed that surface and porosity play a more important role than geometry in the fate of NPs. Tissue distribution was found to be dependent upon the porosity and surface charge of the particles. Mesoporous NPs accumulated more in the lungs, while nonporous NPs accumulate in liver, as the primary amine group on the surface reduced accumulation in the lungs and kidneys.<sup>[336]</sup> A recent study by Lu et al., who used amino- and carboxy-functionalized  $\text{SiO}_2$  NPs of different sizes (30, 70, and 300 nm), showed that charge—and not size—plays a crucial role in the fate of the NPs.<sup>[335]</sup> Furthermore, Souris et al. also investigated  $\text{SiO}_2$  NPs of dif-

ferent charges, functionalized with a far-red-absorbing dye. The authors observed a signal in the liver immediately after injection, which was followed by a signal in the duodenum, indicating that hepatobiliary excretion is the preferred mode of clearance. Most of the fluorescence was detected in the feces, and ICP MS data revealed that secretion was complete within 3 d.<sup>[334]</sup> Exposure can be divided into single and chronic exposure scenarios, as well as according to the route of administration, as mentioned above. Different exposure routes, as well as single versus repeated doses, were studied with 110 nm mesoporous  $\text{SiO}_2$  NPs.<sup>[337,338]</sup> The investigated routes of administration were intravenous, hypodermic, intramuscular, and oral, whereby it was shown that the highest tolerated dose could be achieved through oral administration. Interestingly, NPs administered orally, intramuscularly and hypodermically were not initially observed in the liver and spleen, in contrast to intravenous administration. Upon inspection via ICP OES, NPs were detected in the liver regardless of the administration route, although differential biodistribution was observed. After 7 d postexposure, the amount of NPs in the liver and spleen increased in the case of intravenously administered NPs, while for oral administration a change was not observed. The concentrations of NPs found in the liver, spleen, feces, and urine increased slightly for hypodermic administration.<sup>[337]</sup> In a different study, where  $\text{SiO}_2$  NPs (20 and 100 nm) were administered orally, the NPs were observed in the kidneys, liver, lungs, and spleen. Elevation of the silica concentration in the lungs and spleen was observed after 2 d while the same was observed in the kidneys and liver after 3 d. Even 7 d after oral administration, no increased NP concentration was observed in the GI, esophagus, stomach, and intestine. Transmission electron microscopy analysis revealed that NPs (both sizes) were localized in the hepatocytes in the liver. Most of the NPs (75–80%) were excreted in the feces, while 7–8% were excreted via the urine. Although the amount of NPs was found to significantly decrease after 7 d, longer retention was observed in the liver and kidneys than in the lungs and spleen, and distribution was not significantly size dependent.<sup>[339]</sup> Retention of 150 nm NP in the lungs (lung air sac) and kidneys (glomerulus) was observed after 4 d, and the overall NP retention was 10–15%. Biodegradation of these NPs was suggested since silicic acid has been detected. Interestingly, in some biodistribution studies using silica nanoparticles, NPs were observed in the cell nucleus.<sup>[339,340,382–384]</sup> In a repeated exposure study it was demonstrated that even for potentially biodegradable NPs such as silica,<sup>[341]</sup> in certain cases it took longer than four weeks for complete clearance, while most of the NPs were found to persist trapped in the liver and spleen.<sup>[338]</sup> As anticipated, ultrasmall  $\text{SiO}_2$  NPs (2–3 nm) were predominantly and efficiently excreted via the kidneys,<sup>[330]</sup> but in some cases even significantly larger biodegradable NPs (100 nm) were cleared efficiently, albeit via other routes.<sup>[341]</sup>

## 7.6. Polymers

A wide variety of polymers, including biological, synthetic, and hybrid examples, are used for a range of medical applications,

such as drug delivery systems, coatings, or implants.<sup>[342]</sup> They can be modified in their physical, chemical, and biological properties to be optimized for specific applications. Polymers can be used as building blocks for applications such as drug delivery systems mimicking cellular membranes and organelles or by imitating viral mechanisms. Next to liposomes, polymers have also attracted considerable attention as promising materials for medical applications since they can provide prolonged circulation lifetimes and controlled release of their cargo such as small molecules, proteins, nucleic acids, and hydrophilic and hydrophobic drugs.<sup>[343,382–390]</sup>

Polymer conjugates have shown promising results as therapeutics in clinical trials and some have also found their way onto the market. Polymeric therapeutics can be subdivided into polymer–protein and polymer–drug conjugates. The conjugation of a protein to a polymer reduces its immunogenicity while increasing its stability and blood circulation time.<sup>[344]</sup> Drug conjugates show improved aqueous solubility, increased blood circulation time, reduced toxicity, and an improved therapeutic index through linkage to polymers.<sup>[345,346]</sup> However, since both subgroups show binding via a single linker and limited binding sites, the loading of the conjugates is reduced compared to vesicular structures.

Several protein–polymer conjugates have already been used for clinical trials. The first conjugate approved for the treatment of acute lymphoblastic leukemia (ALL) by the FDA was PEGylated-asparaginase in 1994, better known by the name Pegaspargase or Oncaspar.<sup>[347,348]</sup> Data from pediatric and adult clinical trials show that the elimination half-life of Pegaspargase is  $\approx 5.5$ – $6$  d, about five times longer than non-PEGylated asparaginase derived from *Escherichia coli*.<sup>[349]</sup> Deamination of asparagine occurred 2 h after intravenous application of a dose of  $2000 \text{ IU m}^{-2}$  Pegaspargase and sustained up to three weeks in adult ALL patients, and about five weeks a dose of  $2500 \text{ IU m}^{-2}$  was given to pediatric ALL patients.<sup>[350,351]</sup> Single intravenous infusion of 500, 750, 1000, or  $2500 \text{ IU m}^{-2}$  Pegaspargase revealed that asparaginase activity levels remained  $>0.1 \text{ IU mL}^{-1}$  in 60%, 40%, and 20% of patients two weeks after treatment with 2500, 1000, and  $500 \text{ IU m}^{-2}$  Pegaspargase, respectively, but the levels became undetectable after three weeks in all cases.<sup>[352]</sup> As also seen with liposomes, PEGylation is a commonly used technique to improve in vivo biodistribution of bioactive molecules or whole drug delivery systems. This technique supports the blockage of potentially immunogenic epitopes, thus reducing the dose-limiting hypersensitivity reactions associated with native asparaginase delays in the clearance by the RES.<sup>[353,354]</sup> Despite this fact, rapid clearance of Pegaspargase has been reported in up to one-third of patients treated for ALL. Hypersensitivity reactions to Pegaspargase lead to the formation of antibodies against PEG.<sup>[355]</sup> Therefore, screening for anti-PEG antibodies may allow the modification of the dosing strategy or the use of a non-PEGylated drug version to overcome clearance. Further polymer–protein conjugates available in the market involve, e.g., the antitumor protein neocarzinostatin linked to styrene maleic anhydride, known as Zinostatin, for the treatment of hepatocellular carcinoma, interferon- $\alpha$  linked to PEG (PEGasys) for hepatitis C treatment, the protein adenosine deaminase linked to PEG (Adagen) for the treatment of severe combined immunodeficiency, and granulocyte colony-stimulating factor

linked to PEG (Neulasta) for neutropenia prevention associated with chemotherapy.<sup>[356–359]</sup> Numerous clinical trials of novel polymer–protein conjugates including enzymes and biological response modifiers have been performed or are ongoing.<sup>[360–363]</sup> Maeda investigated the tumor and tissue distribution of poly(maleic acid–styrene)-conjugated neocarzinostatin (Zinostatin) 24 h after intravenous injection in mice. In comparison to its nonconjugated form, the polymer-conjugated neocarzinostatin revealed fivefold higher concentration in the tumor tissue and tenfold and sixfold higher concentrations in the liver and spleen, respectively, compared to the tumor tissue.<sup>[356]</sup> Take-shita et al. investigated the organ specificity of the same formulation in rats. After intravenous injection, the drug was found in the kidney, lymph nodes, and bladder in very high concentrations, and in lesser concentrations in the bone marrow, lung, small intestine, liver, and spleen.<sup>[364]</sup> In addition, Maeda showed that due to albumin binding, the half-life of poly(maleic acid–styrene)-conjugated neocarzinostatin increased to 19 min compared to 1.9 min for naked neocarzinostatin in mice.<sup>[356]</sup> Due to its very short half-life, long term studies of poly(maleic acid–styrene)-conjugated neocarzinostatin do not exist. Further therapeutic applications of styrene–maleic acid copolymer conjugates involve the linkage to pirarubicin, revealing a 8.4-fold increase in tumor tissue accumulation compared to free pirarubicin.<sup>[365]</sup> After 72 h the concentration of the polymer conjugate found in the liver, spleen, and kidney decreased to 24.5%, 27%, and 19% compared to that observed at 24 h. In contrast to all other tissues, the concentration of the polymer conjugate in the tumor after 72 h remained 75% of that observed at 24 h, which was the highest concentration, followed by the liver, spleen, and kidney.

Polymer–drug conjugates have already been studied for more than 30 years, with increasing numbers of applications entering clinical trials. However, so far no polymer–drug conjugates have been approved.<sup>[366]</sup> Several biodistribution studies have been published, mainly focusing on early time points (less than one week; see Table 4).<sup>[367–369]</sup> Borgman et al. investigated the biodistribution of  $^{125}\text{I}$ -radiolabeled *N*-(2-hydroxypropyl) methacrylamide (HPMA) copolymer–geldanamycin-RGDfK conjugates in mice to improve geldanamycin chemotherapy by reducing unspecific toxicity and improving tumor response through higher localized concentrations of the drug.<sup>[370]</sup> Time-dependent biodistribution studies were carried out after 1, 6, 24, 48, and 72 h postinjection. Rapid blood clearance was observed with very little activity remaining in blood after 24 h. It has been shown that the dose of the polymer received by the tumor at 1 h was retained, with a modest increase between 1 and 24 h, as well as prolonged accumulation of the polymer–drug conjugate for the duration of the study. At 24 h, the tumor accumulation was significantly higher than in the blood, heart, lung, spleen, and stomach. Additionally, the accumulation in the tumor after 72 h was significantly higher than all organs except the kidneys (see Figure 11). Etrych et al. investigated the effects of the molecular weight and architecture of HPMA copolymer–doxorubicin conjugates on biodistribution and in vivo activity.<sup>[371]</sup> Copolymer–doxorubicin conjugates of linear and star architectures were compared. With increasing molecular weight (MW), renal clearance decreased, and the conjugates displayed extended blood circulation and enhanced tumor accumulation, which resulted in significantly improved

**Table 4.** Long-term biodistribution data on polymeric nanomaterials.

Material	Size [nm]	Animal	Investigated tissue <sup>a)</sup>	Longest timepoint	Reference
PEG-asparaginase	N/A	Human	Bl	21 d	[352]
Zinostatin	N/A	Mouse	<b>TT, Li, S</b>	24 h	[356]
Styrene–maleic acid copolymer-conjugated pirarubicin	18.9 ± 10.0	Mouse	<b>TT, Li, S, K</b>	72 h	[365]
HPMA copolymer–geldanamycin-RGDfK	N/A	Mouse	Bl, <b>TT</b> , H, L, Li, S, St, <b>K</b>	72 h	[370]
HPMA copolymer–doxorubicin	N/A	Mouse	Bl, <b>U</b> , Li, <b>TT</b>	96 h	[371]
PMMA/ <i>N</i> -isopropylacrylamide	130	Mouse	<b>Li, K, S, H, LN</b>	22 d	[372]
HPMA copolymer–doxorubicin	N/A	Mouse	Bl, <b>S</b> , Li, K, <b>TT</b> , H	168 h	[385]
HPMA copolymer–9-aminocamptothecin	N/A	Mouse	L, H, Li, S, K, <b>SI, C, Co</b>	24 h	[386]
(HPMA) copolymer–dexamethasone	N/A	Rat	Bl, H, L, K, L, <b>S, J</b>	7 d	[387]
PVP-TNF- $\alpha$	N/A	Mouse	<b>Bl</b>	3 h	[388]
Camptothecin–polymer conjugate IT-101	N/A	Mouse and rat	<b>Bl, Li, S, L, TT, H</b>	48 h	[389]
Etoposide-loaded PLGA	105; 160	Mouse	H, L, <b>Li, S, K</b> , St, Si, M, <b>Br</b>	24 h	[390]

<sup>a)</sup>TT: tumor tissue; H: heart; L: lung; K: kidney; Br: brain; M: muscle; SI: small intestine; Bl: blood; Li: liver; S: spleen; J: joints; St: stomach; C: cecum; Co: colon; U: urine; LN: lymph nodes; N/A: data not available; and bold letters indicate that the organ tested positive for nanoparticles.

anti-tumor activities. The linear conjugates with flexible polymer chains were eliminated by kidney clearance more quickly. Only star conjugates with MWs below 50 000 Da were removed by kidney filtration, while linear polymer conjugates with MWs near 70 000 Da were detected in the urine 36–96 h after injection. Falzarano et al. investigated PMMA/*N*-isopropylacrylamide polymer NPs, administered both intraperitoneally and orally, delivering antisense oligonucleotides for the treatment of Duchenne muscular dystrophy.<sup>[372]</sup> After a single IP administration, the polymers remained mainly in the peritoneal cavity for about 24 h and then diffused throughout the whole body, whereas the fluorescence persisted for up to 22 d. Multiple administrations of the polymers for up to two months led to biodistribution in all muscles, including the heart, and revealed a fluorescence signal until 60 d. The fluorescence, while absent in the liver, persisted in kidneys, spleen, and lymph nodes. Although many polymer–drug conjugates based on chemistries such as PEG or HPMA have progressed into clinical development, their progression toward market approval has undoubtedly been hindered by their nonbiodegradable nature. High-MW polymer carriers exceeding the renal excretion threshold should be biodegradable to prevent long-term retention in the body.

## 8. Outlook and Conclusion

In order to take advantage of the full potential of nanomaterials for medical applications it is essential to have a profound (fundamental) comprehension of the interactions of such materials on the level of single cells, tissue barriers, and the human body

as whole. While many studies have been performed to investigate and develop potential nanomaterials for application in drug delivery or as theranostic devices, their biodistribution and long-term fate, although crucial for drug applicability as well as efficacy, have only rarely been investigated. This is also especially important if one considers a repeated use of such nanomedicines over a prolonged time period. One possible hurdle for the relatively low number of studies might be the difficulty in accessing reproducible and reliable analytical methods for the intracellular-, tissue-, and organ-specific quantification of nanomaterials. Up to date no standardized and validated method is recommended, also because of the very different requirements of the analytical procedure depending on the particle type in combination with the different specifications and limitations for each of the analytical techniques.<sup>[373,374]</sup>

The biodistribution and clearance of a specific nanomaterial depends not only on the physicochemical properties of the materials but also on how the material is applied to a (human) body. Although there seems to be an agreement that size and surface charge are the most important determinants of a material's fate in vivo, a grouping of the materials is not yet possible due to the variety of approaches applied to nanomaterial synthesis. This results in differing surface structures, which can strongly affect the interaction of a material with physiological fluids, cells, and organs. However, several efforts are being made to harness the advantages of nanosized systems for medical applications. Instead of trying to exploit the particles' inherent properties, some researchers focus very successfully on them as efficient nanocarriers for drug delivery. Through combination with nanotechnology, some

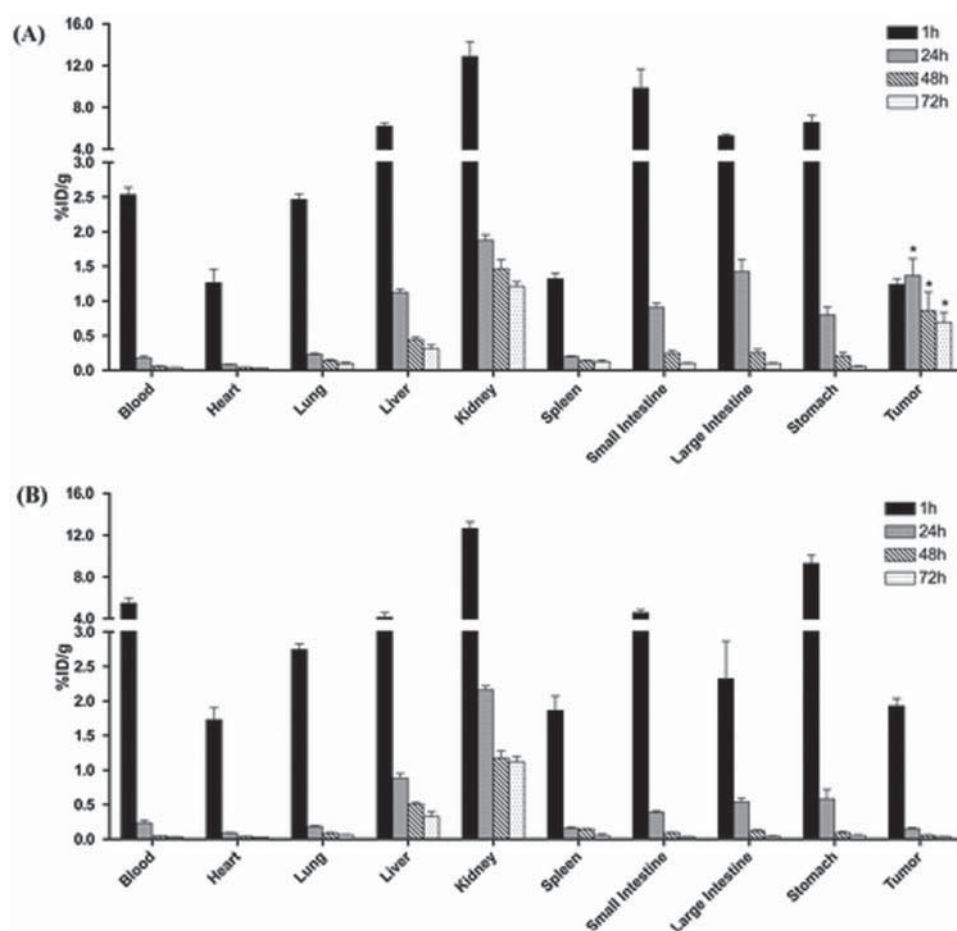


**Figure 11.** Biodistribution of  $^{125}\text{I}$ -radiolabeled HPMA copolymer-AH-GDM conjugates: A,B) biodistribution of  $^{125}\text{I}$ -radiolabeled HPMA copolymer-AH-GDM conjugates with (A) and without (B) RGDfK in prostate-tumor-bearing mice. Activity per organ is expressed as % injected dose per gram of tissue ( $\% \text{ID g}^{-1}$ ) following necropsy at 1, 24, 48, and 72 h postintravenous injection. Rapidly decreasing blood concentrations are observed with no significant accumulation differences in normal organs. Significantly higher localization of the targeted conjugate occurs in the tumor after 1 h compared with the nontargeted conjugate, as indicated in the graph as  $*p < 0.05$ . Data are expressed as mean  $\pm$  SD. Reproduced with permission.<sup>[370]</sup> Copyright 2009, American Chemical Society.

key medical features of drugs (i.e., half-life, solubility, and toxicity) can be improved.<sup>[375]</sup> Examples that are now routinely used in clinics consist of liposomal-encapsulated doxorubicin (Doxil), paclitaxel-loaded albumin nanoparticles (Abraxane), or polymeric micelles containing paclitaxel (Genexol PM).<sup>[376]</sup> Hence, in order to promote the safe-by-design approach of biomedical nanomaterials, nanoscience researchers should focus future research on studies of the long-term effects of nanomaterials in the human body and their possible chronic effects. A special emphasis must also be placed on detailed reporting of the nanomaterial's properties as well as the biological systems used. Taking into account that data collection in long-term studies requires a significant amount of time, and also considering ethical issues for in vivo studies, it is recommended that the methodology should be standardized and follow published and accepted guidelines as much as possible in order to make studies comparable. Additionally, (novel) analytical methods should be developed and optimized to allow detection and quantification of the distribution of nanomaterials in cells, tissues, and/or organs.

## Acknowledgements

J.B., A.M., D.H., and R.L. contributed equally to this work. The authors would like to acknowledge the Swiss National Science Foundation (310030\_159847/1), the National Center of Competence in Research for Bio-Inspired Materials, and the Adolphe Merkle Foundation for financial support. The authors kindly thank Dr. Miguel Spuch Calvar for the graphical designs.

## Conflict of Interest

The authors declare no conflict of interest.

## Keywords

biodistribution, clearance, long-term fate, nanomaterials, routes of exposure

Received: July 31, 2017  
Revised: October 20, 2017  
Published online:

- [1] M. R. Gwinn, V. Vallyathan, *Environ. Health Perspect.* **2006**, *114*, 1818.
- [2] A. D. Maynard, R. J. Aitken, T. Butz, V. Colvin, K. Donaldson, G. Oberdörster, M. A. Philbert, J. Ryan, A. Seaton, V. Stone, S. S. Tinkle, L. Tran, N. J. Walker, D. B. Warheit, *Nature* **2006**, *444*, 267.
- [3] ISO/TS 80004-2:2015(en), Nanotechnologies—Vocabulary. Part 2: Nano-Objects, <https://www.iso.org/obp/ui/#iso:std:iso:ts:80004-2:ed-1:v1:en> (accessed: June 2017).
- [4] F. Piccinno, F. Gottschalk, S. Seeger, B. Nowack, *J. Nanoparticle Res.* **2012**, *14*, 1109.
- [5] S. C. Baetke, T. Lammers, F. Kiessling, *Br. J. Radiol.* **2015**, *88*, 20150207.
- [6] R. Wang, P. S. Billone, W. M. Mullett, *J. Nanomater.* **2013**, *2013*, 1.
- [7] V. Leiro, P. M. Moreno, B. Sarmiento, J. Durão, L. Gales, A. P. Pêgo, C. C. Barrias, in *Bioinspired Materials for Medical Applications*, (Eds.: L. Rodrigues, M. Mota), Elsevier **2017**, pp. 1–44.
- [8] K. J. Koudelka, A. S. Pitek, M. Manchester, N. F. Steinmetz, *Annu. Rev. Virol.* **2015**, *2*, 379.
- [9] A. D. Friedman, S. E. Claypool, R. Liu, *Curr. Pharm. Des.* **2013**, *19*, 6315.
- [10] V. J. Venditto, F. C. Szoka, *Adv. Drug Delivery Rev.* **2013**, *65*, 80.
- [11] H. Nirschl, K. Keller, *Upscaling of Bio-Nano-Processes*, Springer, Berlin/Heidelberg, Germany **2014**.
- [12] R. Paliwal, R. J. Babu, S. Palakurthi, *AAPS PharmSciTech* **2014**, *15*, 1527.
- [13] L. Yildirim, N. T. K. Thanh, M. Loizidou, A. M. Seifalian, *Nano Today* **2011**, *6*, 585.
- [14] D. Bobo, K. J. Robinson, J. Islam, K. J. Thurecht, S. R. Corrie, *Pharm. Res.* **2016**, *33*, 2373.
- [15] E. Connor, J. Mwamuka, A. Gole, C. Murphy, M. Wyatt, *Small* **2005**, *1*, 325.
- [16] C. Kim, P. Ghosh, V. M. Rotello, *Nanoscale* **2009**, *1*, 61.
- [17] M. E. Davis, Z. (Georgia) Chen, D. M. Shin, *Nat. Rev. Drug Discovery* **2008**, *7*, 771.
- [18] D. W. Bartlett, H. Su, I. J. Hildebrandt, W. A. Weber, M. E. Davis, *Proc. Natl. Acad. Sci. USA* **2007**, *104*, 15549.
- [19] A. Grenha, M. E. Gomes, M. Rodrigues, V. E. Santo, J. F. Mano, N. M. Neves, R. L. Reis, *J. Biomed. Mater. Res., Part A* **2010**, *92*, 1265.
- [20] I. L. Medintz, H. Mattoussi, A. R. Clapp, *Int. J. Nanomed.* **2008**, *3*, 151.
- [21] K. M. Tsoi, Q. Dai, B. A. Alman, W. C. W. Chan, *Acc. Chem. Res.* **2013**, *46*, 662.
- [22] H. Soo Choi, W. Liu, P. Misra, E. Tanaka, J. P. Zimmer, B. Itty Ipe, M. G. Bawendi, J. V. Frangioni, *Nat. Biotechnol.* **2007**, *25*, 1165.
- [23] R. Hardman, *Environ. Health Perspect.* **2006**, *114*, 165.
- [24] X. Michalet, *Science* **2005**, *307*, 538.
- [25] A. K. Gupta, M. Gupta, *Biomaterials* **2005**, *26*, 3995.
- [26] O. Veis, J. W. Gunn, F. M. Kievit, C. Sun, C. Fang, J. S. H. Lee, M. Zhang, *Small* **2008**, *5*, 256.
- [27] J. Rautio, H. Kumpulainen, T. Heimbach, R. Oliyai, D. Oh, T. Järvinen, J. Savolainen, *Nat. Rev. Drug Discovery* **2008**, *7*, 255.
- [28] A. E. Hawley, S. S. Davis, L. Illum, *Adv. Drug Delivery Rev.* **1995**, *17*, 129.
- [29] I. Brigger, C. Dubernet, P. Couvreur, *Adv. Drug Delivery Rev.* **2002**, *54*, 631.
- [30] C.-H. Heldin, K. Rubin, K. Pietras, A. Östman, *Nat. Rev. Cancer* **2004**, *4*, 806.
- [31] M. Gänsslen, *Klin. Wochenschr.* **1925**, *71*.
- [32] P. Gehr, M. Bachofen, E. R. Weibel, *Respir. Physiol.* **1978**, *32*, 121.
- [33] J. S. Patton, *Adv. Drug Delivery Rev.* **1996**, *19*, 3.
- [34] J. S. Patton, P. R. Byron, *Nat. Rev. Drug Discovery* **2007**, *6*, 61.
- [35] J. Heyder, J. Gebhart, G. Rudolf, C. F. Schiller, W. Stahlhofen, *J. Aerosol Sci.* **1986**, *17*, 811.
- [36] G. Oberdörster, A. Elder, A. Rinderknecht, *J. Nanosci. Nanotechnol.* **2009**, *9*, 4996.
- [37] M. Arredouani, Z. Yang, Y. Ning, G. Qin, R. Soininen, K. Tryggvason, L. Kobzik, *J. Exp. Med.* **2004**, *200*, 267.
- [38] M. Gumbleton, *Adv. Drug Delivery Rev.* **2001**, *49*, 281.
- [39] J. Rejman, V. Oberle, I. S. Zuhorn, D. Hoekstra, *Biochem. J.* **2004**, *377*, 159.
- [40] W. Möller, W. G. Kreyling, O. Schmid, M. Semmler-Behnke, H. Schluz, in *Particle-Lung Interactions*, 2nd ed., Vol. 241, (Eds: P. Gehr, C. Mühlfeld, B. Rothen-Rutishauser, F. Plank), Informa Healthcare USA, New York **2009**, pp 79–107.
- [41] L. Müller, A. D. Lehmann, B. D. Johnston, F. Blank, P. Wick, A. Fink, B. Rothen-Rutishauser, in *Handbook of Nanotoxicology, Nanomedicine and Stem Cell Use in Toxicology*, John Wiley & Sons, Ltd. **2014**, pp. 205–222.
- [42] A. Bianchi, S. Dufort, F. Lux, P.-Y. Fortin, N. Tassali, O. Tillement, J.-L. Coll, Y. Cremillieux, *Proc. Natl. Acad. Sci. USA* **2014**, *111*, 9247.
- [43] S. Dufort, A. Bianchi, M. Henry, F. Lux, G. Le Duc, V. Josserand, C. Louis, P. Perriat, Y. Cremillieux, O. Tillement, J. L. Coll, *Small* **2015**, *11*, 215.
- [44] W. Yang, J. I. Peters, R. O. Williams, *Int. J. Pharm.* **2008**, *356*, 239.
- [45] M. Simkó, M.-O. Mattsson, *Part. Fibre Toxicol.* **2010**, *7*, 42.
- [46] Y. Yun, Y. W. Cho, K. Park, *Adv. Drug Delivery Rev.* **2013**, *65*, 822.
- [47] P. P. Desai, A. A. Date, V. B. Patravale, *Drug Discovery Today Technol.* **2012**, *9*, e87.
- [48] The Project on Emerging Nanotechnologies, <http://www.nano-techproject.org/> (accessed: July 2017).
- [49] M. Cushen, J. Kerry, M. Morris, M. Cruz-Romero, E. Cummins, *J. Agric. Food Chem.* **2014**, *62*, 1403.
- [50] C. McCracken, P. K. Dutta, W. J. Waldman, *Environ. Sci. Nano* **2016**, *3*, 256.
- [51] H. I. Labouta, M. Schneider, *Nanomed. Nanotechnol., Biol. Med.* **2013**, *9*, 39.
- [52] R. Alvarez-Román, A. Naik, Y. N. Kalia, R. H. Guy, H. Fessi, *J. Controlled Release* **2004**, *99*, 53.
- [53] P. R. Wheeler, G. Burkitt, V. G. Daniels, *Ulster Med. J.* **1979**, *48*, 180.
- [54] B. W. Barry, *Eur. J. Pharm. Sci.* **2001**, *14*, 101.
- [55] N. A. Monteiro-Riviere, K. Wienck, R. Landsiedel, S. Schulte, A. O. Inman, J. E. Riviere, *Toxicol. Sci.* **2011**, *123*, 264.
- [56] R. Dunford, A. Salinaro, L. Cai, N. Serpone, S. Horikoshi, H. Hidaka, J. Knowland, *FEBS Lett.* **1997**, *418*, 87.
- [57] M. D. Newman, M. Stotland, J. I. Ellis, *J. Am. Acad. Dermatol.* **2009**, *61*, 685.
- [58] I. Schreiber, B. Hesse, C. Seim, H. Castillo-michel, J. Villanova, P. Laux, N. Dreier, R. Penning, R. Toucoulou, M. Cotte, A. Luch, *Sci. Rep.* **2017**, *7*, 11395.
- [59] B. W. Barry, *Eur. J. Pharm. Sci.* **2001**, *14*, 101.
- [60] M. Lodén, H. Beitner, H. Gonzalez, D. W. Edström, U. Åkerström, J. Austad, I. Buraczewska-Norin, M. Mattsson, H. C. Wulf, *Br. J. Dermatol.* **2011**, *165*, 255.
- [61] C. H. A. Boakye, K. Patel, R. Doddapaneni, A. Bagde, S. Marepally, M. Singh, *J. Controlled Release* **2017**, *246*, 120.
- [62] R. Yang, T. Wei, H. Goldberg, W. Wang, K. Cullion, D. S. Kohane, *Adv. Mater.* **2017**, *1606596*, 1.
- [63] S. Liu, L. Jones, F. X. Gu, *Macromol. Biosci.* **2012**, *12*, 608.
- [64] I. Sondi, B. Salopek-Sondi, *J. Colloid Interface Sci.* **2004**, *275*, 177.
- [65] M. Priebe, J. Widmer, N. Suhartha, S. L. Abram, I. Mottas, A. K. Woischnig, P. S. Brunetto, N. Khanna, C. Bourquin, K. M. Fromm, *Nanomed. Nanotechnol., Biol. Med.* **2017**, *13*, 11.

- [66] S. K. Nandi, A. Shivaram, S. Bose, A. Bandyopadhyay, *J. Biomed. Mater. Res., Part B* **2017**, <https://doi.org/10.1002/jbm.b.33910>.
- [67] S. Türker, E. Onur, Y. Özer, *Pharm. World Sci.* **2004**, *26*, 137.
- [68] S. Salatin, J. Barar, M. Barzegar-Jalali, K. Adibkia, M. A. Milani, M. Jelvehgari, *Arch. Pharm. Res.* **2016**, *39*, 1181.
- [69] E. Ahmad, Y. Feng, J. Qi, W. Fan, Y. Ma, H. He, F. Xia, X. Dong, W. Zhao, Y. Lu, W. Wu, *Nanoscale* **2017**, *9*, 1174.
- [70] J. W. Suh, J. S. Lee, S. Ko, H. G. Lee, *J. Agric. Food Chem.* **2016**, *64*, 5384.
- [71] A. C. Marques, A. I. Rocha, P. Leal, M. Estanqueiro, J. M. S. Lobo, *Int. J. Pharm.* **2017**, *533*, 455.
- [72] A. Keramanizadeh, D. Balharry, H. Wallin, S. Loft, P. Møller, *Crit. Rev. Toxicol.* **2015**, *45*, 837.
- [73] A. E. Nel, L. Mädler, D. Velegol, T. Xia, E. M. V. Hoek, P. Somasundaran, F. Klaessig, V. Castranova, M. Thompson, *Nat. Mater.* **2009**, *8*, 543.
- [74] T. L. Moore, L. Rodriguez-Lorenzo, V. Hirsch, S. Balog, D. Urban, C. Jud, B. Rothen-Rutishauser, M. Lattuada, A. Petri-Fink, *Chem. Soc. Rev.* **2015**, *44*, 6287.
- [75] D. A. Urban, L. Rodriguez-Lorenzo, S. Balog, C. Kinnear, B. Rothen-Rutishauser, A. Petri-Fink, *Colloids Surf., B* **2016**, *137*, 39.
- [76] M. Lundqvist, J. Stigler, G. Elia, I. Lynch, T. Cedervall, K. A. Dawson, *Proc. Natl. Acad. Sci. USA* **2008**, *105*, 14265.
- [77] T. Cedervall, I. Lynch, S. Lindman, T. Berggård, E. Thulin, H. Nilsson, K. A. Dawson, S. Linse, *Proc. Natl. Acad. Sci. USA* **2007**, *104*, 2050.
- [78] M. P. Monopoli, D. Walczyk, A. Campbell, G. Elia, I. Lynch, F. Baldelli Bombelli, K. A. Dawson, *J. Am. Chem. Soc.* **2011**, *133*, 2525.
- [79] M. Lundqvist, J. Stigler, T. Cedervall, T. Berggård, M. B. Flanagan, I. Lynch, G. Elia, K. Dawson, *ACS Nano* **2011**, *5*, 7503.
- [80] I. Lynch, K. A. Dawson, *Nano Today* **2008**, *3*, 40.
- [81] I. Lynch, A. Salvati, K. A. Dawson, *Nat. Nanotechnol.* **2009**, *4*, 546.
- [82] M. P. Monopoli, C. Åberg, A. Salvati, K. A. Dawson, *Nat. Nanotechnol.* **2012**, *7*, 779.
- [83] A. C. Dudley, *Cold Spring Harbor Perspect. Med.* **2012**, *2*, a006536.
- [84] F. Balkwill, A. Mantovani, *Lancet* **2001**, *357*, 539.
- [85] R. K. Jain, L. T. Baxter, *Cancer Res.* **1988**, *48*, 7022.
- [86] R. K. Jain, T. Stylianopoulos, *Nat. Rev. Clin. Oncol.* **2010**, *7*, 653.
- [87] P. A. Netti, D. A. Berk, M. A. Swartz, A. J. Grodzinsky, R. K. Jain, *Cancer Res.* **2000**, *60*, 2497.
- [88] M. J. Cipolla, *The Cerebral Circulation*, Morgan & Claypool Life Sciences, San Rafael, CA, USA **2009**.
- [89] A. R. Pries, W. M. Kuebler, *Handb. Exp. Pharmacol.* **2006**, *176*, 1.
- [90] A. M. Grabrucker, B. Ruozi, D. Belletti, F. Pederzoli, F. Forni, M. A. Vandelli, G. Tosi, *Tissue Barriers* **2016**, *4*, e1153568.
- [91] B. Obermeier, R. Daneman, R. M. Ransohoff, *Nat. Med.* **2013**, *19*, 1584.
- [92] C. Y. Cheng, D. D. Mruk, *Pharmacol. Rev.* **2012**, *64*, 16.
- [93] A. Pietroiusti, L. Campagnolo, B. Fadeel, *Small* **2013**, *9*, 1557.
- [94] L. Su, D. D. Mruk, C. Y. Cheng, *J. Endocrinol.* **2010**, *208*, 207.
- [95] Z. Lan, W.-X. Yang, *Nanomedicine* **2012**, *7*, 579.
- [96] D. Evseenko, J. W. Paxton, J. A. Keelan, *Expert Opin. Drug Metab. Toxicol.* **2006**, *2*, 51.
- [97] V. Ganapathy, P. D. Prasad, M. E. Ganapathy, F. H. Leibach, *J. Pharmacol. Exp. Ther.* **2000**, *294*, 413.
- [98] A. Pietroiusti, M. Massimiani, I. Fenoglio, M. Colonna, F. Valentini, G. Palleschi, A. Camaioni, A. Magrini, G. Siracusa, A. Bergamaschi, A. Sgambato, L. Campagnolo, *ACS Nano* **2011**, *5*, 4624.
- [99] B. D. Chithrani, W. C. W. Chan, *Nano Lett.* **2007**, *7*, 1542.
- [100] B. D. Chithrani, J. Stewart, C. Allen, D. A. Jaffray, *Nanomedicine* **2009**, *5*, 118.
- [101] W. G. Kreyling, S. Hirn, W. Möller, C. Schleh, A. Wenk, G. Celik, J. Lipka, M. Schäffler, N. Haberl, B. D. Johnston, R. Sperling, G. Schmid, U. Simon, W. J. Parak, M. Semmler-Behnke, *ACS Nano* **2014**, *8*, 222.
- [102] A. P. Walczak, E. Kramer, P. J. M. Hendriksen, P. Tromp, J. P. F. G. Helsper, M. van der Zande, I. M. C. M. Rietjens, H. Bouwmeester, *Nanotoxicology* **2015**, *9*, 453.
- [103] S. McClean, E. Prosser, E. Meehan, D. O'Malley, N. Clarke, Z. Ramtoola, D. Brayden, *Eur. J. Pharm. Sci.* **1998**, *6*, 153.
- [104] G. Warren, W. Wickner, *Cell* **1996**, *84*, 395.
- [105] K. Ritchie, J. Spector, *Biopolymers* **2007**, *87*, 95.
- [106] S. J. Singer, G. L. Nicolson, *Science* **1972**, *175*, 720.
- [107] T. Wang, J. Bai, X. Jiang, G. U. Nienhaus, *ACS Nano* **2012**, *6*, 1251.
- [108] H. Hillaireau, P. Couvreur, *Cell. Mol. Life Sci.* **2009**, *66*, 2873.
- [109] B. Yameen, W. Il Choi, C. Vilos, A. Swami, J. Shi, O. C. Farokhzad, *J. Controlled Release* **2014**, *190*, 485.
- [110] R. Lehner, X. Wang, S. Marsch, P. Hunziker, *Nanomed. Nanotechnol., Biol. Med.* **2013**, *9*, 742.
- [111] H. Maeda, J. Wu, T. Sawa, Y. Matsumura, K. Hori, *J. Controlled Release* **2000**, *65*, 271.
- [112] V. Bagalkot, L. Zhang, E. Levy-Nissenbaum, S. Jon, P. W. Kantoff, R. Langer, O. C. Farokhzad, *Nano Lett.* **2007**, *7*, 3065.
- [113] R. Alshehri, A. M. Ilyas, A. Hasan, A. Arnaout, F. Ahmed, A. Memic, *J. Med. Chem.* **2016**, *59*, 8149.
- [114] X. Zhang, L. Meng, Q. Lu, Z. Fei, P. J. Dyson, *Biomaterials* **2009**, *30*, 6041.
- [115] M. Dominska, D. M. Dykxhoorn, *J. Cell Sci.* **2010**, *123*, 1183.
- [116] K. F. Ferri, G. Kroemer, *Nat. Cell Biol.* **2001**, *3*, E255.
- [117] M. L. Boland, A. H. Chourasia, K. F. Macleod, *Front. Oncol.* **2013**, *3*, 292.
- [118] L. Galluzzi, E. Morselli, O. Kepp, I. Vitale, A. Rigoni, E. Vacchelli, M. Michaud, H. Zischka, M. Castedo, G. Kroemer, *Mol. Aspects Med.* **2010**, *31*, 1.
- [119] V. Gogvadze, S. Orrenius, B. Zhivotovsky, *Trends Cell Biol.* **2008**, *18*, 165.
- [120] Z.-P. Chen, M. Li, L.-J. Zhang, J.-Y. He, L. Wu, Y.-Y. Xiao, J.-A. Duan, T. Cai, W.-D. Li, *J. Drug Target.* **2016**, *24*, 492.
- [121] E. Oh, J. B. Delehanty, K. E. Sapsford, K. Susumu, R. Goswami, J. B. Blanco-Canosa, P. E. Dawson, J. Granek, M. Shoff, Q. Zhang, P. L. Goering, A. Huston, I. L. Medintz, *ACS Nano* **2011**, *5*, 6434.
- [122] C. Pouton, K. Wagsaff, D. Roth, G. Moseley, D. Jans, *Adv. Drug Delivery Rev.* **2007**, *59*, 698.
- [123] I. G. Macara, *Microbiol. Mol. Biol. Rev.* **2001**, *65*, 570.
- [124] S. D. Conner, S. L. Schmid, *Nature* **2003**, *422*, 37.
- [125] G. J. Doherty, H. T. McMahon, *Annu. Rev. Biochem.* **2009**, *78*, 857.
- [126] A. Aderem, D. M. Underhill, *Annu. Rev. Immunol.* **1999**, *17*, 593.
- [127] R. G. W. Anderson, *Science* **2002**, *296*, 1821.
- [128] M. Edidin, *Sci. Signaling* **2001**, *2001*, pe1.
- [129] S. L. Schmid, *Annu. Rev. Biochem.* **1997**, *66*, 511.
- [130] F. M. Brodsky, C. Chen, M. C. Towler, D. E. Wakeham, *Annu. Rev. Cell Dev. Biol.* **2001**, *17*, 517.
- [131] C. Mühlfeld, P. Gehr, B. Rothen-Rutishauser, *Swiss Med. Wkly.* **2008**, *138*, 387.
- [132] T. G. Iversen, T. Skotland, K. Sandvig, *Nano Today* **2011**, *6*, 176.
- [133] D. A. Kuhn, D. Vanhecke, B. Michen, F. Blank, P. Gehr, A. Petri-Fink, B. Rothen-Rutishauser, *Beilstein J. Nanotechnol.* **2014**, *5*, 1625.
- [134] M. Mahmoudi, S. N. Saeedi-Eslami, M. A. Shokrgozar, K. Azadmanesh, M. Hassanlou, H. R. Kalhor, C. Burtea, B. Rothen-Rutishauser, S. Laurent, S. Sheibani, H. Vali, *Nanoscale* **2012**, *4*, 5461.
- [135] M. Geiser, B. Rothen-Rutishauser, N. Kapp, S. Schürch, W. Kreyling, H. Schulz, M. Semmler, V. Im Hof, J. Heyder, P. Gehr, *Environ. Health Perspect.* **2005**, *113*, 1555.
- [136] Q. Mu, N. S. Hondow, Ł. Krzemiński, A. P. Brown, L. J. Jeuken, M. N. Routledge, *Part. Fibre Toxicol.* **2012**, *9*, 29.
- [137] W. Lesniak, A. U. Bielinska, K. Sun, K. W. Janczak, X. Shi, J. R. Baker Jr., L. P. Balogh, *Nano Lett.* **2005**, *5*, 2123.

- [138] B. M. Rothen-Rutishauser, S. Schürch, B. Haenni, N. Kapp, P. Gehr, *Environ. Sci. Technol.* **2006**, *40*, 4353.
- [139] D. Rimai, D. Quesnel, A. Busnaina, *Colloids Surf., A* **2000**, *165*, 3.
- [140] F. R. Maxfield, T. E. McGraw, *Nat. Rev. Mol. Cell Biol.* **2004**, *5*, 121.
- [141] M. Hao, F. R. Maxfield, *J. Biol. Chem.* **2000**, *275*, 15279.
- [142] P. Ukkonen, V. Lewis, M. Marsh, A. Helenius, I. Mellman, *J. Exp. Med.* **1986**, *163*, 952.
- [143] S. Mukherjee, F. R. Maxfield, *Annu. Rev. Cell Dev. Biol.* **2004**, *20*, 839.
- [144] J. S. Bonifacino, J. H. Hurley, *Curr. Opin. Cell Biol.* **2008**, *20*, 427.
- [145] R. N. Majzoub, C.-L. Chan, K. K. Ewert, B. F. B. Silva, K. S. Liang, C. R. Safinya, *Biochim. Biophys. Acta, Biomembr.* **2015**, *1848*, 1308.
- [146] M. S. Cartiera, K. M. Johnson, V. Rajendran, M. J. Caplan, W. M. Saltzman, *Biomaterials* **2009**, *30*, 2790.
- [147] J. S. Bonifacino, R. Rojas, *Nat. Rev. Mol. Cell Biol.* **2006**, *7*, 568.
- [148] C. Raiborg, T. E. Rusten, H. Stenmark, *Curr. Opin. Cell Biol.* **2003**, *15*, 446.
- [149] M. Sachse, S. Urbé, V. Oorschot, G. J. Strous, J. Klumperman, *Mol. Biol. Cell* **2002**, *13*, 1313.
- [150] I. Kadiu, A. Nowacek, J. McMillan, H. E. Gendelman, *Nanomedicine* **2011**, *6*, 975.
- [151] M. Liu, Q. Li, L. Liang, J. Li, K. Wang, J. Li, M. Lv, N. Chen, H. Song, J. Lee, J. Shi, L. Wang, R. Lal, C. Fan, *Nat. Commun.* **2017**, *8*, 15646.
- [152] S. R. Pfeffer, *Nat. Cell Biol.* **1999**, *1*, E145.
- [153] E. Granger, G. McNee, V. Allan, P. Woodman, *Semin. Cell Dev. Biol.* **2014**, *31*, 20.
- [154] G. M. Cooper, R. E. Hausman, *The Cell: A Molecular Approach*, 4th ed., Sinauer Associates, Sunderland, MA, USA **2007**, p. 1.
- [155] J. P. Luzio, P. R. Pryor, N. A. Bright, *Nat. Rev. Mol. Cell Biol.* **2007**, *8*, 622.
- [156] M. Schwake, B. Schröder, P. Saftig, *Traffic* **2013**, *14*, 739.
- [157] B. Alberts, A. Johnson, J. Lewis, M. Raff, K. Roberts, P. Walter, *Molecular Biology of the Cell*, 4th ed., Garland Science, New York **2002**.
- [158] K. K. Huynh, E.-L. Eskelinen, C. C. Scott, A. Malevanets, P. Saftig, S. Grinstein, *EMBO J.* **2007**, *26*, 313.
- [159] J. Huotari, A. Helenius, *EMBO J.* **2011**, *30*, 3481.
- [160] Y.-B. Hu, E. B. Dammer, R.-J. Ren, G. Wang, *Transl. Neurodegener.* **2015**, *4*, 18.
- [161] C. H. Lee, S. H. Cheng, I. P. Huang, J. S. Souris, C. S. Yang, C. Y. Mou, L. W. Lo, *Angew. Chem., Int. Ed.* **2010**, *49*, 8214.
- [162] H. Meng, M. Xue, T. Xia, Z. Ji, D. Y. Tarn, J. I. Zink, A. E. Nel, *ACS Nano* **2011**, *5*, 4131.
- [163] A. M. Sauer, A. Schlossbauer, N. Ruthardt, V. Cauda, T. Bein, C. Bräuchle, *Nano Lett.* **2010**, *10*, 3684.
- [164] G. C. Baltazar, S. Guha, W. Lu, J. Lim, K. Boesze-battaglia, A. M. Laties, P. Tyagi, U. B. Kompella, C. H. Mitchell, *PLoS One* **2012**, *7*, 1.
- [165] S. Müller, J. Dennemärker, T. Reinheckel, *Biochim. Biophys. Acta, Proteins Proteomics* **2012**, *1824*, 34.
- [166] M. Fukuda, *J. Biol. Chem.* **1991**, *266*, 21327.
- [167] F. Wang, L. Yu, M. P. Monopoli, P. Sandin, E. Mahon, A. Salvati, K. A. Dawson, *Nanomed. Nanotechnol., Biol. Med.* **2013**, *9*, 1159.
- [168] V. Sée, P. Free, Y. Cesbron, P. Nativo, U. Shaheen, D. J. Rigden, D. G. Spiller, D. G. Fernig, M. R. H. White, I. A. Prior, M. Brust, B. Lounis, R. Lévy, *ACS Nano* **2009**, *3*, 2461.
- [169] Z. Ma, J. Bai, X. Jiang, *ACS Appl. Mater. Interfaces* **2015**, *7*, 17614.
- [170] W. G. Kreyling, A. M. Abdelmonem, Z. Ali, F. Alves, M. Geiser, N. Haberl, R. Hartmann, S. Hirn, D. J. de Aberasturi, K. Kantner, G. Khadem-Saba, J.-M. Montenegro, J. Rejman, T. Rojo, I. R. de Larramendi, R. Ufartes, A. Wenk, W. J. Parak, *Nat. Nanotechnol.* **2015**, *10*, 619.
- [171] B. E. Wildt, A. Celedon, E. I. Maurer, B. J. Casey, A. M. Nagy, S. M. Hussain, P. L. Goering, *Nanotoxicology* **2016**, *10*, 710.
- [172] E. I. Maurer, M. Sharma, J. J. Schlager, S. M. Hussain, *Nanotoxicology* **2013**, *5390*, 1.
- [173] X. Jiang, T. Miclăuş, L. Wang, R. Foldbjerg, D. S. Sutherland, H. Autrup, C. Chen, C. Beer, *Nanotoxicology* **2015**, *9*, 181.
- [174] S. Sabella, R. P. Carney, V. Brunetti, M. A. Malvindi, N. Al-Juffali, G. Vecchio, S. M. Janes, O. M. Bakr, R. Cingolani, F. Stellacci, P. P. Pompa, *Nanoscale* **2014**, *6*, 7052.
- [175] J. O. Martinez, M. Evangelopoulos, C. Chiappini, X. Liu, M. Ferrari, E. Tasciotti, *J. Biomed. Mater. Res., Part A* **2014**, *102*, 3540.
- [176] J. O. Martinez, C. Chiappini, A. Ziemys, A. M. Faust, M. Kojic, X. Liu, M. Ferrari, E. Tasciotti, *Biomaterials* **2013**, *34*, 8469.
- [177] J. G. Croissant, Y. Fatieiev, N. M. Khashab, *Adv. Mater.* **2017**, *1604634*.
- [178] T. L. Burgess, R. B. Kelly, *Annu. Rev. Cell Biol.* **1987**, *3*, 243.
- [179] C. Y. Dombu, M. Kroubi, R. Zibouche, R. Matran, D. Betbeder, *Nanotechnology* **2010**, *21*, 355102.
- [180] R. E. Yanes, D. Tarn, A. a. Hwang, D. P. Ferris, S. P. Sherman, C. R. Thomas, J. Lu, A. D. Pyle, J. I. Zink, F. Tamanoi, *Small* **2013**, *9*, 697.
- [181] N. Symens, S. J. Soenen, J. Rejman, K. Braeckmans, S. C. De Smedt, K. Remaut, *Adv. Drug Delivery Rev.* **2012**, *64*, 78.
- [182] N. Oh, J.-H. Park, *Int. J. Nanomed.* **2014**, *9*, 51.
- [183] B. D. Chithrani, A. A. Ghazani, W. C. W. Chan, *Nano Lett.* **2006**, *6*, 662.
- [184] Z. Chu, Y. Huang, Q. Tao, Q. Li, *Nanoscale* **2011**, *3*, 3291.
- [185] R. Sakhtianchi, R. F. Minchin, K.-B. Lee, A. M. Alkilyan, V. Serpooshan, M. Mahmoudi, *Adv. Colloid Interface Sci.* **2013**, *201–202*, 18.
- [186] E. Mahon, A. Salvati, F. Baldelli Bombelli, I. Lynch, K. A. Dawson, *J. Controlled Release* **2012**, *161*, 164.
- [187] N. A. Monteiro-Riviere, C. L. Tran, *Nanotoxicology: Characterization, Dosing and Health Effects*, Informa Healthcare, New York **2007**.
- [188] H. F. Krug, P. Wick, *Angew. Chem., Int. Ed.* **2011**, *50*, 1260.
- [189] W. Utembe, K. Potgieter, A. B. Stefaniak, M. Gulumian, *Part. Fibre Toxicol.* **2015**, *12*, 11.
- [190] A. M. Studer, L. K. Limbach, L. Van Duc, F. Krumeich, E. K. Athanassiou, L. C. Gerber, H. Moch, W. J. Stark, *Toxicol. Lett.* **2010**, *197*, 169.
- [191] G. Oberdörster, *Int. Arch. Occup. Environ. Health* **2000**, *73*, S60.
- [192] R. M. Abra, M. E. Bosworth, C. A. Hunt, *Res. Commun. Chem. Pathol. Pharmacol.* **1980**, *29*, 349.
- [193] K. Xiao, Y. Li, J. Luo, J. S. Lee, W. Xiao, A. M. Gonik, R. G. Agarwal, K. S. Lam, *Biomaterials* **2011**, *32*, 3435.
- [194] F. Alexis, E. Pridgen, L. K. Molnar, O. C. Farokhzad, *Mol. Pharm.* **2008**, *5*, 505.
- [195] X. Huang, L. Li, T. Liu, N. Hao, H. Liu, D. Chen, F. Tang, *ACS Nano* **2011**, *5*, 5390.
- [196] N. Khlebtsov, L. Dykman, *Chem. Soc. Rev.* **2011**, *40*, 1647.
- [197] W. G. Kreyling, M. Geiser, in *Nanoparticles in Medicine and Environment: Inhalation and Health Effects*, (Eds: J. C. Marijnissen, L. Gradon), Springer, Dordrecht, The Netherlands **2010**, pp. 145–171.
- [198] M. Geiser, W. G. Kreyling, *Part. Fibre Toxicol.* **2010**, *7*, 2.
- [199] E. S. Kostewicz, B. Abrahamsson, M. Brewster, J. Brouwers, J. Butler, S. Carlet, P. A. Dickinson, J. Dressman, R. Holm, S. Klein, J. Mann, M. McAllister, M. Minekus, U. Muenster, A. Möllertz, M. Verwei, M. Vertzoni, W. Weitschies, P. Augustijnen, *Eur. J. Pharm. Sci.* **2014**, *57*, 342.
- [200] G. Oberdörster, *Environ. Health Perspect.* **2012**, *120*, A13 (author reply A13).
- [201] M. Gonzalez, *Draft: Assessment of Biodurability of Nanomaterials and their Surface Ligands, ENV/CHEM/NANO2015)9/REV*, Organisation for Economic Co-operation and Development, Paris, France **2016**.

- [202] S. Hirn, M. Semmler-Behnke, C. Schleh, A. Wenk, J. Lipka, M. Schäffler, S. Takenaka, W. Möller, G. Schmid, U. Simon, W. G. Kreyling, *Eur. J. Pharm. Biopharm.* **2011**, *77*, 407.
- [203] C. Schleh, U. Holzwarth, S. Hirn, A. Wenk, F. Simonelli, M. Schäffler, W. Möller, N. Gibson, W. G. Kreyling, *J. Aerosol Med. Pulm. Drug Delivery* **2013**, *26*, 24.
- [204] W. G. Kreyling, U. Holzwarth, N. Haberl, J. Kozempel, S. Hirn, A. Wenk, C. Schleh, M. Schäffler, J. Lipka, M. Semmler-Behnke, N. Gibson, *Nanotoxicology* **2017**, *11*, 434.
- [205] W. G. Kreyling, U. Holzwarth, C. Schleh, J. Kozempel, A. Wenk, N. Haberl, S. Hirn, M. Schäffler, J. Lipka, M. Semmler-Behnke, N. Gibson, *Nanotoxicology* **2017**, *11*, 443.
- [206] W. G. Kreyling, U. Holzwarth, N. Haberl, J. Kozempel, A. Wenk, S. Hirn, C. Schleh, M. Schäffler, J. Lipka, M. Semmler-Behnke, N. Gibson, *Nanotoxicology* **2017**, *11*, 454.
- [207] M. Li, K. T. Al-Jamal, K. Kostarelos, J. Reineke, *ACS Nano* **2010**, *4*, 6303.
- [208] M. Li, P. Zou, K. Tyner, S. Lee, *AAPS J.* **2017**, *19*, 26.
- [209] U. Carlander, D. Li, O. Jolliet, C. Emond, G. Johanson, *Int. J. Nanomed.* **2016**, *11*, 625.
- [210] G. Bachler, S. Losert, Y. Umehara, N. von Goetz, L. Rodriguez-Lorenzo, A. Petri-Fink, B. Rothen-Rutishauser, K. Hungerbuehler, *Part. Fibre Toxicol.* **2015**, *12*, 18.
- [211] B. D. Gerard, J. Tortora, *Principles of Anatomy and Physiology*, John Wiley and Sons, Inc., Hoboken, NJ, USA **2006**.
- [212] M. Yu, J. Zheng, *ACS Nano* **2015**, *9*, 6655.
- [213] W. Deen, M. Lazzara, B. Myers, *Am. J. Physiol. Renal Physiol* **2001**, *281*, F579.
- [214] M. Ohlson, J. Sörensson, B. Haraldsson, *Am. J. Physiol. Renal Physiol.* **2001**, *280*, 396.
- [215] M. Longmire, P. L. Choyke, H. Kobayashi, *Nanomedicine* **2008**, *3*, 703.
- [216] H. Kobayashi, N. Le, I. S. Kim, M. K. Kim, J. E. Pie, D. Drumm, D. S. Paik, T. A. Waldmann, C. H. Paik, J. A. Carrasquillo, *Cancer Res.* **1999**, *59*, 422.
- [217] X. Huang, F. Zhang, L. Zhu, K. Y. Choi, N. Guo, J. Guo, K. Tackett, P. Anilkumar, G. Liu, Q. Quan, H. S. Choi, G. Niu, Y. Sun, S. Lee, *ACS Nano* **2013**, *7*, 5684.
- [218] X. He, H. Nie, K. Wang, W. Tan, X. Wu, P. Zhang, *Anal. Chem.* **2008**, *80*, 9597.
- [219] Q. He, Z. Zhang, F. Gao, Y. Li, J. Shi, *Anal. Chem.* **2011**, *7*, 271.
- [220] J. Lu, M. Liong, Z. Li, J. I. Zink, F. Tamanoi, *Small* **2010**, *6*, 1794.
- [221] M. A. Malfatti, H. A. Palko, E. A. Kuhn, K. W. Turteltaub, *Nano Lett.* **2012**, *12*, 5532.
- [222] S. J. Cheong, C. M. Lee, S. L. Kim, H. J. Jeong, E. M. Kim, E. H. Park, D. W. Kim, S. T. Lim, M. H. Sohn, *Int. J. Pharm.* **2009**, *372*, 169.
- [223] E. Sadauskas, G. Danscher, M. Stoltenberg, U. Vogel, A. Larsen, H. Wallin, *Nanomed. Nanotechnol., Biol. Med.* **2009**, *5*, 162.
- [224] K. Ogawara, M. Yoshida, K. Higaki, T. Kimura, K. Shiraishi, M. Nishikawa, Y. Takakura, M. Hashida, *J. Controlled Release* **1999**, *59*, 15.
- [225] M.-Y. Lee, J.-A. Yang, H. S. Jung, S. Beack, J. E. Choi, W. Hur, H. Koo, K. Kim, S. K. Yoon, S. K. Hahn, *ACS Nano* **2012**, 9522.
- [226] Y. Yang, S. X. Yuan, L. H. Zhao, C. Wang, J. S. Ni, Z. G. Wang, C. Lin, M. C. Wu, W. P. Zhou, *Mol. Pharm.* **2015**, *12*, 644.
- [227] L. Wang, Y. F. Li, L. Zhou, Y. Liu, L. Meng, K. Zhang, X. Wu, L. Zhang, B. Li, C. Chen, *Anal. Bioanal. Chem.* **2010**, *396*, 1105.
- [228] K. Poelstra, J. Prakash, L. Beljaars, *J. Controlled Release* **2012**, *167*, 188.
- [229] M. Bartsch, A. H. Weeke-Klimp, D. K. F. Meijer, G. L. Scherphof, J. A. A. M. Kamps, *Pharm. Res.* **2002**, *19*, 676.
- [230] Y. N. Zhang, W. Poon, A. J. Tavares, I. D. McGilvray, W. C. W. Chan, *J. Controlled Release* **2016**, *240*, 332.
- [231] M. R. Knowles, R. C. Boucher, *J. Clin. Invest.* **2002**, *109*, 571.
- [232] B. Button, L.-H. Cai, C. Ehre, M. Kesimer, D. B. Hill, J. K. Sheehan, R. C. Boucher, M. Rubinstein, *Science* **2012**, *337*, 937.
- [233] A. Livraghi, S. H. Randell, *Toxicol. Pathol.* **2007**, *35*, 116.
- [234] I. Ibanez-Tallon, *Hum. Mol. Genet.* **2003**, *12*, 27R.
- [235] K. H. Kilburn, *Am. Rev. Respir. Dis.* **1968**, *98*, 449.
- [236] L. Morgan, M. Pearson, R. de longh, D. Mackey, H. van der Wall, M. Peters, J. Rutland, *Eur. Respir. J.* **2004**, *23*, 518.
- [237] M. Meeks, A. Bush, *Pediatr. Pulmonol.* **2000**, *316*, 307.
- [238] S. H. Randell, R. C. Boucher, *Am. J. Respir. Cell Mol. Biol.* **2006**, *35*, 20.
- [239] W. D. Bennett, E. Daviskas, A. Hasani, J. Mortensen, J. Fleming, G. Scheuch, *J. Aerosol Med. Pulm. Drug Delivery* **2010**, *23*, 261.
- [240] J. Kirch, A. Schneider, B. Abou, A. Hopf, U. F. Schaefer, M. Schneider, C. Schall, C. Wagner, C.-M. Lehr, *Proc. Natl. Acad. Sci. USA* **2012**, *109*, 18355.
- [241] X. Murgia, P. Pawelzyk, U. F. Schaefer, C. Wagner, N. Willenbacher, C.-M. Lehr, *Biomacromolecules* **2016**, *17*, 1536.
- [242] S. Yona, S. Gordon, *Front. Immunol.* **2015**, *6*, 1.
- [243] P. Rous, J. W. Bearad, *Science* **1933**, *77*, 92.
- [244] P. Rio-Hortega, *Lancet* **1939**, *233*, 1023.
- [245] M. Williams, F. Ginhoux, C. Jakubzick, S. H. Naik, N. Onai, B. U. Schraml, E. Segura, R. Tussiwand, S. Yona, *Nat. Rev. Immunol.* **2014**, *14*, 571.
- [246] G. Renaud, R. L. Hamilton, R. J. Havel, *Hepatology* **1989**, *9*, 380.
- [247] P. P. Karmali, D. Simberg, *Expert Opin. Drug Delivery* **2011**, *8*, 343.
- [248] N. Desai, *AAPS J.* **2012**, *14*, 282.
- [249] A. Hochreiter-Hufford, K. S. Ravichandran, *Cold Spring Harbor Perspect. Biol.* **2013**, *5*, a008748.
- [250] C. D. Gregory, A. Devitt, *Immunology* **2004**, *113*, 1.
- [251] J. Cho, F. Caruso, *Chem. Mater.* **2005**, *17*, 4547.
- [252] S. Nie, *Nanomedicine* **2010**, *5*, 523.
- [253] P. L. Rodriguez, T. Harada, D. a. Christian, D. a. Pantano, R. K. Tsai, D. E. Discher, *Science* **2013**, *339*, 971.
- [254] M. Gulati, M. Grover, S. Singh, M. Singh, *Int. J. Pharm.* **1998**, *165*, 129.
- [255] G. L. Scherphof, J. Dijkstra, H. H. Spanjer, J. T. Derksen, F. H. Roerdink, *Ann. N. Y. Acad. Sci.* **1985**, *446*, 368.
- [256] C. R. Alving, E. A. Steck, W. L. Chapman, V. B. Waits, L. D. Hendricks, G. M. Swartz, W. L. Hanson, *Proc. Natl. Acad. Sci. USA* **1978**, *75*, 2959.
- [257] A. K. Agrawal, C. M. Gupta, *Adv. Drug Delivery Rev.* **2000**, *41*, 135.
- [258] M. K. Basu, S. Lala, *Curr. Mol. Med.* **2004**, *4*, 681.
- [259] H. M. Patel, *Crit. Rev. Ther. Drug Carrier Syst.* **1992**, *9*, 39.
- [260] D. J. Falcone, *J. Leukoc. Biol.* **1986**, *39*, 1.
- [261] A. Chonn, S. C. Semple, P. R. Cullis, *J. Biol. Chem.* **1995**, *270*, 25845.
- [262] J. E. Volanakis, A. J. Narkates, *J. Immunol.* **1981**, *126*, 1820.
- [263] M. Murai, Y. Aramaki, S. Tsuchiya, *Immunology* **1995**, *86*, 64.
- [264] T. Ishida, H. Kojima, H. Harashima, H. Kiwada, *Int. J. Pharm.* **2000**, *205*, 183.
- [265] J. Senior, G. Gregoriadis, *Life Sci.* **1982**, *30*, 2123.
- [266] H. Harashima, Y. Ochi, H. Kiwada, *Biopharm. Drug Dispos.* **1994**, *15*, 217.
- [267] K. Funato, R. Yoda, H. Kiwada, *Biochim. Biophys. Acta, Biomembr.* **1992**, *1103*, 198.
- [268] K. Nishikawa, H. Arai, K. Inoue, *J. Biol. Chem.* **1990**, *265*, 5226.
- [269] J. H. Senior, *Crit. Rev. Ther. Drug Carrier Syst.* **1987**, *3*, 123.
- [270] Y. J. Kao, R. L. Juliano, *Biochim. Biophys. Acta* **1981**, *677*, 453.
- [271] T. M. Allen, C. Hansen, F. Martin, C. Redemann, A. Yau-Young, *Biochim. Biophys. Acta, Biomembr.* **1991**, *1066*, 29.
- [272] T. M. Allen, C. Hansen, J. Rutledge, *Biochim. Biophys. Acta* **1989**, *981*, 27.
- [273] A. Gabizon, D. Papahadjopoulos, *Proc. Natl. Acad. Sci. USA* **1988**, *85*, 6949.

- [274] J. Morgenstern, P. Baumann, C. Brunner, J. Hubbuch, *Int. J. Pharm.* **2017**, 519, 408.
- [275] J. M. Harris, R. B. Chess, *Nat. Rev. Drug Discovery* **2003**, 2, 214.
- [276] G. Blume, G. Cevc, M. D. Crommelin, I. A. Bakker-Woudenberg, C. Kluff, G. Storm, *Biochim. Biophys. Acta* **1993**, 1149, 180.
- [277] M. Vert, D. Domurado, *J. Biomater. Sci., Polym. Ed.* **2000**, 11, 1307.
- [278] K. J. Harrington, G. Rowlinson-Busza, K. N. Syrigos, R. M. Abra, P. S. Uster, A. M. Peters, J. S. Stewart, *Br. J. Cancer* **2000**, 83, 684.
- [279] K. J. Harrington, G. Rowlinson-Busza, K. N. Syrigos, P. S. Uster, R. M. Abra, J. S. Stewart, *Br. J. Cancer* **2000**, 83, 232.
- [280] W. C. Zamboni, A. C. Gervais, M. J. Egorin, J. H. M. Schellens, E. G. Zuhowski, D. Pluim, E. Joseph, D. R. Hamburger, P. K. Working, G. Colbern, M. E. Tonda, D. M. Potter, J. L. Eiseman, *Cancer Chemother. Pharmacol.* **2004**, 53, 329.
- [281] S. Zalipsky, M. Qazen, J. A. Walker, N. Mullah, Y. P. Quinn, S. K. Huang, *Bioconjugate Chem.* **1999**, 10, 703.
- [282] D. E. Lopes de Menezes, M. J. Kirchmeier, J.-F. Gagne, L. M. Pilarski, T. M. Allen, *J. Liposome Res.* **1999**, 9, 199.
- [283] P. Sapra, T. M. Allen, *Prog. Lipid Res.* **2003**, 42, 439.
- [284] O. P. Medina, Y. Zhu, K. Kairemo, *Curr. Pharm. Des.* **2004**, 10, 2981.
- [285] P. Laverman, O. C. Boerman, Oyen WJG, Corstens FHM, G. Storm, *Crit. Rev. Ther. Drug Carrier Syst.* **2001**, 18, 551.
- [286] A. S. Abu Lila, H. Kiwada, T. Ishida, *J. Controlled Release* **2013**, 172, 38.
- [287] T. Ishida, H. Kiwada, *Yakugaku Zasshi* **2008**, 128, 233.
- [288] C. Wang, X. Cheng, Y. Su, Y. Pei, Y. Song, J. Jiao, Z. Huang, Y. Ma, Y. Dong, Y. Yao, J. Fan, H. Ta, X. Liu, H. Xu, Y. Deng, *Int. J. Nanomed.* **2015**, 10, 3533.
- [289] L. Sercombe, T. Veerati, F. Moheimani, S. Y. Wu, A. K. Sood, S. Hua, *Front. Pharmacol.* **2015**, 6, 1.
- [290] K. Knop, R. Hoogenboom, D. Fischer, U. S. Schubert, *Angew. Chem., Int. Ed.* **2010**, 49, 6288.
- [291] T. H. Chow, Y. Y. Lin, J. J. Hwang, H. E. Wang, Y. L. Tseng, S. J. Wang, R. S. Liu, W. J. Lin, C. S. Yang, G. Ting, *Anticancer Res.* **2009**, 29, 2111.
- [292] M. L. Immordino, F. Dosio, L. Cattel, *Int. J. Nanomed.* **2006**, 1, 297.
- [293] T.-H. Chow, Y.-Y. Lin, J.-J. Hwang, H.-E. Wang, Y.-L. Tseng, V. F. Pang, R.-S. Liu, W.-J. Lin, C.-S. Yang, G. Ting, *J. Nucl. Med.* **2009**, 50, 2073.
- [294] A. Soundararajan, A. Bao, W. T. Phillips, R. Perez, B. A. Goins, *Nucl. Med. Biol.* **2009**, 36, 515.
- [295] Y. Chang, C. Chang, T. Chang, C. Yu, L. Chen, M. Jan, T. Luo, G. Ting, *Anticancer Res.* **2007**, 27, 2217.
- [296] N. Zhang, P. R. Wardwell, R. A. Bader, *Pharmaceutics* **2013**, 5, 329.
- [297] S. W. Kim, K. Park, in *Targeted Delivery of Small and Macromolecular Drugs: Problems Faced and Approaches Taken*, (Eds: A. Narang, R. Mahato), Taylor and Francis Group **2010**, pp. 513–551.
- [298] C. M. R. Oda, R. S. Fernandes, S. C. de Araújo Lopes, M. C. de Oliveira, V. N. Cardoso, D. M. Santos, A. M. de Castro Pimenta, A. Malachias, R. Paniago, D. M. Townsend, P. M. Colletti, D. Rubello, R. J. Alves, A. L. B. de Barros, E. A. Leite, *Biomed. Pharmacother.* **2017**, 89, 268.
- [299] A. Al Zaki, J. Z. Hui, E. Higbee, A. Tsourkas, *J. Biomed. Nanotechnol.* **2015**, 11, 1836.
- [300] J. Wang, W. Mao, L. L. Lock, J. Tang, M. Sui, W. Sun, H. Cui, D. Xu, Y. Shen, *ACS Nano* **2015**, 9, 7195.
- [301] A. B. Ebrahim Attia, C. Yang, J. P. K. Tan, S. Gao, D. F. Williams, J. L. Hedrick, Y. Y. Yang, *Biomaterials* **2013**, 34, 3132.
- [302] C. Louis, O. Pluchery, *Gold Nanoparticles for Physics, Chemistry and Biology*, World Scientific Publishing Europe Ltd., London, UK **2017**.
- [303] N. Khlebtsov, L. Dykman, *Chem. Soc. Rev.* **2011**, 40, 1647.
- [304] A. M. Alkilany, C. J. Murphy, *J. Nanopart. Res.* **2010**, 12, 2313.
- [305] Y. S. Chen, Y. C. Hung, I. Liao, G. S. Huang, *Nanoscale Res. Lett.* **2009**, 4, 858.
- [306] J. Y. Wang, J. Chen, J. Yang, H. Wang, X. Shen, Y. M. Sun, M. Guo, X. D. Zhang, *Int. J. Nanomed.* **2016**, 11, 3475.
- [307] F. Naz, V. Koul, A. Srivastava, Y. K. Gupta, A. K. Dinda, *J. Drug Target.* **2016**, 24, 720.
- [308] S. Fraga, A. Brandão, M. E. Soares, T. Morais, J. A. Duarte, L. Pereira, L. Soares, C. Neves, E. Pereira, M. de L. Bastos, H. Carmo, *Nanomed. Nanotechnol., Biol. Med.* **2014**, 10, 1757.
- [309] S. K. Balasubramanian, J. Jittiwat, J. Manikandan, C. N. Ong, L. E. Yu, W. Y. Ong, *Biomaterials* **2010**, 31, 2034.
- [310] D. Hessl, D. V. Nguyen, C. Green, A. Chavez, F. Tassone, J. Hagerman, D. Senturk, A. Schneider, A. Lightbody, A. L. Reiss, S. Hall, *J. Neurodev. Disord.* **2009**, 1, 33.
- [311] R. Goel, N. Shah, R. Visaria, G. F. Paciotti, J. C. Bischof, *Nanomedicine* **2009**, 4, 401.
- [312] C. Alric, I. Miladi, D. Kryza, J. Taleb, F. Lux, R. Bazzi, C. Billotey, M. Janier, P. Perriat, S. Roux, O. Tillement, *Nanoscale* **2013**, 5, 5930.
- [313] N. Lee, D. Yoo, D. Ling, M. H. Cho, T. Hyeon, J. Cheon, *Chem. Rev.* **2015**, 115, 10637.
- [314] M. Bañobre-López, A. Teijeiro, J. Rivas, *Rep. Pract. Oncol. Radiother.* **2013**, 18, 397.
- [315] T. Kobayashi, *Biotechnol. J.* **2011**, 6, 1342.
- [316] L. Li, W. Jiang, K. Luo, H. Song, F. Lan, Y. Wu, Z. Gu, *Theranostics* **2013**, 3, 595.
- [317] Circ, P. Release, W. H. O. (Who), S.-H. Xie, A.-L. Liu, Y.-Y. Chen, L. Zhang, H.-J. Zhang, B.-X. Jin, W.-Q. W.-H. Lu, X.-Y. Li, W.-Q. W.-H. Lu, P. a. White, J. B. Rasmussen, C. Blaise, S.-H. Xie, A.-L. Liu, Y.-Y. Chen, L. Zhang, H.-J. Zhang, B.-X. Jin, W.-Q. W.-H. Lu, X.-Y. Li, W.-Q. W.-H. Lu, *Environ. Mol. Mutagen.* **2010**, 51, 229.
- [318] J. E. Hall, A. C. Guyton, *J. Chem. Inf. Model.* **2011**, 53, 160.
- [319] T. Skotland, T. G. Iversen, K. Sandvig, *Nanomed. Nanotechnol., Biol. Med.* **2010**, 6, 730.
- [320] L. Lartigue, D. Alloyeau, J. Kolosnjaj-Tabi, A. Javed, J. Riedinger, P. Guardia, A. Riedinger, C. Péchoux, T. Pellegrino, C. Wilhelm, F. Gazeau, *ACS Nano* **2013**, 7, 3939.
- [321] K. Briley-Saebø, S.-O. Hustvedt, A. Haldorsen, A. Bjørnerud, *J. Magn. Reson. Imaging* **2004**, 20, 622.
- [322] J. E. Wagenseil, L. O. Johansson, C. H. Lorenz, *J. Magn. Reson. Imaging* **1999**, 10, 784.
- [323] M. Levy, N. Luciani, D. Alloyeau, D. Elgrabli, V. Deveaux, C. Pechoux, S. Chat, G. Wang, N. Vats, F. Gendron, C. Factor, S. Lotersztajn, A. Luciani, C. Wilhelm, F. Gazeau, *Biomaterials* **2011**, 32, 3988.
- [324] P. Keselman, E. Y. Yu, X. Y. Zhou, P. W. Goodwill, P. Chandrasekharan, R. M. Ferguson, A. P. Khandhar, S. J. Kemp, K. M. Krishnan, B. Zheng, S. M. Conolly, *Phys. Med. Biol.* **2017**, 62, 3440.
- [325] K. Unger, H. Rupperecht, B. Valentin, W. Kircher, *Drug Dev. Ind. Pharm.* **1983**, 9, 69.
- [326] L. Sancey, S. Kotb, C. Truillet, F. Appaix, A. Marais, E. Thomas, B. van der Sanden, J.-P. Klein, B. Laurent, M. Cottier, R. Antoine, P. Dugourd, G. Panczer, F. Lux, P. Perriat, V. Motto-Ros, O. Tillement, *ACS Nano* **2015**, 9, 2477.
- [327] M. Longmire, P. L. Choyke, H. Kobayashi, *Nanomedicine* **2008**, 3, 703.
- [328] H. S. Choi, J. V. Frangioni, *Mol. Imaging* **2010**, 9, 291.
- [329] E. Phillips, O. Penate-Medina, P. B. Zanzonico, R. D. Carvajal, P. Mohan, Y. Ye, J. Humm, M. Gönen, H. Kalaigian, H. Schöder, H. W. Strauss, S. M. Larson, U. Wiesner, M. S. Bradbury, *Sci. Transl. Med.* **2014**, 6, 260ra149.

- [330] A. A. Burns, J. Vider, H. Ow, E. Herz, O. Penate-Medina, M. Baumgart, S. M. Larson, U. Wiesner, M. Bradbury, *Nano Lett.* **2009**, 9, 442.
- [331] Q. He, Z. Zhang, F. Gao, Y. Li, J. Shi, *Small* **2011**, 7, 271.
- [332] M. Cho, W.-S. S. Cho, M. Choi, S. Jun, B. Seok, S. Hee, H. Ook, Y. Yhong, J. Jeong, S. H. S. J. Kim, B. S. Han, S. H. S. J. Kim, H. O. Kim, Y. Y. Sheen, J. Jeong, *Toxicol. Lett.* **2009**, 189, 177.
- [333] G. Xie, J. Sun, G. Zhong, L. Shi, D. Zhang, *Arch. Toxicol.* **2010**, 84, 183.
- [334] J. S. Souris, C.-H. Lee, S.-H. Cheng, C.-T. Chen, C.-S. Yang, J. A. Ho, C.-Y. Mou, L.-W. Lo, *Biomaterials* **2010**, 31, 5564.
- [335] X. Lu, C. Ji, T. Jin, X. Fan, *Nanotechnology* **2015**, 26, 175101.
- [336] T. Yu, D. Hubbard, A. Ray, H. Ghandehari, *J. Controlled Release* **2012**, 163, 46.
- [337] C. Fu, T. Liu, L. Li, H. Liu, D. Chen, F. Tang, *Biomaterials* **2013**, 34, 2565.
- [338] T. Liu, L. Li, X. Teng, X. Huang, H. Liu, D. Chen, J. Ren, J. He, F. Tang, *Biomaterials* **2011**, 32, 1657.
- [339] J.-A. Lee, M.-K. Kim, H.-J. Paek, Y.-R. Kim, M.-K. Kim, J.-K. Lee, J. Jeong, S.-J. Choi, S.-J. Choi, *Int. J. Nanomed.* **2014**, 9, 251.
- [340] B. Borak, P. Biernat, A. Prescha, A. Baszczuk, J. Pluta, *Adv. Clin. Exp. Med.* **2012**, 21, 13.
- [341] E. J. Park, K. Park, *Toxicol. Lett.* **2009**, 184, 18.
- [342] M. F. Maitz, *Biosurf. Biotribol.* **2015**, 1, 161.
- [343] W. B. Liechty, D. R. Kryscio, B. V Slaughter, N. A. Peppas, *Annu. Rev. Chem. Biomol. Eng.* **2010**, 1, 149.
- [344] R. Duncan, *Nat. Rev. Drug Discovery* **2003**, 2, 347.
- [345] R. Duncan, *Nat. Rev. Cancer* **2006**, 6, 688.
- [346] L. Bildstein, C. Dubernet, P. Couvreur, *Adv. Drug Delivery Rev.* **2011**, 63, 3.
- [347] P. A. Dinndorf, J. Gootenberg, M. H. Cohen, P. Keegan, R. Pazdur, *Oncologist* **2007**, 12, 991.
- [348] R. Masetti, A. Pession, *Biologics* **2009**, 3, 359.
- [349] V. I. Avramis, S. Sencer, A. P. Periclou, H. Sather, B. C. Bostrom, L. J. Cohen, A. G. Ettinger, L. J. Ettinger, J. Franklin, P. S. Gaynon, J. M. Hilden, B. Lange, F. Majlessipour, P. Mathew, M. Needle, J. Neglia, G. Reaman, J. S. Holcenberg, L. Stork, *Blood* **2002**, 99, 1986.
- [350] K. A. Wenner, J. P. Vieira Pinheiro, G. Escherich, R. Wessalowski, N. Jorch, J. Wolff, M. Stehn, A. Kohlschütter, J. Boos, G. E. Janka-Schaub, *Klin. Padiatr.* **2005**, 217, 321.
- [351] D. Douer, H. Yampolsky, L. J. Cohen, K. Watkins, A. M. Levine, A. P. Periclou, V. I. Avramis, *Blood* **2006**, 109, 2744.
- [352] J. P. V. Pinheiro, C. Lanvers, G. Würthwein, R. Beier, J. Casimiro da Palma, A. von Stackelberg, J. Boos, *Leuk. Lymphoma* **2002**, 43, 1911.
- [353] A. Abuchowski, G. M. Kazo, C. R. Verhoest, T. Van Es, D. Kafkewitz, M. L. Nucci, A. T. Viau, F. F. Davis, *Cancer Biochem. Biophys.* **1984**, 7, 175.
- [354] Y. Kamisaki, H. Wada, T. Yagura, A. Matsushima, Y. Inada, *J. Pharmacol. Exp. Ther.* **1981**, 216, 410.
- [355] J. K. Armstrong, G. Hempel, S. Koling, L. S. Chan, T. Fisher, H. J. Meiselman, G. Garratty, *Cancer* **2007**, 110, 103.
- [356] H. Maeda, *Adv. Drug Delivery Rev.* **2001**, 46, 169.
- [357] P. Bailon, A. Palleroni, C. A. Schaffer, C. L. Spence, W. J. Fung, J. E. Porter, G. K. Ehrlich, W. Pan, Z. X. Xu, M. W. Modi, A. Farid, W. Berthold, M. Graves, *Bioconjugate Chem.* **2001**, 12, 195.
- [358] C. Booth, H. B. Gaspar, *Biologics* **2009**, 3, 349.
- [359] G. Molineux, *Curr. Pharm. Des.* **2004**, 10, 1235.
- [360] P. N.-M. Cheng, T.-L. Lam, W.-M. Lam, S.-M. Tsui, A. W.-M. Cheng, W.-H. Lo, Y.-C. Leung, *Cancer Res.* **2007**, 67, 309.
- [361] R. M. Bukowski, J. Young, G. Goodman, F. Meyers, B. F. Issell, J. S. Sergi, D. McLain, G. Fyfe, J. Finke, *Invest. New Drugs* **1993**, 11, 211.
- [362] J. C. Yang, S. L. Topalian, D. J. Schwartzentruber, D. R. Parkinson, F. M. Marincola, J. S. Weber, C. A. Seipp, D. E. White, S. A. Rosenberg, *Cancer* **1995**, 76, 687.
- [363] C. Mueller, S. Al-Batran, E. Jaeger, B. Schmidt, M. Bausch, C. Unger, N. Sethuraman, *J. Clin. Oncol.* **2008**, 26, 2533.
- [364] J. Takeshita, H. Maeda, R. Kanamaru, *Gan* **1982**, 73, 278.
- [365] K. Tsukigawa, L. Liao, H. Nakamura, J. Fang, K. Greish, M. Otagiri, H. Maeda, *Cancer Sci.* **2015**, 106, 270.
- [366] R. Duncan, M. J. Vicent, *Adv. Drug Delivery Rev.* **2013**, 65, 60.
- [367] P. Chytil, M. Šírová, E. Koziolová, K. Ulbrich, B. Íhová, T. Etrych, *Physiol. Res.* **2015**, 64, S41.
- [368] F. M. Veronese, O. Schiavon, G. Pasut, R. Mendichi, L. Andersson, A. Tsirk, J. Ford, G. Wu, S. Kneller, J. Davies, R. Duncan, *Bioconjugate Chem.* **2005**, 16, 775.
- [369] G. S. Kwon, M. Yokoyama, T. Okano, Y. Sakurai, K. Kataoka, *Pharm. Res.* **1993**, 10, 970.
- [370] M. P. Borgman, O. Aras, S. Geysler-Stoops, E. A. Sausville, H. Ghandehari, *Mol. Pharm.* **2009**, 6, 1836.
- [371] T. Etrych, V. Šubr, J. Strohalm, M. Šírová, B. Říhová, K. Ulbrich, *J. Controlled Release* **2012**, 164, 346.
- [372] M. S. Falzarano, E. Bassi, C. Passarelli, P. Braghetta, A. Ferlini, *Hum. Gene Ther.* **2014**, 25, 927.
- [373] A. Elsaesser, A. Taylor, G. S. de Yanés, G. McKerr, E.-M. Kim, E. O'Hare, C. V. Howard, *Nanomedicine* **2010**, 5, 1447.
- [374] B. Drasler Barbara, D. Vanhecke, L. Rodriguez-Lorenzo, A. Petri-Fink, B. Rothen-Rutishauser, *Nanomedicine (Lond.)* **2017**, 12, 1095.
- [375] Y. Min, J. M. Caster, M. J. Eblan, A. Z. Wang, *Chem. Rev.* **2015**, 115, 11147.
- [376] S. Kunjachan, J. Ehling, G. Storm, F. Kiessling, T. Lammers, *Chem. Rev.* **2015**, 115, 10907.
- [377] E. Markovsky, H. Baabur-Cohen, A. Eldar-Boock, L. Omer, G. Tiram, S. Ferber, P. Ofek, D. Polyak, A. Scomparin, R. Satchi-Fainaro, *J. Controlled Release* **2012**, 161, 446.
- [378] K. Tryggvason, J. Wartiovaara, *Physiology* **2005**, 20, 96.
- [379] K. M. Tsoi, S. A. MacParland, X.-Z. Ma, V. N. Spetzler, J. Echeverri, B. Ouyang, S. M. Fadel, E. A. Sykes, N. Goldaracena, J. M. Kathis, J. B. Conneely, B. A. Alman, M. Selzner, M. A. Ostrowski, O. A. Adeyi, A. Zilman, I. D. McGilvray, W. C. W. Chan, *Nat. Mater.* **2016**, 1, 1.
- [380] F. Naz, V. Koul, A. Srivastava, Y. K. Gupta, A. K. Dinda, *J. Drug Target.* **2016**, 24, 720.
- [381] W. D. James, L. R. Hirsch, J. L. West, P. D. O'Neal, J. D. Payne, *J. Radioanal. Nucl. Chem.* **2007**, 271, 455.
- [382] R. Kumar, I. Roy, T. Y. Ohulchanskyy, L. A. Vathy, E. J. Bergey, M. Sajjad, P. N. Prasad, *ACS Nano* **2010**, 4, 699.
- [383] H.-J. Paek, H.-E. Chung, J.-A. Lee, M.-K. Kim, Y.-J. Lee, M.-S. Kim, S.-H. Kim, E.-H. Maeng, J. K. Lee, J. Jeong, S.-J. Choi, *Sci. Adv. Mater.* **2014**, 6, 1605.
- [384] L. Li, T. Liu, C. Fu, L. Tan, X. Meng, H. Liu, *Nanomedicine* **2015**, 11, 1915.
- [385] J. G. Shiah, M. Dvorák, P. Kopecková, Y. Sun, C. M. Peterson, J. Kopeček, *Eur. J. Cancer* **2001**, 37, 131.
- [386] S.-Q. Gao, Z.-R. Lu, P. Kopečková, J. Kopeček, *J. Controlled Release* **2007**, 117, 179.
- [387] L. Quan, F. Yuan, X. Liu, J. Huang, Y. Alnouti, D. Wang, *Mol. Pharm.* **2010**, 7, 1041.
- [388] Y. Kaneda, Y. Tsutsumi, Y. Yoshioka, H. Kamada, Y. Yamamoto, H. Kodaira, S. Tsunoda, T. Okamoto, Y. Mukai, H. Shibata, S. Nakagawa, T. Mayumi, *Biomaterials* **2004**, 25, 3259.
- [389] T. Schluep, J. Cheng, K. T. Khin, M. E. Davis, *Cancer Chemother. Pharmacol.* **2006**, 57, 654.
- [390] K. S. Yadav, K. Chuttani, A. K. Mishra, K. K. Sawant, *PDA J. Pharm. Sci. Technol.* **2011**, 65, 131.